University of Kentucky Master's Theses   Graduate School

2010

CHROMIUM, COPPER, AND ARSENIC CONCENTRATION AND SPECIATION IN SOIL ADJACENT TO CHROMATED COPPER ARSENATE (CCA) TREATED LUMBER ALONG A TOPOHYDROSEQUENCE

Donald Roy Schwer III
University of Kentucky, don.schwer@uky.edu

Recommended Citation

ABSTRACT OF THESIS

CHROMIUM, COPPER, AND ARSENIC CONCENTRATION AND SPECIATION IN
SOIL ADJACENT TO CHROMATED COPPER ARSENATE (CCA) TREATED
LUMBER ALONG A TOPOHYDROSEQUENCE

Arsenic (As), Chromium (Cr), and Copper (Cu) are ubiquitous in soils as a result of anthropogenic and geogenic processes. The fate of As, Cr, and Cu in the environment is largely governed by their speciation, which is influenced by soil physiochemical properties. This study investigated the influence of soil physiochemical properties and landscape position on As, Cr, and Cu concentration and speciation in soils adjacent to Chromated Copper Arsenate (CCA) treated lumber fence posts. Concentration gradients showed elevated total As and Cu adjacent to the three fence posts, which decreased with increasing distance from the posts. In addition, As and Cu had higher concentrations in the surface soil samples than the subsoil samples possibly due to enhanced weathering of the CCA treated posts at the surface. Concentrations of As, Cr, and Cu were similar among the Maury and Donerail silt loam, however, they were closer to the background concentration in the Newark silt loam, a partially hydric soil, indicating mobility of the metals. Extended X-ray Absorption Fine Structure (EXAFS) spectroscopy indicates As(V) is the predominate species which is principally coordinated with Fe and Al whereas, Cu(II) is coordinated with soil organic matter. Overall, the use of CCA treated lumber as a metal source can help determine how soil properties influence mobility and speciation of As, Cr, and Cu across the soil landscape.

KEYWORDS: Arsenic, Chromium, Copper, Extended X-Ray Absorption Fine Structure (EXAFS), Chromated Copper Arsenic (CCA) lumber

___Donald R. Schwer III____
_____5/5/2010_____

CHROMIUM, COPPER, AND ARSENIC CONCENTRATION AND SPECIATION IN
SOIL ADJACENT TO CHROMATED COPPER ARSENATE (CCA) TREATED
LUMBER ALONG A TOPOHYDROSEQUENCE

By

Donald Roy Schwer III

<div align="right">

Dr. David H. McNear
(Director of Thesis)

Dr. Charles T. Dougherty
(Director of Graduate Studies)

5/5/2010

</div>

RULES FOR THE USES OF THESES

Unpublished theses submitted for the Master's degree and deposited in the University of Kentucky Library are as a rule open for inspection, but are to be used only with due regard to the right of the authors. Bibliographical references may be noted, but quotations or summaries of parts may be published only with the permission of the author, and with the usual scholarly acknowledgments.

Extensive copying or publication of the thesis in whole or in part also requires the consent of the Dean of the Graduate School of the University of Kentucky.

A library that borrows this thesis for use by its patrons is expected to secure the signature of each user.

Name   Date

_____

_____

_____

_____

_____

_____

_____

_____

_____

_____

_____

_____

_____

THESIS

Donald Roy Schwer III

The Graduate School

University of Kentucky

2010

CHROMIUM, COPPER, AND ARSENIC CONCENTRATION AND SPECIATION IN
SOIL ADJACENT TO CHROMATED COPPER ARSENATE (CCA) TREATED
LUMBER ALONG A TOPOHYDROSEQUENCE

THESIS

A thesis submitted in partial fulfillment of the
requirements for the degree of Master of Science in the
College of Agriculture
at the University of Kentucky

By

Donald Roy Schwer III

Lexington, Kentucky

Director: Dr. David H. McNear Jr., Professor of Rhizosphere Science

Lexington, Kentucky

2010

In the loving memory of my grandfather, Donald R. Schwer Sr.

Table of Contents

List of Tables

List of Figures

List of Files

Thesis_Donald_Schwer.pdf

Chapter 1: Introduction and Literature Review

1.0 Introduction

One unique aspect of the Central Bluegrass Region of Kentucky is its distinction as the "horse capital of the world". With horses, come fences and the type of fence post commonly used in the region is Chromated Copper Arsenate (CCA) treated lumber. From an environmental perspective the release of these three metal(loid)s (chromium, copper, and arsenic) can have a detrimental impact on ecosystem and human health even at very low concentrations. The extent of release of these metal(loid)s from CCA posts must be determined in Kentucky soils. Fence posts, however, are not the only sources of these metal(liod)s, other sources include land application of manure and biosolids and metal release during coal mining. The novelty of this project is to use CCA treated lumber fence posts as a source of these metal(loid)s and evaluate how soil physiochemical properties influence the mobility and speciation of Cr, Cu, and As in the soil.

The following sections of this chapter will provide an overview of i.) general soil chemistry properties influencing metal mobility, ii.) sources of metal(liod)s in the environment, iii.) specific chemistry regarding As, Cr, and Cu in the soil, iiii.) chemistry of CCA treated wood, and v.) the objectives of this study. Chapter 2 will cover how soil physicochemical properties influence the mobility and speciation of Arsenic in the soil and Chapter 3 will address how soil physicochemical properties influence the mobility and speciation of Copper and Chromium. Finally, Chapter 4 will be an overall summary and conclusion of the findings.

1.1 Review of Literature

1.1.1 Metal Sequestration in Soils

1.1.1.1 pH and Eh: Master Variables

The pH of the soil is dictated by a confluence of physical, chemical, and biological components. The main sources of hydrogen ions (protons) in the soil are from carbonic acid, as well as other acids, dissolved in rain water, dissociation of H^+ from mineral and organic material functional groups, the oxidation of compounds (e.g. oxidation of ammonium ions), and the plant uptake of ions (Sparks, 2003). The principal properties dictated by the pH of the soil are the speciation of the metal present and the charge on the soil constituents. Overall, as the pH of the soil increases the charge on the metal species present as well as on the soil constituents become increasingly negative. The inherent chemical properties of each chemical species will dictate its protonation/deprotonation properties at various pH conditions, thus influencing the charge. The coupling of the protonation constants between the metal species and soil constituents will dictate the adsorption properties of the soil.

Like pH, Eh dictates the speciation present due to alteration of metal and mineral oxidation states. However, unlike pH, the transfer of electrons in a system requires close chemical contact. The redox conditions of the soil dictate whether it is thermodynamically favorable for a reduced or oxidized species of metal to be present. In most cases, soil is well aerated and thus in an oxidized state; however, in landscape positions where drainage pathways converge or ponding conditions occur reducing conditions develop through the depletion of oxygen in the water. The occurrence of

reducing conditions alters the electronic state of metals in the soil and thus will alter mobility and speciation in the environment.

1.1.1.2 Soil Surface Charge

The soil surface charge is a function of the chemical constituents of the soil, as well as the pH and Eh conditions of the soil. The physical and chemical weathering of the soil and the organic matter accumulation over time leads to the development of a specific surface charge. This surface charge can be further broken down to the surface charge of mineral phases and organic matter phases in the soil.

1.1.1.2.1 Mineral-Metal Interaction

The surface charge of minerals can be attributed to two phenomena the first being a permanent charge due to isomorphic substitution of cations of lower charge and site vacancies in mineral structures. This charge is independent of pH and is characteristic of the mineral type present. Secondly, there exists a surface charge dependent on pH due to the protonation or deprotenation of surface functional groups on soil minerals. This surface charge is dependent on the number and type of functional groups present on the mineral surface. The most abundant surface functional groups are hydroxyl groups associated with the edge of mineral structures. The hydroxyl groups possess protonation/ deprotonation characteristics that are a function of the mineral and coordination environment of oxygen.

The balance of the charge created on mineral surfaces with the ions in solution determines the type and extent of metal sorption. Sorption mechanisms in the soil are generally inner-sphere and outer-sphere sorption complexes. With inner-sphere sorption

complexes there exists direct coordination of the metal with the mineral functional group. However, with outer- sphere sorption complexes there exists a water molecule between the metal and the mineral functional group, and are generally considered electrostatic interactions therefore, less stable than inner sphere complexes (Sposito, 2008). The properties of the metal, mineral, and ions in solution determine the type and extent of sorption at different pH/Eh conditions.

1.1.1.2.2 Organic Matter-Metal Interaction

The composition of organic matter in the soil is highly complex consisting of organic residues, soil biomass, humus, humic acids, and humin (Sparks, 2003). Perhaps the most important of these with respect to metal interaction are the humic substances (humic and fulvic acids and humin) because of their stability in soil and relative abundance (up to 80% soil organic matter) (Sposito, 2008). The surface charge of soil organic material is generated through the pH dependence of a wide variety of functional groups and is principally negatively charged at pH values greater than 3. As the pH increases more deprotonation of functional groups occurs, thus an increasingly negative charge develops (Sparks, 2003). Although, nearly every possible organic functional group may exist in soil organic matter, the predominant functional groups of interest are carboxylic and phenolic OH groups because there deprotonation constants are within the range of most soil pH values (Sparks, 2003). Similar to mineral surfaces, humic substances can bind metals as both inner and outer-sphere adsorption complexes.

1.1.1.3 Biotic Controls on Metal Mobility

Biological organisms control metal mobility through the alteration of their immediate environment. The biological alteration of the environment develops through

changes in pH, alterations in soil solution, release of chelating molecules, and utilization of metals as nutrients, terminal electron acceptors, and/or energy sources. The change of pH and alteration of soil solution properties can influence the charge properties of the metal, mineral, and organic matter present. Also, chelating molecules can solubilize metals, increasing mobility and the use of the metal as a biological agent (nutrient, electron acceptor, and energy source) can work to further increase metal mobility. Many times microorganisms speed the rate thermodynamically favorable chemical reactions will occur, especially in fluctuating reducing and oxidizing conditions.

1.1.2 Sources of Arsenic, Chromium, and Copper in the Environment

Heavy metals copper (Cu) and chromium (Cr) and metalloid arsenic (As) in the unperturbed soil are considered trace elements, elements with concentrations of <0.1%. The sources of these elements, natural or anthropogenic, can provide information on concentrations and mobility in the environment. Naturally, the main source of trace elements in the soil is due to the weathering of soil parent material. In natural systems, the levels of As, Cr, and Cu are generally low and in most cases are necessary for the proper function of the ecosystem, because the background concentrations provide essential nutrients (Cu,Cr) for the resident flora and fauna. However, due to anthropogenic activities, and under some natural circumstances, the trace metals concentrations in soils can become highly elevated with respect to background concentrations. Under these circumstances trace nutrients can be damaging to the local environment, as well as, causing a potential threat to humans through the intake of food and water containing elevated metal concentrations. The following sections will address

Cr, Cu and As sources in the environment, evaluate their distribution on a local, national, and global scale and describe the chemical and physical interactions that control their mobility and bioavailability in the environment.

1.1.3 Arsenic

1.1.3.1 Natural Sources

Arsenic (As) is a highly toxic element that is ubiquitous in the pedosphere, hydrosphere, and biosphere at trace amounts. Arsenic is present in greater than 200 mineral forms on earth (Mandal and Suzuki, 2002). Some common As minerals are orpiment(As_2S_3), realgar (As_4S_4), arsenolite (As_2O_3), olivenite (Cu_2OHAsO_4), and the arsenide's, with the most common being arsenopyrite (FeAsS) (Zhang and Selim, 2008). As these minerals weather, the dissolution of As bearing minerals can release As into the soil solution where it can then be sorbed, precipitated or lost from the system.

The mean concentration of arsenic in the earth crust is 1.5 – 1.7 mg kg^{-1} with a mean concentration in the soil 5.2- 7.2 mg kg^{-1} (Sparks, 2003; Sposito, 2008). Arsenic is therefore slightly enriched in the soil and commonly occurs coprecipitated with the secondary soil minerals of Fe, Al, and Mn oxides (Sposito, 2008). Arsenic can be precipitated with iron hydroxides and sulfide and is also associated with iron deposits and manganese nodules (Mandal and Suzuki, 2002). The concentrations of As in soils of the state of Kentucky range from 0.1 – 10 mg kg^{-1}(Baldwin, 1998). In general As concentrations in the soils of the United States reside in the 3 – 11 mg kg^{-1} range (Figure 1.1).
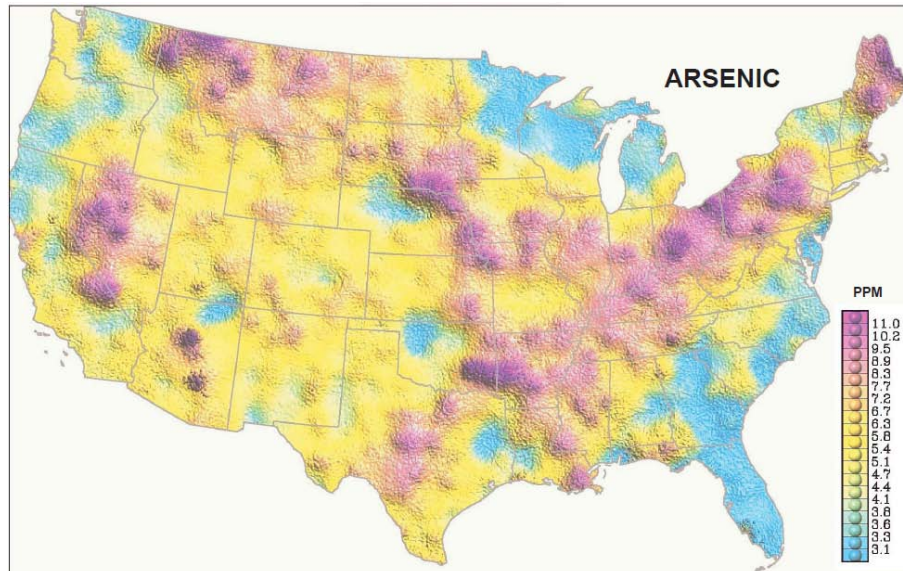
Figure 1.1: Arsenic distribution in soils of the United States (Gustavsson, 2001)

1.1.3.2 Anthropogenic Sources

Though there is a wide array of natural sources of arsenic in the soil environment, concentration of As can be significantly increased in the soil as a result of anthropogenic processes. The anthropogenic mobilization factor (AMF), defined as the mass of As anthropogenically extracted annually verses the mass released by crustal weathering and volcanic activity annually, is ~ 27, indicating that humans are significantly perturbing the As cycle (Sposito, 2008). Common anthropogenic practices that have increased concentrations of As in the soil are applications of As containing pesticides and animal manure (e.g. Roxarsone (3-nitro-4-hydroxyphenylarsonic acid) in poultry litter), as part of waste material in mine tailings, and as the wood preservative Chromated Copper Arsenate (CCA). Arsenic was widely used as a pesticide in the form of lead arsenate,

Ca_3AsO_4, Paris-Green (copper acetoarsenite), H_3AsO_4, MSMA (monosodium methanearsonate), DSMA (disodium methanearsonate), sodium arsenite, organic arsenical herbicides, and cacodylic acid (Mandal and Suzuki, 2002). These products were used to exterminate insect and plant pests in the soil and its extended use has led to localized soil As concentrations of 10 - 892 mg kg^{-1} (Kabata-Pendias, 2001). The use of arsenic in the form of Roxarsone in poultry feed to control parasites and stimulate the production of eggs in poultry has increased total As concentration by 14 - 76 mg kg^{-1} in poultry litter (Arai et al., 2003). The application of this litter onto soil can thus elevate the As concentrations in the soil. Because As is often associated with mineral deposits, the mining of Pb, Cu, Zn, Co, Ni, and Au often can produce tailings with elevated As concentrations (Paktunc et al., 2003; Paktunc et al., 2004). In some cases, arsenic concentrations have reached ~ 30,000 mg kg^{-1} in soils close to tailing dump sites (O'Neill, 1995). Perhaps the most common yet over looked source of As in the soil is from the extensive use of CCA treated lumber, which can significantly increase As concentrations in soils adjacent to where it is used, where the treatment process took place, or where improperly disposed.

1.1.3.3 General Arsenic Chemistry

Arsenic is a metalloid with atomic number 33 and atomic mass 74.922. It is in the 15th group of the periodic table along with nitrogen, phosphorus, antimony, and bismuth. Arsenic chemically reacts much like phosphorus and antimony in many ways. The electronic structure of ground state As ($[Ar]3d^{10}4s^24p^3$) results in the primary oxidation states of 5 ($[Ar]3d^{10}$), 3 ($[Ar]3d^{10}4s^2$), and -3 ($[Ar]3d^{10}4s^24p^6$), all resulting from the filling of an electron orbital. These oxidative states are referred to as arsenate (As^{5+}),

arsenite (As^{3+}), and arsine (As^{3-}). Arsine is produced in highly reducing conditions resulting in the formation of AsH_3, the most toxic form of As; however, this form of arsenic rarely exists in soils. The most common oxidation states in the soil environment are As^{5+} (oxic conditions) and As^{3+} (anoxic conditions). The ionic radii of these states are 0.034 nm and 0.058 nm, respectively. Thus, in the As^{5+} valence state, As coordinates with 4 counter ions in tetrahedral configuration, and in the As^{3+} valence state As is capable of coordinating with 6 counter ions in octahedral configuration (Sposito, 2008).

Arsenic exists in many chemical states and forms in the environment each of which ultimately dictates its toxicity, mobility, and bioavailability. The processes that govern the chemical form and/or bioavailability of As in soils include adsorption/desorption, dissolution/precipitation, reduction/oxidation, and biological interactions each of which are affected by pH, pE, mineralogy, organic matter content, temperature, and time (Zhang and Selim, 2008). These processes will be discussed in more detail in the following sections.

1.1.3.4 Arsenic Sequestration in Soils

Arsenic adsorption/desorption is a dynamic process that is affected by a variety of factors including, but not limited to, As concentration, As speciation, ionic strength, soil solution composition, pH, and, perhaps most importantly, the inorganic and organic soil constituents. Arsenic adsorption is largely controlled by the metal oxide content (particularly Fe-oxides) of the soil (Elkhatib et al., 1984; Livesey and Huang, 1981; Manning and Goldberg, 1997a; Masscheleyn et al., 1991; Smith et al., 1999; Smith et al., 2002) and to a lesser extent, the clay content (specifically short range order aluminosilicates) (Frost and Griffin, 1977; Goldberg and Glaubig, 1988; Hopp et al.,

2008; Manning and Goldberg, 1996; Wauchope, 1975) as well as, calcite(Goldberg and Glaubig, 1988) and soil organic matter (Elkhatib et al., 1984; Grafe et al., 2001).

The extent of arsenic adsorption to these soil constituents is strongly affected by the pH of the soil solution. The pH governs the surface charge on the soil particles as well as the speciation of As present. At low pH conditions in an oxic soil, the principle As species will be $H_2AsO_4^-$ while as the pH increases deprotenation will occur (pK_2=6.97) and $HAsO_4^{2-}$ will become the principal As component. In an anoxic soil, the principle As species will be $H_3AsO_3^0$. The surface charge of soil minerals are vastly different, however, the point of zero charge (PZC) are generally low for clays (2-5) while higher for metal oxides (5-9.1) (Sparks, 2003). At a pH below the PZC the mineral has a positive surface charge and at a pH above the PZC the mineral has a negative surface charge. This is a principal reason why metal oxides have such an influence on As adsorption, because at most soil pH conditions the metal oxides will have positive charges while the As species are negatively charged or neutral, causing a net attraction. The sorption of As can also be influenced by the presence of competing components in the soil solution. These competing components can effectively reduce the adsorption potential of As on soil sorption sites by taking up sites where arsenic could be held, as well as, desorbing arsenic species. Also, competing ligands can aid in the desorption of arsenic from mineral surfaces. The next sections will cover the general sorption sites of As in the soil, kinetics and extent of adsorption, pH effects on adsorption, soil solution effects on adsorption, and desorption.

1.1.3.5 Sorption Sites in Soil

Metal oxides play a major role in adsorption of arsenic. The most common forms of As adsorption onto metal oxides involve the formation of inner- sphere complexes (Sun and Doner, 1996) and in some cases outer - sphere complexes (Goldberg and Johnston, 2001). There are several types of inner sphere complexes including monodentate, mononuclear bidentate, and binuclear bidentate. Work by Fendorf et. al., (1997) on arsenate sorption to goethite showed that at low As surface coverage the monodentate complex occurs most frequently, whereas, at higher As surface coverage the binuclear bidentate complex occurs (Fendorf et al., 1997). This has become the main model for defining As adsorption on goethite, however, recent work conducted by Loring et al, 2009 has shown that the trait used to evaluate the sorption type (Fe-As distances) is not always indicative of the coordination environment of As and that As may be principally coordinated to goethite in a monodentate complex, the results also suggest that there is no change in coordination environment as effected by pH (Loring et al., 2009). Arsenate was found to form inner sphere complexes on both Fe and Al oxides, while arsenite formed inner sphere complexes on Fe but outer sphere complexes on Al oxides (Goldberg and Johnston, 2001).

Clays are negatively charged, thus, sorption of arsenic is much smaller than with metal oxides however it can still be significant in some soils (Goldberg and Glaubig, 1988). Arsenic is proposed to be sorbed by clays through $AlOH_2^+$ functional groups exposed at clay edges (Manning and Goldberg, 1996). Also, the possibility for $Al(OH)_x$ in interlayers of clays as well as isomorphic substitution of Fe in the crystal structure of clays may provide additional sorption sites (Frost and Griffin, 1977). It is generally

regarded that clay's with higher surface area will exhibit more sorption sites for As (Frost and Griffin, 1977; Lin, 2000). In certain clays the formation of a hydroxyl-arsenate interlayer may also be possible (Lin, 2000). Goldberg, 1988 showed that at pH<9 clay minerals controlled As sorption, however, at pH>9 calcite controlled sorption (Goldberg and Glaubig, 1988).

1.1.3.6 Kinetics and Extent of Adsorption

In soils, a bulk of the As adsorption occurs very quickly (Raven et al., 1998; Smith et al., 1999; Zhang and Selim, 2008). However, there can be an additional phase in which arsenic is adsorbed more slowly related to the difference in sorption sites on mineral surfaces (Zhang and Selim, 2008). For example, on ferrihydrite Raven et al. (1998) found that the adsorption process best fit the condition of a parabolic diffusion equation indicating that arsenic may be diffusion controlled, having an initial high adsorption rate and then a slow rate dictated by diffusion into the mineral structure (Raven et al., 1998). The authors also noted that the adsorption of arsenite was kinetically quicker than the adsorption of arsenate on ferrihydrite (Raven et al., 1998).

The extent of adsorption is governed by the mineralogy present in the system. In general the amorphous Fe and Al oxides have the highest sorption potentials, followed by the Fe oxides and Al oxides (Dixit and Hering, 2003; Goldberg, 1986). Goldberg (2002) determined that sorption curves on kaolinite and montmorillonite are similar to oxides however sorption capacities are much lower (Goldberg, 2002). In natural soils systems the adsorption of As^V was determined to be higher than the adsorption of As^{III} (Manning and Goldberg, 1997a; Smith et al., 1999). Frost and Griffin (1977) determined higher adsorption of As^V than As^{III} occurred on montmorillonite and kaolinite (Frost and Griffin,

1977). Similarly, goethite and amorphous Fe-oxide showed higher sorption of arsenate than arsenite (Bauer and Blodau, 2006; Dixit and Hering, 2003). Ferrihydrite shows the reverse, however, with arsenite sorption occurring to a higher degree than arsenate (Raven et al., 1998).

1.1.3.7 Effects of pH on Adsorption

The adsorption of arsenic in soils has been found to increase with pH (Elkhatib et al., 1984; Goldberg and Glaubig, 1988) however, more recent studies indicate that at low Fe content pH had little effect on As sorption while at high Fe content As sorption was decreased with increasing pH (Smith et al., 1999). The differences in these observations are likely related to the differences in mineralogy between the soils. In pure mineral systems of goethite and amorphous Fe- oxide the sorption of As^V is more favorable at low pH (5-6) and the sorption of As^{III} is more favorable at higher pH (7-8) meaning the reduction of As^V to As^{III} at higher pH values may decrease mobility of As (Dixit and Hering, 2003). The crossover pH, pH in which As^V and As^{III} were adsorbed equally, on both goethite and amorphous Fe-oxide decreased with increasing total arsenic in solution (Dixit and Hering, 2003). This may indicate different preferential sorption sites for As^V and As^{III} because if sites that preferentially adsorb As^V filled this may begin to shift the crossover point towards lower pH values. Overall, the crossover pH was between 6-8.5 depending on solution concentration of arsenate, and arsenate adsorbed on goethite and amorphous Fe-oxides. Through competition with arsenate, phosphate lowered the crossover pH by about 1 at lower concentrations (10 μM - 25 μM) of total arsenic, meaning As^{III} was sorbed preferentially at a wider range of pH's (Dixit and Hering, 2003). Ferrihydrite showed a higher sorption of arsenite than arsenate, except at pH 4.6

with As concentrations < 1 mol kg^{-1} ferrihydrite; both arsenite and arsenate were expected to be present as inner sphere species (Raven et al., 1998). The sorption of arsenate on ferrihydrite decreased with pH, however, the adsorption of arsenite only slightly increased with pH (Raven et al., 1998). This arsenate adsorption process can be attributed to net positive charge on ferrihydrite and negative charge on $H_2AsO_4^{-1}$ at lower pH causing higher adsorption rates, however as the pH is increased the ferrihydrite becomes more negatively charge and the principal arsenate species shifts to $HAsO_4^{-2}$ possibly resulting in a higher net repulsion thus decreasing the sorption of arsenate on ferrihydrite (Raven et al., 1998). Arsenite, which is expected to be in a neutral state, $H_3AsO_3^{0}$ doesn't exhibit this behavior, instead resulting in a slight increase in arsenite adsorption with pH (Raven et al., 1998). Additionally, when arsenate and arsenite are added simultaneously to the system the crossover pH was 7.5 (Raven et al., 1998). Amorphous aluminum oxides, kaolinite, illite and montmorillonite behave very similar to Fe oxides, in which arsenate adsorption decreases with pH and arsenite sorption increases with pH (Goldberg, 1986; Goldberg, 2002). Manning and Goldberg (1997) found that the max adsorption of arsenite on kaolinite, illite, montmorillonite, and amorphous aluminum hydroxide occurred at pH of 7.5-9.5(Manning and Goldberg, 1997b). Frost and Griffin(1977) determined that on montmorillonite and kaolinite As[V] sorption with respect to pH looked very similar to the pH curve for $H_2AsO_4^{-}$ in solution using acid protonation constants and that adsorption of As[III] was increased with pH (Frost and Griffin, 1977).

1.1.3.8 Soil Solution Constituents Effect on Arsenic Adsorption

The most recognized competing anion with arsenic is the phosphate anion. Phosphate greatly decreases As sorption in low Fe soils (< 100 mmol kg^{-1}) but had little effect on soils with high Fe content (> 800 mmol kg^{-1}) (Smith et al., 2002). This occurs because at high iron content there are enough sorption sites to hold both arsenic and phosphate. Also, it may indicate that soils have sites that preferentially adsorb P and As (Smith et al., 2002). With the addition of phosphate to goethite and amorphous iron oxides considerably less As^V and As^{III} was adsorbed and the cross over pH was lowered, indicating As^{III} was adsorbed preferentially at a wider range of pH's (Dixit and Hering, 2003). Manning and Goldberg(1996) found that As^V adsorption was decreased through the competition of phosphate and molybdenate (Manning and Goldberg, 1996). The presence of Ca^{2+} increased arsenate sorption, however had little effect on arsenite adsorption, this process possibly resulted through altering the surface charge, although the presence of Na$^+$ had no effect on As sorption (Smith et al., 2002). Appelo et al. (2002) also found that dissolved Ca enhanced sorption of As, whereas phosphate and carbonate reduced adsorption by competition (Appelo et al., 2002). The presence of Cl$^-$, NO$_3^-$, and SO$_4^{2-}$ has little effect on As^V sorption in soil (Livesey and Huang, 1981).

Soil organic matter can compete with As for sorption sites on hematite, this can cause limited sorption to the Fe surfaces or desorption of adsorbed arsenic (Redman et al., 2002). Natural organic matter also has the capability of changing the redox status of As, generally causing oxidation in the case of As^{III} and also little reduction of As^V to As^{III} (Redman et al., 2002) which has implications for changing adsorption properties and thus effects mobility. Interestingly, natural organic matter, despite its anionic characteristics,

can form complexes with As in solution. It was observed that natural organic matter with higher metal content exhibited greater As sorption, the proposed mechanism of adsorption is through ternary complexation with cationic metals in the natural organic matter structure (Redman et al., 2002). After addition of natural organic matter to the solution a substantial portion of As was desorbed, however, depending on the metal content of the organic matter the desorbed As could exist principally as a free ion or complexed with the organic matter (Redman et al., 2002). Additionally, Bauer and Blodau (2005) determined that dissolved organic matter was able to desorb As from iron oxides, soils, and sediments (Bauer and Blodau, 2006). This process targeted weakly adsorbed As and acted through competition for sorption sites, as well as, complexed with As causing increased mobilization (Bauer and Blodau, 2006). Bauer and Blodau (2009) also found that dissolved organic matter inhibits the formation and growth of Fe oxides and when dissolved organic matter was added to the system dissolved As concentration increased as well as the percentage of As bound to colloids, both causing considerable mobility of arsenic from the system (Bauer and Blodau, 2009).

The presence of humic and fulvic acid decreased As^V adsorption on goethite (α-FeOOH) while citric acid had no effect. However, As^{III} adsorption was inhibited by all three (humic<fulvic <citric acid) (Grafe et al., 2001). The presence of As^V reduced sorption of all three acids on goethite. Because of this it is likely that type, density and functional group behavior on dissolved organic carbon species greatly influence As^{III} and As^V sorption on goethite (Grafe et al., 2001). Phenolic OH and COOH groups on acids compete with As species. In a similar study conducted by Grafe et al. (2002) As^V adsorption on ferrihydrite was decreased in the presence of citric acid but not humic or

16

fulvic acid, opposite that of goethite indicating sorption processes depended on mineralogy. Fulvic and citric acid decreased sorption of As^{III} on ferrihydrite, however, humic acids had little influence (Grafe et al., 2002). The presence of As^V and As^{III} decreased fulvic and citric acid adsorption, while having little effect on humic acid suggesting the adsorption of As species and humic acid are independent of each other (Grafe et al., 2002). The reduction in As^V sorption by citric acid as explained by Geelhoed et al. (1998) is due to the bidentate surface complexes of 2 COO^- and hydrogen bonding of 1 COO^- competing with arsenate(Geelhoed et al., 1998).

1.1.3.9 Desorption

After arsenic is adsorbed onto mineral surfaces it is not easily desorbed (Zhang and Selim, 2008). Through sequential extractions only a small fraction of the arsenic on the soil mineral is exchangeable, even in highly contaminated soils (Keon et al., 2001; La Force et al., 2000; Zhang and Selim, 2008). It is also documented that desorption from Fe oxides (Pigna et al., 2006), Al oxides (Arai et al., 2001; Pigna et al., 2006), and clays (Lin, 2000) decreases over time. In the case of clays this process was speculated to occur as a result of diffusion into the internal pores of clay aggregates (Lin, 2000). As^V was found to be mobilized at high pH in oxic conditions (Smedley and Kinniburgh, 2002) which likely occurs because of the pH dependent properties inherent on the mineral surfaces and arsenic species. Also, As desorption occurs through the reductive dissolution of Fe – oxyhydroxides through the decomposition of organic matter (Nath et al., 2009). Furthermore, as stated above, changes in pH may possibly make the sorption of some species less favorable because competing species such as phosphate and soil organic

matter can desorb arsenic. Perhaps the most pronounced desorption events are caused as a result of reduction/oxidation reactions.

1.1.3.10 Reduction/ Oxidation

Reduction and oxidation reactions of arsenic occur as a result of both abiotic and biotic processes in the soil. These properties have pronounced effects on the solubility and thus the mobility of arsenic in soils. The species present is generally dictated by the Eh condition of the soil. The acid dissociation constants for arsenic acid are $pK_1=2.20$ for $H_2AsO_4^-$, $pK_2=6.97$ for $HAsO_4^{2-}$, and $pK_3=11.53$ for AsO_4^{3-} and for arsenous acid the dissociation constants are $pK_1=9.22$ for $H_2AsO_3^-$, $pK_2=12.13$ for $HAsO_3^{2-}$, and $pK_3=13.4$ for AsO_3^{3-} (Zhang and Selim, 2008). As such, for an oxic (oxidizing conditions) soil with pH from 5-9 the arsenic will be present as $H_2AsO_4^-$ and $HAsO_4^{2-}$ while, in an anoxic (reducing conditions) soil arsenic will be in the form of $H_3AsO_3^0$ (Figure 1.2).
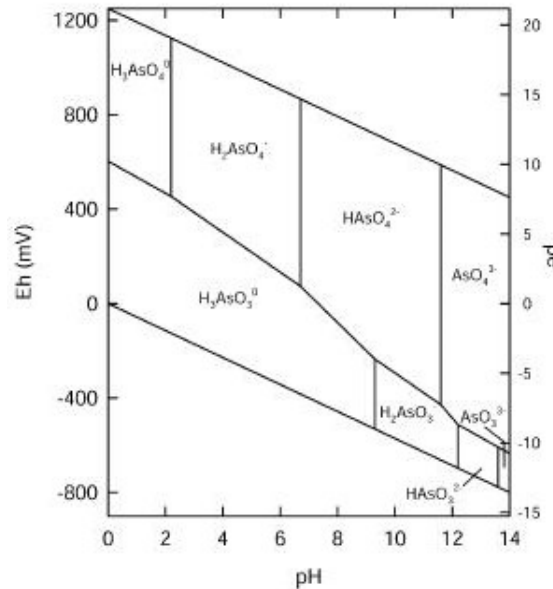
Figure 1.2: Eh vs. pH diagram for arsenic (Smedley and Kinniburgh, 2002).

18

Soil constituents also play an important role in oxidation processes in the soil. The most recognized soil oxidants are manganese (Mn) oxides. Mn oxides effectively oxidize arsenite to arsenate under many soil conditions (Oscarson et al., 1981). Birnessite, a Mn oxide, can oxidize arsenite in solution as well as arsenite adsorbed to Fe- oxides (Sun and Doner, 1998; Tournassat et al., 2002). Fe^{II} can act as a catalyst in the oxidation of arsenite (Bisceglia et al., 2005). The oxidation of arsenite has been reported on kaolinite and illite, however this may be due to Mn oxide contamination of the clays (Manning and Goldberg, 1997b). Lin(2000) observed the oxidation of arsenite on many clay surfaces, however, found no arsenic reduction occurred (Lin, 2000). In addition, as discussed above organic matter has the capability of oxidizing arsenite and in some cases reducing arsenate. However, perhaps more important than the abiotic redox process are biotic redox process in which microbes take an active role in altering arsenic speciation.

1.1.3.11 Microbial Transformations of Arsenic

Generally, microbial transformations of arsenic occur as redox conversions of inorganic forms or conversions between inorganic to organic form through methylation and demethylation. Microbes can obtain energy through the oxidation of arsenic (Paez-Espino et al., 2009). Also, the reduction of arsenic can occur through dissimilatory reduction where microorganisms utilize arsenic as a terminal electron acceptor for anaerobic respiration (Oremland and Stolz, 2005). In addition, microorganisms possess reduction mechanisms that are thought to be linked to detoxification processes. For instance, arsenic reduction occurs through a reductase enzyme (arsC) to facilitate the removal of arsenic from the cell by another enzyme (arsB) (Paez-Espino et al., 2009). The organic forms of arsenic are methylarsine [CH_3AsH_2], dimethylarsine [$(CH_3)_2AsH$],

19

trimethylarsine [[(CH$_3$)$_3$As], methylarsonic acid [CH$_3$AsO(OH)$_2$], dimethylarsinic [(CH$_3$)$_2$AsO(OH)], trimethylarsine oxide [(CH$_{36}$)$_3$AsO], and the tetramethylarsonium ion [(CH$_3$)$_4$As$^+$], (Paez-Espino et al., 2009; Smith et al., 1998). The methylated arsenic species are created primarily through microbial processes (Paez-Espino et al., 2009) and are considered to be in low concentrations, and are often disregarded in the soil system (Zhang and Selim, 2008). However, the alteration of the oxidation of arsenic is not the only process effecting arsenic mobility in the environment, in respect to reduction/ oxidation conditions. The reduction of the soil constituents holding arsenic may also provide mobilization of arsenic in the soil (Oremland and Stolz, 2005). In column experiments using Fe and As reducing bacteria with ferrihydrite coated sand the reduction of As^V to As^{III} was found to be the predominant method of mobilization and that the reduction of Fe^{III} to Fe^{II} actually suppressed the initial mobilization with respect to abiotic controls through the precipitation of secondary Fe minerals (Kocar et al., 2006). A similar study shows initial reduction in As mobilization due to the transformation of Fe phases, however, after the Fe transformation is in equilibrium prolonged release of As^{III} to solution occurs (Tufano and Fendorf, 2008).

1.1.4 Chromium

1.1.4.1 Natural Sources

As for Arsenic, Chromium (Cr) exists in soils as a result of weathering of Cr containing parent materials. The concentrations of Cr in the parent rock varies, with higher Cr content found in mafic (170-200ppm) and ultramafic (1600-3400 ppm) rock and lower concentrations in igneous and sedimentary rocks(5-120 ppm) (Kabata-

Pendias, 2001). The most common Cr mineral is Chromite ($FeCr_2O_4$) which is resistant

to chemical weathering and therefore is the main source of Cr in residual material. Also,

the substitution of Cr^{3+} for Fe^{3+} or Al^{3+} in spinel structures may occur extensively

because of their similar ionic radius and chemical properties (Kabata-Pendias, 2001).

The mean concentration of Cr in the earth's crust is 100- 126 mg kg^{-1} with a mean

average soil concentration of 54 – 70 mg kg^{-1} (Sparks, 2003; Sposito, 2008).   Therefore,

Cr is not enriched in the soil in relation to the earth's crust. The average concentration of

chromium in limestone is 5-16 mg kg^{-1} (Kabata-Pendias, 2001). The soil concentrations

of Cr in the U.S. are generally between 20 mg kg^{-1} and 120 mg kg^{-1} with the mean being

50 mg kg^{-1} (Figure 1.3) (Gustavsson, 2001). The concentrations of Cr in silt or loam

soils are 10-100 mg kg^{-1} in the U.S. (Shacklette and Boerngen, 1984). An investigation of

six Northern Kentucky soils found Cr concentrations in surface soils to be 14.5 mg kg^{-1}

and subsoil concentrations 21.2 mg kg^{-1} (Pils et al., 2004).
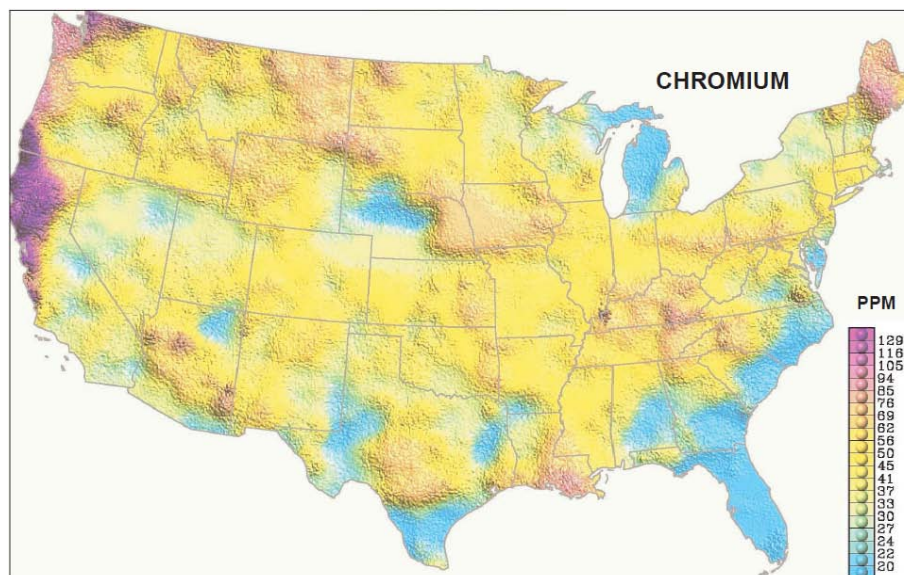
Figure 1.3: Chromium distribution in soils of the United States(Gustavsson, 2001)

1.1.4.2 Anthropogenic Sources

The anthropogenic sources of Cr in the environment stem from the use of Cr in the metallurgy, refractory and chemical industries. In the metallurgy industry Cr is used to create alloys or to plate metals, making them more corrosion resistant. The refractory industry uses chromite to cast metals and the chemical industry uses Cr as a paint pigments (e.g. yellow road markings) or as basic chromium sulfate $(Cr_2(SO_4)_3)$ in leather tanneries. During the conversion of chromite ore to the ferrochromium and metallic chromium used in the aforementioned industries, significant amounts of Cr can be introduced into the surrounding environment. Byproducts from the smelting process (e.g. Cr laden ash) along with atmospheric deposition and simple chemical leaching from raw and processed ore piles represent the most prevalent direct sources of Cr enrichment in soils. For example, Uminska, (1988) found metal concentrations in excess of 10,000 mg kg^{-1} in the proximity of Cr smelter heaps (Uminska, 1988). In addition, because of the ubiquity of Cr containing products produced, a significant amount of Cr is introduced into agricultural soils via the application of municipal sewage sludge, with reported concentrations exceeding 700 mg kg^{-1} (Kabata-Pendias, 2001). As a result the anthropogenic mobilization factor of Cr is 273 , indicating substantial human influence on the Cr cycle (Sposito, 2008).

1.1.4.3 Chromium in the environment

Chromium (Cr) principally exists in the environment in two oxidation states, Cr^{III} and Cr^{VI}, which differ widely in chemical properties resulting in differences in speciation and toxicity. While hexavalent chromium is highly toxic to many organisms, trivalent chromium is required as a trace nutrient, and in mammals controls glucose and lipid

metabolism (Anderson, 1989). At the pH and Eh of most soils chromium exists in the trivalent forms of Cr^{III} cation and CrO_2^- anion, and in the hexavalent forms of $Cr_2O_7^{2-}$ and CrO_4^{2-}. The solubility of Cr^{III} decreases with pH and complete precipitation occurs at pH 5.5. In soils high in pH and phosphorus a significant proportion of Cr forms hydroxides and phosphates rather that organic complexes (Bartlett and Kimble, 1976b). Hexavalent Cr forms occur to a much lesser extent compared to trivalent forms and the addition of Cr^{VI} to soil usually results in complete reduction to Cr^{III} by soil organic matter (Bartlett and Kimble, 1976a). However, if Cr^{VI} does occur to some extent its solubility is low in most soil pH conditions (6-8), thus limiting mobility (Bartlett and Kimble, 1976a). The mobilization of chromium from CCA treated wood to soil is minimal, the reason for which will be discussed in a later section.

1.1.5 Copper

1.1.5.1 Natural Sources

The highest copper concentrations occur in mafic rocks (60-120 mg kg^{-1}) and in the lowest concentration in limestone rocks (2-10 mg $kg^{-1`}$) (Kabata-Pendias, 2001). On average the concentration of Cu in the earth's crust is 25-50 mg kg^{-1} and is 17 – 30 mg kg^{-1} in the soil (Sparks, 2003; Sposito, 2008). In the U.S. the concentration of Cu in the soil range from 7 – 100 mg kg^{-1} in silty or loamy soil types (Shacklette and Boerngen, 1984). In Northern Kentucky the average soil concentration of Cu is 10.7 mg kg^{-1} in the surface soil and 23.1 mg kg^{-1} in the subsurface soil (Pils et al., 2004). Copper is a component in many primary minerals, the most common being sulfides such as chalcocite (Cu_2S), covellite (CuS), and villamaninite (CuS_2). The sulfide minerals are

quite soluble and provide a continuous release of Cu ions to solution where they can then interact with a variety of soil constituents. The solubilized copper strongly interacts with sulfide, carbonate and hydroxide anions in soil solution resulting in the formation of precipitates and surface complexes which greatly reduces Cu mobility in the soil (Kabata-Pendias, 2001).
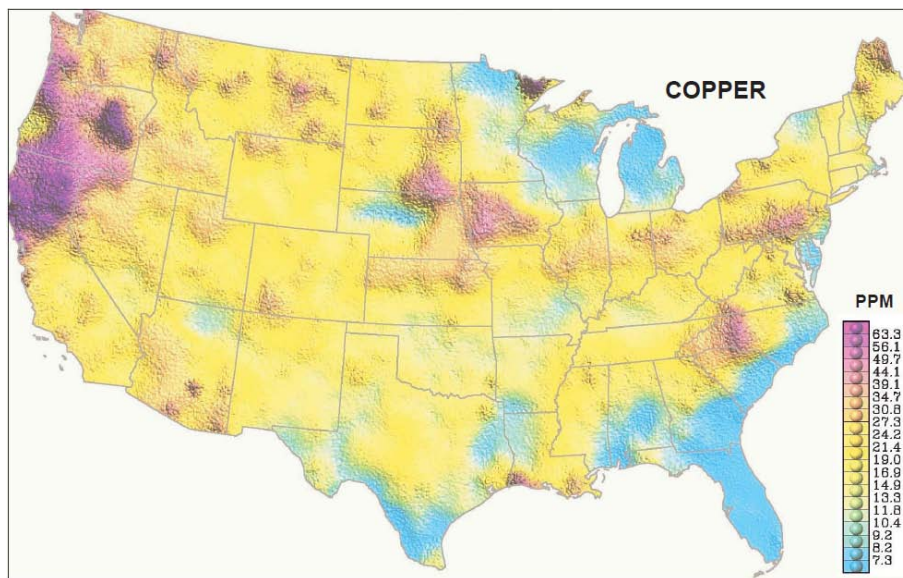
Figure 1.4: Copper distribution in soils of the United States(Gustavsson, 2001)

1.1.5.2 Anthropogenic Sources

Due to the widespread use of copper in many anthropogenic activities, the element can be highly elevated in surface soils. The anthropogenic mobilization factor of copper is 632, meaning human activities are greatly influencing the metal cycling of copper (Sposito, 2008). The anthropogenic sources of Cu in the soil environment are from mining activities, waste emissions, and the application of sewage sludge, fertilizers, and fungicides in agricultural applications (Flemming and Trevors, 1989). In areas of

extensive mining activity, soil Cu concentrations have been found as high as 2,000 mg kg^{-1}, with even higher values (4500 mg kg^{-1}) found in areas adjacent to Cu processing facilities (Barcan and Kovnatsky, 1998; Kabata-Pendias, 2001). As was the case for both As and Cr, the application of sewage sludge to agricultural fields has also led to increased Cu concentrations, with some field soils exceeding 1600 mg kg^{-1} (Kabata-Pendias, 2001). Another activity that has substantially increased soil Cu concentrations is the use of Cu containing fungicides. Perhaps the most recognized Cu containing fungicide is the Bordeaux mixture ($Ca(OH)_2+CuSO_4$) which has been applied to control downy mildew on grapes since the end of the 19th century. This has lead to accumulation of Cu up to 200-500 mg kg^{-1} compared to 5-30 mg kg^{-1} in soils without fungicide addition (Brun et al., 2001; Brun et al., 1998).

1.1.5.3 Copper Chemistry

Copper is a heavy metal with atomic number 29 and atomic mass 63.546. It is in the 11 group of the periodic table along with silver and gold. In its ground state copper's electronic structure is $[Ar]3d^{10}4s^1$. Copper occurs in three oxidation states in the environment; as a solid metal with a charge of zero (Cu^0), as the cuprous ion with a plus one charge Cu^I ($[Ar]3d^{10}$), and as the cupric ion with a plus two charge Cu^{II} ($[Ar]3d^9$). Cu^{II} is a transition Lewis acid, which means it is highly reactive with both hard and soft Lewis bases, while Cu^I is a soft Lewis acid which reacts with soft Lewis bases (Sparks, 2003). Cu^{II} can exhibit an ionic radius of 0.057 nm or 0.073 enabling it to form coordination numbers of 4, a tetrahedral configuration and 6, an octahedral configuration, respectively (Sposito, 2008).

In the environment Cu is partitioned into the aqueous phase, including soluble species and free ions, the solid phase, including sorption to soil constituents and precipitates, and the biological phase, including sorption and incorporation in organic matter (Flemming and Trevors, 1989). Cu^{II} is the most common copper oxidation state in the environment and is classically thought to exist as the free cupric cation $[Cu(H_2O)_6^{2+}]$ in solution, however, recent observation have concluded Cu^{II} can also exhibit fivefold coordination as a result of the Jahn- Teller effect (Pasquarello et al., 2001). The hydrolysis products of $Cu(H_2O)_6^{2+}$ are $CuOH^+$ (pK_1=7.93) and $Cu(OH)_2^0$ (pK_2=8.37) (Paulson and Kester, 1980). It can also be complexed with carbonates forming $CuCO_3$ and $Cu(CO_3)_2^{2-}$ (Sylva, 1976). In the soil, processes that control fixation of Cu include adsorption, precipitation, and biological fixation.

1.1.5.4 Copper Retention Mechanisms

1.1.5.4.1 Adsorption

Copper exhibits strong sorption properties to many mineral surfaces as well as soil organic matter, this makes Cu one of the least mobile of the heavy metals (Kabata-Pendias, 2001). Organic matter controls and dominates the adsorption of Cu in the soil (McBride et al., 1997). This has been demonstrated by many studies, one of the first being a fractionation study in which the authors found that 30% of the Cu was extracted by pyrophosphate, the proportion corresponding to the amount of Cu bound to organic sites (McLaren and Crawford, 1973b). Copper has been shown to adsorb quite strongly to humin in the soil (Sanders and Bloomfield, 1980) and the removal of organic matter reduces Cu adsorption significantly even in cases of high CEC (Elliott et al., 1986). Agbenin and Olojo, (2004) found that the removal of organic matter from the soil

decreased the fraction of adsorbed Cu/soluble Cu nearly 40 times (Agbenin and Olojo, 2004). Organic matter not only controls the adsorption onto the soil solids but also the percent of soluble Cu^{II} as a free cation (McBride et al., 1997). Nearly all copper in the soil solution is complexed with organic substances (McBride and Bouldin, 1984). In general solid organic matter will decrease Cu solubility, whereas, dissolved organic carbon will increase the mobility of Cu through complexation (McBride et al., 1997).

Similarly, Hickey and Kitrick (1984) showed that nearly a third of the copper in soils was complexed with organic matter, while, almost another third was complexed with Fe and Mn oxides (Hickey and Kittrick, 1984). Vega et al. (2007) showed that although organic matter is the main component affecting sorption of Cu, especially at neutral pH, oxides control the adsorption at lower pH (Vega et al., 2007). Fe/Mn oxides controlled Cu distribution with soils low in organic matter (Yu et al., 2004). Through fractionation it was determined that 15 % of Cu was extracted by oxalate, the portion sorbed to free oxides (McLaren and Crawford, 1973b). These studies shows that metal oxides are a significant source controlling Cu distribution, so much so that the removal of amorphous oxides from a soil decreased the fraction of sorbed Cu/ soluble copper 100 times (Agbenin and Olojo, 2004). Although amorphous Fe oxide provide an important sink for Cu they may not lower copper solubility in the soil (Martinez and McBride, 1998).

While Cu sorption is mainly controlled by organic matter and oxides, in calcareous soils Cu sorption has been showed to be enhanced by calcite (Rodriguez-Rubio et al., 2003). Harter (1979) found that Cu sorption was related to the base saturation of the soil and strongly correlated with vermiculite content in the subsurface,

while, organic matter content had little influence on adsorption in surface horizons, contrarily to many other observations (Harter, 1979). In many cases clays have little influence on Cu sorption (Vega et al., 2007). The 1:1 clays such as kaolinite have little affinity for Cu (McBride, 1978a). However, Martinez-Villegas and Martinez (2008) showed that copper sorption was found in the order organic matter> montmorillonite > ferrihydrite (Martinez-Villegas and Martinez, 2008). It was indicated that sequential extraction techniques may be over estimating the % of copper bound to oxides and underestimating the affect clay has on Cu adsorption (Martinez-Villegas and Martinez, 2008). This study was conducted using only leaf compost, montmorillonite, and ferrihydrite. It was noted that dissolved organic carbon was adsorbing onto ferrihydrite and lowering its copper retention and that Fe oxides may not be good competitors for Cu sorption in the presence of dissolved organic matter (Martinez-Villegas and Martinez, 2008). However, dissolved organic matter in the form of humic acid adsorbed on goethite increases copper retention (Tipping et al., 1983). Experimental design may be the cause of the observed discrepancies in these studies.

1.1.5.4.2 Sorption Mechanism/Sites

The specific adsorption of copper were strongest for manganese oxides and organic matter followed by Fe oxides and clay minerals (Mn oxides> organic matter> Fe oxides> clay minerals) (McLaren and Crawford, 1973a). Sorption and fixation of Cu in soils rapidly increases at pH greater than 4 with most adsorption being non exchangeable (Cavallaro and McBride, 1984). Because soluble and exchangeable Cu is generally low in soils it is expected that the primary sorption mechanism is inner-sphere adsorption. The retention of Cu in soils is predicted to be through the specific adsorption of Cu^{2+} and

CuOH$^+$ on most functional groups (Agbenin and Olojo, 2004). Cu is sorbed through Al-OH on aluminum oxides (McBride, 1982) and is specifically adsorbed, possibly through bidentate structures, on allophone and imogolite (Clark and McBride, 1984). The formation of bonds with the direct coordination of Cu and the functional oxygen's of organic substances often occurs, which is often dependent on soil pH (Kabata-Pendias, 2001). Similarly, Cu^{+2} coordinates directly with functional oxygen's of peat, this involves the bonding to 1-2 carboxyl functional groups (Bloom and McBride, 1979). Sorption curves for clays are similar to oxides, however oxides control the fixation of Cu in inorganic soils (Cavallaro and McBride, 1984). For kaolinite, Cu^{2+} showed a higher affinity than Ni^{2+}, Co^{2+}, and Mn^{2+} for binding to silanol and aluminol surface functional groups with sorption conforming to the Langmuir adsorption equation (Yavuz et al., 2003). The adsorption of Cu on illite was due to electrostatic and surface complexation of Cu^{2+}as well as surface complexation of CuOH$^+$. Copper sorption on soils often follows Langmuir or Freundlich isotherms based on Cu concentration, indicating at low concentrations surface complexation was occurring and as concentrations were increased surface precipitation was forming (Vega et al., 2007). Fit of the Freundlich equations was found to depend on pH and CEC, accounting for approximately 80% of the variance (Arias et al., 2005). Through extended x-ray adsorption fine structure (EXAFS) analysis Cu was found to be adsorbed to soil organic matter in a bidentate inner-sphere fashion with carboxyl or amine ligands (Strawn and Baker, 2008). At low ionic strength Cu sorbs in the interlayer's of smectites while preserving its hydration sphere, however, at high ionic strength Cu sorbs to silanol and aluminol functional groups as Cu-Cu dimers (Strawn et al., 2004). At low ionic strength Cu was held weakly and thus exchangeable

as an outer sphere complexed hydrated ion on vermiculite, at high ionic strength Cu took the form of an interlayer dimer (Furnare et al., 2005b).   Copper forms inner or outer sphere complexes with clays, inner sphere adsorption can occur as corner sharing with functional groups or as Cu- dimer adsorbed to interlayers and edges (Furnare et al., 2005a) . Cu bound to ferrihydrite through edge sharing inner-sphere sorption complexes(Scheinost et al., 2001) . For a goethite- humate complex, Cu^{2+} is in a distorted octahedral configuration containing four equatorial oxygen at bond distance of 1.94- 1.97 Å and two axial oxygen at 2.24- 2.32 Å (Alcacio et al., 2001).

1.1.5.4.3 Precipitation

At higher pH surface precipitation, usually of $Cu(OH)_2^0$ or $CuCO_3$, is likely to occur on many soil constituents. On illite increasing pH led to more retention by $CuOH^+$ eventually causing surface precipitation of $Cu(OH)_2$ (Alvarez-Puebla et al., 2005). $CuOH^+$ retention on humic substances rises as pH is increased. At pH 4 Cu begins to precipitate, forming amorphous precipitates, which are the main mode of retention at pH 8 (Alvarez-Puebla et al., 2004a). In a similar study with humin, the same process happened however a botalachite precipitate formed. (Alvarez-Puebla et al., 2004c). In the presence of CO_3 and organic matter, copper possibly precipitated as malachite (Cavallaro and McBride, 1980). Malachite was also found to occur on the surface of dolomitic limestone, while, carbonates promoted Cu hydroxide and carbonate formation in soils (McBride and Bouldin, 1984). Similarly, in calcareous soils precipitation of Cu occurred through retention of Cu by calcium carbonate, forming Cu hydroxide and carbonate precipitates (Ponizovsky et al., 2007; Rodriguez-Rubio et al., 2003).

1.1.5.4.4 pH Effects

In general, the specific sorption of Cu onto soil constituent increases as the pH rises (McLaren and Crawford, 1973b). Sorption and fixation of Cu rapidly increases at a pH greater than 4 with most adsorption being non exchangeable on clays (Cavallaro and McBride, 1984). On allophane and imogolite Cu sorption increases with pH (Clark and McBride, 1984) and the same is true for illite (Alvarez-Puebla et al., 2005). McLaren, 1973 found that the maximum adsorption of Cu occurs at a pH greater than 5 on Fe oxides, Mn oxides, organic matter and clay minerals (McLaren and Crawford, 1973a). Similarly, in soils the maximum Cu sorption has been found at a pH greater than 5.5-6.5 (Agbenin and Olojo, 2004; Elliott et al., 1986). Increasing pH also causes an increase in the complexation of Cu onto humic substances (Sanders and Bloomfield, 1980). Alvarez- Puebla showed that $CuOH^+$ retention on humic substances rises as pH is increased and at pH 4 Cu begins to precipitate (Alvarez-Puebla et al., 2004a). Increasing pH led to higher retention of $CuOH^+$ on illite, eventually causing surface precipitation of $Cu(OH)_2$, much of the sorption was precipitation at pH greater than 6 (Alvarez-Puebla et al., 2005). As adsorption is increased with pH the solubility of Cu in soil solution is decreased, probably due to hydrolysis (Cavallaro and McBride, 1980). McBride and Bouldin (1984) showed that nearly all Cu in solution is complexed to organic matter, however, lowering the pH increased the free Cu in the soil solution (McBride and Bouldin, 1984). Also, the desorption of Cu from humic acid is decreased with increasing pH, however, this is only a small portion of the total Cu adsorbed (Arias et al., 2005).

1.1.5.4.5 Competing species

Cu is strongly retained in soils and competes very well for adsorption sites with other divalent cations/metals and organic matter. Competitive adsorption experiments show that copper is preferentially adsorbed compared to Ni, Zn, and Cd in soils (Echeverria et al., 1998; Elliott et al., 1986). Likewise, copper is the most preferred divalent cation for sorption onto amorphous alumina (McBride, 1978b). Elliot et. al. , (1986) found that the order of adsorption of divalent metals can be determined through the order of increasing pK for the first hydrolysis (Elliott et al., 1986). Lead is the only divalent cation that out competes copper for adsorption sites in soils (Echeverria et al., 1998; Elliott et al., 1986). However, unlike mineral studies, Cu adsorption to humic acid is higher than Pb, Cd, and Zn (Elliott et al., 1986). Similarly, ion adsorption onto brown peat was in the following order Cu>Co>Ni, copper retention was most likely the highest due to Jahn Teller distortion (Alvarez-Puebla et al., 2004b). Copper adsorption onto humified organic matter increases with decreasing ionic strength (Sanders and Bloomfield, 1980).

Desorption of Cu in soil has been shown to occur from competition with humic acid, with the desorption decreasing with increasing pH (Arias et al., 2005). However, overall less than 6% of adsorbed copper was able to be desorbed in 80% of the 27 soils studied (Arias et al., 2005). In general, dissolved organic carbon controls Cu solubility through the formation of dissolved organic carbon-Cu complexes, and by lowering copper retention by competition (Martinez-Villegas and Martinez, 2008). It has been found that dissolved organic carbon sorption can block Cu sorption sites (Ponizovskii et

al., 1999). Also, dissolved organic carbon can increase the solubility of Cu in the soil, increasing mobility (Martinez-Villegas and Martinez, 2008).

1.1.6 Toxicity and Regulation of Arsenic, Chromium, and Copper

1.1.6.1 Toxicity

Arsenic is very toxic to humans and the consumption of food and water with elevated levels of arsenic and contact with the skin are the main modes of entry into the body. The toxicity of arsenic depends on its chemical form with toxic effects decreasing as follows :arsines>As^{III} anion> organic As^{III} > As^V anion (Mandal and Suzuki, 2002). Acute As^{III} toxicity acts through binding to sulfhydryl groups and disrupting enzymatic processes while, As^V acts as a phosphate analog and blocks oxidative phosphorylation (Valko et al., 2005). Chronic toxicity from arsenic exposure is more prevalent than acute toxicity, and is documented to effect many of the major systems of the body (respiratory, pulmonary, cardiovascular, dermal, reproductive, immune, etc.) with possible carcinogenic and mutagenic effects (Mandal and Suzuki, 2002). There are many documented cases of arsenic poisoning throughout the world resulting from the consumption of naturally elevated As in ground water or contaminated foods and beverages, or via direct exposure from industrial sources (Mandal and Suzuki, 2002). Perhaps the most know case of arsenic poisoning is in the Indian subcontinent, including the areas of West Bengal and Bangladesh, in which elevated arsenic concentrations are found in groundwater due to aquifer material enriched in As (Chakraborti et al., 2002; Nickson et al., 1998).

Unlike arsenic, copper and chromium are micronutrients essential for proper human nutrition. Copper serves as a cofactor for many proteins involved in respiration, iron metabolism, and free radical eradication (Valko et al., 2005) . Chromium in the Cr^{VI} oxidation state is toxic, however, as Cr^{III} it is required for the proper functioning of glucose metabolism (Valko et al., 2005). The main mode of toxicity for excess Cu and Cr is through the formation of free radicals which can then modify DNA and calcium and sulfhydryl homeostasis, while also causing oxidative degradation of lipids. Lipid peroxides, formed through the oxidation of lipids, can react with copper and chromium to form carcinogenic malondialdehyde, 4-hydroxynonenal, and DNA adducts (Valko et al., 2005).

Heavy metals in the soil have been shown to decrease the microbial biomass (Giller et al., 1998). High concentrations of heavy metals have also effected the utilization of C substrates, decreasing the rate of mineralization and in some cases increasing the leaf litter on the forest surface (Giller et al., 1998). Soil enriched in heavy metals through application of sewage sludge has also led to a decrease in microbial symbiotic N_2 – fixation (Giller et al., 1998).

1.1.6.2 Governmental Regulation

The United States Environmental Protection Agency (USEPA) maximum contaminant level goal (MCLG) for arsenic in drinking water is currently set to zero, however, this is unenforced and reflects the overall concern for arsenic in the water system. The maximum contaminant level (MCL) for arsenic in drinking water is .01 mg L^{-1} and 0.1 mg L^{-1} for chromium. There is no MCL established for copper because it is required to control the corrosiveness of the water and is regulated by the treatment

technique. The action level set by the treatment technique is 1.3 mg L^{-1} for copper (EPA, 2009). According to the CERCLA, arsenic is the #1 contaminant of concern at superfund sites, while Cr is #77, with hexavalent chromium at #18, and copper is #128. The ranking is based on the amount of sites contaminated, the proximity to the population, and the toxicity of the contaminant (USDHHS, 2007).

1.1.7 Chromated Copper Arsenate (CCA) Treated Lumber as a Metal Source

The tight regulations governing the allowable quantity of arsenic, chromium, and copper release into the environment only goes to demonstrate the realized potential that these elements have to cause human and ecosystem degradation. In order to make informed policy decisions and properly dispose of metal laden wastes, it is essential to assess the relative mobility and bioavailability of the metals. The over arching parameter influencing the mobility and bioavailability of the metal is its' speciation, or chemical form in the soil, which is governed by a host of soil properties such as pH, Eh, organic matter content, mineralogy, etc. Chromated Copper Arsenate (CCA) treated lumber is used quite extensively for the construction of decks, docks and many kilometers of fences (especially here in the central bluegrass). The close contact CCA treated wood has with the soil often results in the release of Cr, Cu and As (again, the amount of release being dictated by a variety of soil properties) which can be used as a consistent metal source to assess which soil properties, or combination of properties, have the greatest influence on the metal(loid) speciation and subsequent bioavailability.

1.1.7.1 The CCA Treatment Process

Pressure treated lumber has been used for decades to help preserve the integrity of wooden structures. This is done by applying a treatment that will resist the attack of pests to the wood. In the case of CCA treated lumber the chemical treatment is CrO_3, CuO, and As_2O_5 applied under pressure. The resistance stems from arsenic acting as an insecticide and copper acting as a fungicide (Warner and Solomon, 1990). There are three types of CCA solutions used each differing in the amount of Cr, Cu and As depending on the final use intended for the wood. The three CCA formulations are **A**- 65.5% CrO_3, 18.1% CuO, 16.4% As_2O_5, **B**- 35.3% CrO_3, 19.6% CuO, 45.1% As_2O_5, and **C**- 47.5% CrO_3, 18.5% CuO, 35% As_2O_5, with type C being the most commonly used (Association, 2005; AWPA, 2005). Above-ground applications require low retention levels, 4.0 and 6.4 kg/m^3. Wood treated to 9.6 kg/m^3 is used for load-bearing structures and retention levels of 12.8 and 40.0 kg/m^3 are used for saltwater applications (Association, 2005; AWPA, 2005). On a mass basis this leaves approximately 1000-5000 mg kg^{-1} of each constituent in the wood depending on type and loading rate (Aceto and Fedele, 1994).

1.1.7.2 Chemistry of Fixation

The chemistry of CCA treated lumber is still not completely understood, however, there is a reduction of hexavalent chromium to trivalent chromium through the oxidation of functional groups on lignin and cellulose (Bull, 2001). The level of unreacted Cr(VI) in wood can give an indication of the extent of fixation and the potential leaching of all constituents (Cooper et al., 1995). There is strong association of Cr with As after fixation, with the main products being $CrAsO_4$ and CrO_4^{2-} complexation with lignin, and Cu^{2+} complexation and precipitation products with lignin (Hingston et al., 2001). The

association between Cr and As was confirmed through x-ray absorption spectroscopy which has shown that all As and half of Cr is fixed as $CrAsO_4 \cdot nH_2O$ (Bull et al., 2000) . It is currently considered that the dominant fixation products are chromium (III) arsenate, chromium (III) hydroxide, and carboxylate- copper(II) complexes (Bull, 2001). Also, Cu was found to not be associated with any other metal after the fixation process(Bull et al., 2000). However, this was in contrast to initial fixation models that report large amounts of Cu(II) arsenates(Dahlgren, 1974; Dahlgren and Hartford, 1972). Another analysis of CCA treated wood has show no differences in XANES and EXAFS spectra through an aging process of 1-4 years, however the Cr:As ratio has been increased from 1.5:1 in fresh wood to 2.2:1 in aged wood (Nico et al., 2004). The ratio of Cr:As dictates As leaching because Cr concentrations control As complexation (i.e. insufficient Cr enhances As leaching) (Henshaw, 1979).Some of the more recent findings indicate that clusters of Cr/As occur through the bridging of a Cr dimer by an As(V) oxyanion within the wood (Nico et al., 2006).

1.1.7.3 Extent of Use

The current quantity of CCA treated lumber sold in the U.S. has not been assessed. However, as of 1999 approximately 75% of the treated wood market was CCA treated lumber (Solo-Gabriele and Townsend, 1999). Also, it was estimated that 1/3 of annual timber production was CCA treated (Townsend and Solo-Gabriele, 2001). The residential use of CCA treated lumber has been phased out as of 2004 (Registar, 2002). With CCA treated lumber consuming 95% of the arsenic commodity pre-2004, this phase out caused a dramatic decrease in the estimated consumption of arsenic in the U.S. (21,600 metric tons in 2003 to 6, 800 metric tons in 2004, the current estimate of arsenic

consumption is 7,200 metric tons) (USGS, 2009). Because of the substantial reduction of arsenic consumption it is estimated that far less CCA treated wood is being used then what studies pre-2004 indicate. However, CCA treated lumber in still used in non-residential sectors and the proper care and disposal of the existing and new CCA treated timber is still a concern. This concern becomes particularly obvious in the case such as Hurricane Katrina, in which it is estimated that 1,740 tons of arsenic contained in CCA treated lumber were left in the debris (USGS, 2009). Proper disposal of this quantity of CCA lumber is essential to limit the leaching of As, Cr, and Cu into the soil or water systems. Because of such large quantities of CCA treated lumber in the soil environment it is essential to address the mobility; speciation and bioavailability of these trace metals in the soil environment both in the surface and often disregarded subsurface soil. Substitutes to CCA treatment lumber include ammoniacal copper quaternary, copper azole, copper citrate, and copper dimethyldithiocarbamate(USGS, 2009).

1.1.7.4 Leaching/Retention studies

It has been determined through various sources that As, Cr, and Cu are leaching into the environment from CCA treated lumber (Cooper, 1991; Khan et al., 2004; Kim et al., 2007; Lebow et al., 2004b; Robinson et al., 2006; Stilwell et al., 2003; Stilwell and Gorny, 1997; Stilwell and Graetz, 2001). The leachable components of CCA treated lumber have been speculated to be individual ions, Cr or Cu arsenates, or organometallic complexes (Lebow, 1996). Khan et al.(2004) detected only inorganic As leachates in both new and weathered CCA treated wood, as opposed to chromium arsenates or organic arsenic complexes (Khan et al., 2004). In new wood the principal leachate was in the form of As^V but in the weathered both As^V and As^{III} were leached (Khan et al., 2004).

The rate of leaching from the wooden structures is different for the metals and decreases in the following order: Cu>As>Cr (Breslin and Adler-Ivanbrook, 1998; Robinson et al., 2006; Stilwell and Gorny, 1997). Also, the rate of leaching increases with acidity (Aceto and Fedele, 1994; Warner and Solomon, 1990).

As reviewed previously, the amount of Cu, As and Cr retention depends on many factors in the soil, most notably, pH, organic matter content and clay content. Chromium concentrations in soil adjacent to CCA treated lumber were found to be related with the pH of the soil solution, arsenic concentration was related with the O.M content of the soil, and Cu concentration was related with both O.M and clay content (Kim et al., 2007). The movement of As extended the farthest vertically, compared to Cr and Cu, indicating it was the most mobile of the three (Kim et al., 2007). Another study showed that Cu and Cr sorption in the soil was increased with increasing organic matter content; however, kaolinite content had little influence on Cr retention, which was low for mineral soils (Balasoiu et al., 2001). Likewise, Cu retention was not influenced by kaolinite content except for soils particularly low in organic matter (Balasoiu et al., 2001). Arsenic behaves differently than both Cu and Cr; it was retained by the soil regardless of the amount of organic matter or kaolinite content (Balasoiu et al., 2001). The adsorption of As was high in both mineral and organic soils; at high levels of organic matter there was formation of As^{III} species (Balasoiu et al., 2001). Partitioning of Cr and Cu is different between mineral and organic soils, in mineral soils Cu and Cr are predominantly in an exchangeable form, however in organic soils exchangeable concentrations are much lower (Balasoiu et al., 2001). An assessment of sandy Florida soils indicates that leaching

had occurred principally within .3 m from posts; however retention by the soil was low because of low organic matter and clay content (Chirenje et al., 2003).

1.2 Research Justification and Objectives

Many studies indicate that Cr, Cu, and As are leaching from CCA treated fence posts. However, limited studies have addressed the resultant speciation of Cr, Cu, and As leachates in soils adjacent to CCA treated fence posts. Previous studies have investigated CCA enriched soils in CCA treated lumber processing plants. These studies have shown that arsenic is principally coordinated as As(V) adsorbed to Fe or proto-imogolite allophone (Hopp et al., 2008), also, Cu may play a large role in the sequestration of arsenic as poorly ordered precipitates along with Fe and Al oxide complexes (Grafe et al., 2008b). To my knowledge, no studies have evaluated the coordination environment of Cu in soils adjacent to CCA fence posts and CCA leachate behavior and speciation has not been assessed in subsurface soil horizons.

Because of this lack of knowledge, the widespread use of CCA treated lumber, especially in the bluegrass region of central Kentucky, and concern for the toxicity of its metal constituents leaching into the soil and water environment, an evaluation of these metals in the Kentucky soil environment needs to be addressed. In addition, CCA treated lumber is composed of relatively the same amount and form of its metal constituents and CCA treated fences transect the landscape. These metal sources can be used to study the soil properties which influence the leaching, concentration, speciation, and bioavailability of As, Cr, and Cu in the soil. Ultimately, this will provide information on the fate of these trace metals in the soil environment.

The specific objectives of the study are (1) to determine the amount and distribution of Cr, Cu and As around CCA treated fence posts along a topohydrosequence; (2) determine the speciation of Cr, Cu and As (and therefore, the potential mobility, and bioavailability) in these soils and (3) determine which soil properties most strongly influenced the observed speciation.

Chapter 2: Speciation and Spatial Distribution of Arsenic from CCA Treated Fences Across a Toposequence

2.0 Introduction

Arsenic speciation and spatial distribution were assessed adjacent to Chromated Copper Arsenate (CCA) treated fence posts along a toposequence. Metal distribution is evaluated on both macroscopic (soil profile contour maps) and microscopic scales (XRF images), speciation of As was conducted using extended x-ray absorption fine structure (EXAFS) and a myriad of basic soil properties probed to determine which soil properties most influence As spatial distribution and speciation. This study indicates As speciation is controlled through aluminum and iron containing soil minerals and that in acidic soils aluminum predominantly controls As speciation, whereas, in neutral soils Fe and aluminum oxides are favored equally for the adsorption of As. Additionally, the mobility of arsenic tends to increase in the higher pH conditions, in which Fe-As interactions are greater.

Arsenic, and other metal(loid)s, are enriched in environmental systems through many processes, for instance, soil and water can be contaminated through coal mining (mountain top removal, mine drainage, disposal of fly ash), land application of biosolids and manure, and through the installation and disposal of Chromated Copper Arsenate (CCA) treated lumber. The acute and chronic exposure of arsenic is well known, having profound reproductive, mutagenetic, and carcinogenic effects (Mandal and Suzuki, 2002), even at low doses (10 to 100 ppb) it is indicative that arsenic significantly compromises the immune system, increasing the risk of influenza (Kozul et al., 2009) and

other ailments. The toxic effect of exposure to arsenic is attributed not only to the total concentration but also it speciation, or chemical form in the environment (Mandal and Suzuki, 2002). The central Bluegrass region of Kentucky is known for its horse industry and the associated kilometers of fences.   These fences, many of which are treated with chromated copper arsenate (CCA) wood preservative transect a wide array of soil series and landscape positions, thus it is possible to use this consistent arsenic source to evaluate which soil properties influence arsenic mobility and speciation.

Chromated copper arsenate (CCA) is a pesticide treatment introduced under pressure in which As acts as an insecticide and Cu a fungicide in order to preserve the integrity of wooden structures exposed to harsh environmental conditions (Warner and Solomon, 1990).   There are three types of CCA treatments each varying in the proportion of Cr, Cu and As, the most common being form C which is comprised of 47.5% CrO_3 , 18.5% CuO, 35% As_2O_5 applied at rates of 4.0 to 40.0 kg/m^3 depending on use (Association, 2005; AWPA, 2005). The fixation of arsenic in the wood is accomplished through the formation of $CrAsO_4$, where Cr forms a complex with lignin or cellulose (Hingston et al., 2001) or through the bridging of a Cr dimer by an As(V) oxyanion (Nico et al., 2006). Arsenic from CCA treated lumber used in wood decking, play structures, fences, etc. has been shown to leach into the surrounding environment (Cooper, 1991; Khan et al., 2004; Kim et al., 2007; Lebow et al., 2004b; Robinson et al., 2006; Stilwell et al., 2003; Stilwell and Gorny, 1997; Stilwell and Graetz, 2001). Khan et al., (2004) using a variety of leaching procedures detected only inorganic As leachates, predominantly in the pentavalent state, in both new and weathered CCA treated wood, with the weathered wood leaching more total As and a higher proportion of As(III)

compared to the new wood. This manuscript will address how these leachates interact with soils of varying physicochemical properties by determining the speciation of As in soils adjacent to CCA treated fence posts along a toposequence.

The specific objectives of the study are (1) to determine the amount and distribution of As around CCA treated fence posts along a topohydrosequence; (2) determine the speciation of As (and therefore, the potential mobility, and bioavailability) in these soils and (3) determine which soil properties most strongly influenced the observed speciation.

2.1 Materials and Methods

2.1.1 Soil Sample Collection, Description and Preparation

The field site is located in the Inner Bluegrass region of Kentucky on the University of Kentucky Spindletop Research farm. Sampling was conducted along a Chromated-Copper-Arsenate (CCA) treated fenceline which had been in place for ~20 years surrounding a mixed grass pasture. The fence line was chosen because it transects a Bluegrass-Maury silt loam (fine, mixed, semiactive, mesic Typic Paleudalfs), a Donerail silt loam (fine, mixed, active, mesic Oxyaquic Argiudolls), and a Newark silt loam (fine-silty, mixed, active, nonacid, mesic Fluventic Endoaquepts), each having different pH, drainage class and slope. Additional information regarding the site location and soil series specification can be found in Appendix 1.Soil pits were dug by backhoe to a depth of ~1m alongside a fence post at the hill top (HT), a midslope (MS), and a toeslope (TS) position corresponding to the Maury, Donerail, and Newark silt loam soils respectively. A grid pattern was established on the face of the pit containing the fence post from which

about 60 soils samples were collected into Whirl-Pak® (Nasco, Fort Atkinson, Wisconsin) bags and stored on ice (See Appendix 2 for sampling plan schematic). Upon returning to the lab, soils were sieved past 2 mm, placed in new whirl-pack® bags and stored at 4°C until analysis. Additionally, to assess trends along the toposequence soil samples were collect every 8 posts (~20m) from the HT position to the TS position at distances 0-5 cm and 10-15 cm away and depths 0-15 cm and 15-30 cm (See Appendix 10 for additional details).

To establish the influence that changes in redox status may be having on metal mobility, soil samples were collected at the HT, MS, and TS positions after a spring rainfall event using a 30 cm soil probe with a 3 cm diameter. At the time of sampling the groundwater was within 45 cm of the soil surface in the toe slope position. Samples were pulled at a depth of 60-90 cm and again at a depth of 90-120 cm, placed into sterilized Whirl-Paks ® (Nasco, Fort Atkinson, Wisconsin), flash froze under liquid nitrogen and transferred to a glove box filled with an Ar atmosphere for analysis.

2.1.2 Soil chemical properties

In preparation for analysis, sieved soils were dried at 60° C. Soil pH was determined by a glass electrode in a 1:1 soil/water ratio which was stirred manually and allowed to set for $\geq$15 min. Mehlich III -P, K, Ca, Mg, Zn, Cd, Cr, Ni, Pb, Cu, and Mo (Meh-P, Meh-K, etc.) were determined by inductively couples plasma mass spectroscopy (ICP-MS) after 2 cm^3 soil mixed with 20 ml of Mehlich III solution (0.2 N acetic acid, 0.25 N NH_4NO_3, 0.015 N NH_4F, 0.013 N HNO_3, and 0.001 N EDTA), shaken for 5 min. and filtered through Whatman #2 filter paper(Mehlich, 1984). Soil carbon and nitrogen

determined by dry combustion with 0.5 g soil. Cation exchange capacity (CEC) and base saturation determined with 10 g soil by saturation with 1 N ammonium acetate. Soil texture was determined by the micropipette method. Analysis, with the exception of pH, was performed by the University of Kentucky's Division of Regulatory Services.

2.1.3 Redox Characterization through Iron Analysis

Total Fe and Fe(II) were determined in a water extracts and ammonium oxalate extracts, the Fe(II) was assessed by a ferrozine based method(Phillips and Lovley, 1987; Stookey, 1970). For the water extract, one-hundred milliliters of a 100 g anoxic air dried soil L^{-1} deoxygenated water suspension was shaken for 90 minutes and an aliquot was passed through a 0.22 μm filter to obtain 2 ml of filtrate. The filtrate was combined with 1 ml pH 6 MES buffer (0.1M) and 0.3 ml ferrozine (0.01 M). For the ammonium oxalate method a 0.5 ml aliquot of the soil suspension (100 g soil L^{-1} deoxygenated water) was combined with a 1.5 ml of anoxic acid ammonium oxalate (0.2 M at pH 3), shaken in the dark for 24 hrs., passed through a 0.22 μm filter and combined with 1 ml pH 6 MES buffer (0.1M) and 0.3 ml ferrozine (.01 M). The presence of Fe(II) will cause the colorless ferrozine mixture to change to a magenta color which was measure through absorbance at 562 nm on a Shimatzu UV-3101PC UV-VIS-NIR Scanning Spectrophotometer. The total Fe concentration was determined using a Shimatzu Flame Atomic Adsorption Spectroscopy (FAAS).

2.1.4 Total Metal Determination

Total metal content of the soil samples was determined using a modification of EPA method 3052. Briefly, 9 ml of nitric acid and 5 ml hydrofluoric acid were added to 250 mg of dry soil in Teflon pressurized/sealed vessels and rapidly digested in a 1600W MARS (CEM, Matthews, North Carolina) microwave digestion unit. Samples were brought up to 180° C and kept at this temperature for 10 min., after which they were allowed to cool, transferred to 50mL falcon tubes, and brought up to final volume of 50 mL using ultrapure water. Samples were then analyzed on an Agilent 7500 series (Santa Clara, Ca) Inductively Coupled Plasma- Mass Spectrometer (ICP-MS). All reagents used were ultra-pure trace-metal grade.

2.1.5 Metal Speciation via Synchrotron X-ray Absorption Fine Structure Spectroscopy (XAFS)

2.1.5.1 Sample Preparation and Data Collection

Data collection was performed at beamline 13-BM-D [Advanced Photon Source (APS), Argonne National Laboratory, Argonne, IL] and beamline 10.3.2 [Advanced Light Source (ALS), Lawrence Berkeley National Laboratories, Berkeley, CA](Marcus et al., 2004). μ-X-ray Absorption Fine Structure Spectroscopy (μ–XAFS) and μ-Synchrotron X-ray Fluorescence (μ–SXRF) mapping data were collected on beam lines 13-BM-D at APS and 10.3.2 at ALS, while, bulk XAFS data was collected at beamline 13-BM-D at APS. Soil samples were dried at 60° C for 24 hrs and ground with an agate mortar and pedestal. Samples for bulk X-ray analysis were retained in a 20 mm by 5 mm by 3mm hole between two pieces of non-adhesive Kapton film in an acrylic sample holder. For μSXRF and μXAFS data collection an even layer of soil was adhered to

Kapton film using a thin layer of silicone based vacuum grease. Samples were mounted at 45° to the incident beam and data collected in fluorescence mode by a 16- element and 7- element Ge detector at beamlines 13-BM-D and 10.3.2, respectively.

At beamline 13-BM-D, μ–SXRF mapping was conducted over an area of 1 mm^2 at 14 keV using a beam size of 10 μm by 20 μm with 20 μm steps, and a 2 s dwell time while, μSXRF mapping conducted at beamline 10.3.2 was over an area of 1 mm^2 at 13 keV using a beam size of 6 μm by 6 μm using a continuously scanning stage with 6 μm steps. Multiple (≥5) extended X -ray absorption fine structure spectra (EXAFS) were collected in fluorescence mode from 150 below to 650 above the As K-edge (11.867 keV), from each area of interest (AOI) found in the μ–SXRF maps. The beam size was set to 6 mm by 0.9mm for all bulk EXAFS data collected. For μ–SXRF mapping and μ–EXAFS spectra collection a beam size of 10 μm by 20 μm was used at 13-BM-D while, a beam size of 4 μm by 3 μm was used at beam line 10.3.2.

2.1.5.2 Data Analysis

All data reduction was performed using WinXAS 2.1 (Ressler, 1997). Individual spectra were calibrated for shifts in edge energy using the 2nd derivative of the adsorption edge and setting the edge energy equal to 11.874 keV. Then, spectra were background corrected using two polynomials ,the pre-edge and post-edge region were estimated through first order polynomials, however, under some circumstances a second order polynomial provided a better estimate for the post-edge region background correction, the spectra were then normalized. After normalization, multiple scans per AOI were averaged and converted from energy (keV) to photo-electron wave unit's (k (Å^{-1})) by

setting the edge energy origin at 11.874 keV. A single atomic spectra with the absence of back scattering was estimated using a cubic-spline function of 7 knots over an average k space of 2.0 to 13.5 Å^{-1} and subtracted from the spectra to obtain raw $\chi(k)$ data. The $\chi(k)$ was weighted by a factor of k^3 to amplify oscillations at higher k values. Fourier transformation of the $\chi(k)k^3$ was performed over the k ranges of 2.5 – 12.75 Å^{-1} to obtain radial structure functions using a Bessel window with a smoothing parameter of 4.

Traditional fitting procedures are not well suited for multicomponent systems such as soil. Therefore, in order to illicit the species present in the soil a statistical procedure using principal component analysis (PCA) was conducted. The PCA analysis was conducted over a k range of 2.0 to 10 Å^{-1} of the $\chi(k)k^3$. The PCA analysis works by taking the original set of spectra and reducing it to a smaller number of principle components. The number of principal components that can statistically account for a majority of the data is selected based upon the minimization of the indicator value (Malinowski, 1977). A target transformation of standards is conducted with the set of principal components selected that statistically account for a majority of the data. The target transformation consists of removing from the standard spectrum that which cannot be accounted for by the principal components. The standards used were Adamite [$Zn_2(AsO_4)OH$], Allactite [$Mn_7(AsO_4)_2(OH)_8$] , Chalcophyllite [$Cu_9Al(AsO_4)_2(SO_4)_{1.5}(OH)_{12} \cdot 18H_2O$], Ojuelaite [$ZnFe_2^{3+}(AsO4)_2(OH)_2 \cdot 4H_2O$] , Olivenite [$Cu_2(AsO_4)OH$], Scorodite [$FeAsO_4 \cdot 2H_2O$], Mansfieldite [$AlAsO_4 \cdot 2H_2O$] (determined to be an amorphous phase through XRD), As(V) Birnessite, As(V)-Gibbsite, As(V)-Goethite, As(V)Zn(II) Birnessite, As(V)Zn(II)-Gibbsite, As(V)Zn(II)-Goethite, As(V)Zn(II)-Silica Oxide, and Liquid As(V). Additional details on the standards used

can be found in (Grafe et al., 2008a; Grafe et al., 2008b). The less that needs to be

removed from the standard; the more likely the standard is a component in the sample. To

assess the extent of fit a SPOIL value is given to each reference spectra. SPOIL values

<1.5 are considered excellent fit, 1.5-3 good fit, 3-4.5 fair, 4.5-6 poor, and >6

unacceptable (Manceau et al., 2002). After the determination of the standard spectra

present, a linear least squares fitting is used to determine the amount of each standard

spectra within each sample spectra.

2.2 Results

2.2.1 Total Metal Concentration and Spatial Distribution

Geostatistical constructions of contour maps showing the spatial distribution of

total arsenic around the fence posts indicate significant leaching of As adjacent to the

hilltop (HT) and midslope (MS) post, (Figure 2.1). The maximum concentrations of

arsenic (HT: 755 ppm, MS: 685 ppm, and TS: 133 ppm) are located directly adjacent to

the post and fan out toward the surface soil, showing elevated concentrations (75 – 100

ppm) up to 30 – 35 cm from the post. At depth the increased concentrations of arsenic

are confined to the 0-10 cm region adjacent to the CCA post, otherwise arsenic

concentrations approach background. For the hilltop and toeslope positions the highest

arsenic concentrations are located in the 0-15 cm depth directly adjacent to the post and

concentrations decrease with depth. This is not the case for the midslope sampling

position where the highest arsenic concentrations (400-600 ppm) are located at depths of

15- 80 cm in soil adjacent to the post. Although the maximum concentrations of arsenic

are similar at hill top and midslope position,(~755 ppm and ~685 ppm, respectively), the

midslope positions shows a higher total mass of arsenic throughout all depths, with the 60-90 cm depth in the   HT having 0.046 g As/cm depth compared to the MS which has 0.148 g As/cm depth showing the greatest differences (Figure 2.1/Table 2.1) calculations exhibited in Appendix 6**.**   The total sum of arsenic released and remaining in the surrounding soils is estimated to be 21.46 g, 29.27 g, and 4.36 g for the HT, MS, and TS landscape positions, respectively (Appendix 6). The toeslope position has, on average, arsenic concentrations that are much lower than the HT and MS positions, however, the overall spatial distribution is similar. The distribution of copper is similar to that of arsenic, where increased concentrations were observed in the topsoil and emanating farther from the post, whereas, in the subsoil elevated concentrations generally remain close to the post. (A more detailed discussion of the copper and chromium data appears in Chapter 3).

Average As concentration in surface soils along the toposequence exhibits similar if not slightly increasing concentrations of As while moving down the topographic gradient (Figure 2.2). The TS landscape position concentrations are much lower than any of the other soils analyzed. Additionally, the ratio of the directly adjacent to the post (0 – 5cm) to the 10-15 cm away from the post As concentrations indicate that As is enriched to a higher degree away from the post in samples while moving down the topographic gradient (Figure 2.2).
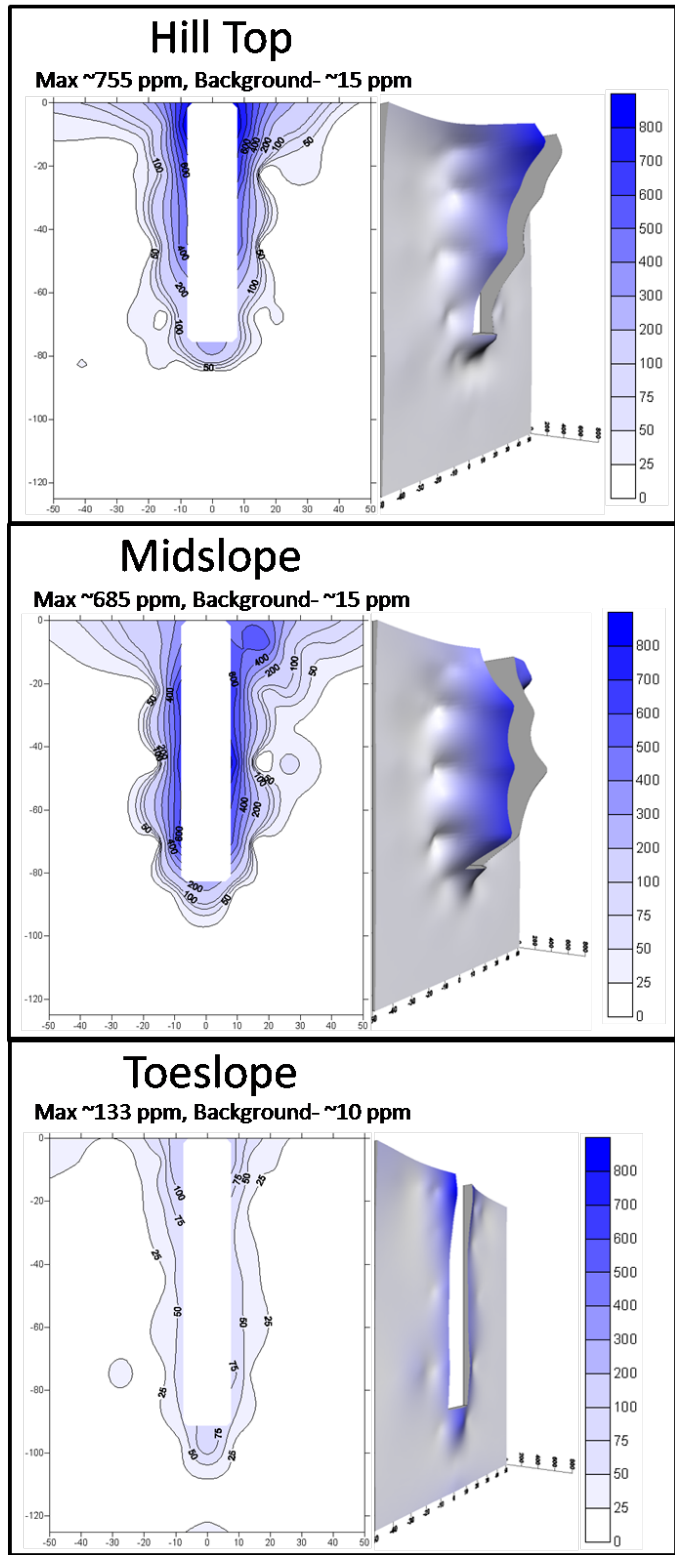
Figure 2. 1: Soil profile contour map of Arsenic concentrations (ppm) in soils along the toposequence. The blanked section indicates regions where the post enters the soil.

Table 2.1: Total mass and normalized enrichment factor (NEF) of arsenic. Detailed explanation of the calculations is provided in the Appendix 6.

	Depth	Mass per unit depth (g/cm)	Normalized Enrichment Factor (NEF)
Hilltop			
	0 to 15 cm	0.662	15
	15 to 30 cm	0.268	8
	30 to 60 cm	0.200	6
	60 to 90cm	0.046	2
	90 to 105 cm	0.009	2
	Total g (0-105cm)	21.463	
Midslope			
	0 to 15 cm	0.771	16
	15 to 30 cm	0.347	10
	30 to 60 cm	0.268	10
	60 to 90cm	0.148	6
	90 to 110 cm	0.003	2
	Total g (0-105cm)	29.269	
Toeslope			
	0 to 15 cm	0.100	4
	15 to 30 cm	0.049	2
	30 to 60 cm	0.030	2
	60 to 90cm	0.033	2
	90 to 120 cm	0.017	2
	Total g (0-105cm)	4.363	
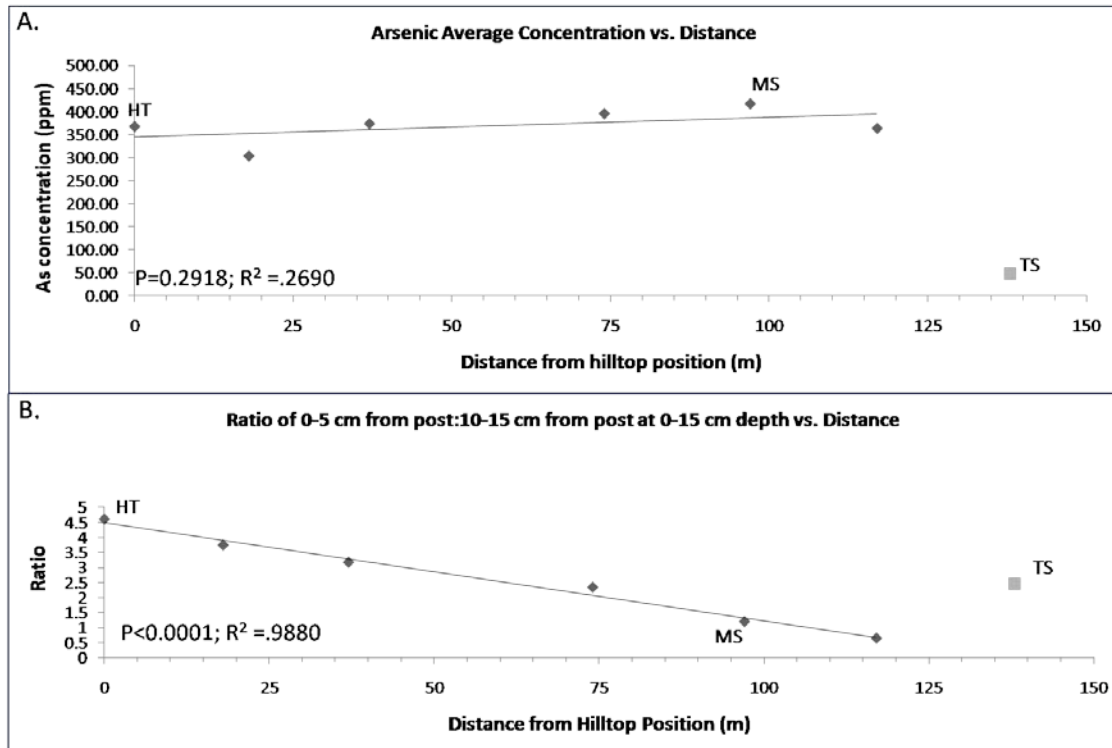
Figure 2. 2: Concentration and mobilization of arsenic across the topographic gradient. A.)Average arsenic concentration of samples collected along the toposequence and B.) ratio of 0-5 cm from post: 10-15 cm from post at 0-15 cm depth along the toposequence. Hilltop (HT), Midslope (MS), Toeslope (TS). See Appendix 10 for additional details.

2.2.2 Basic Soil Properties

Basic soil properties are exhibited in Table 2.2, principally; the soil texture class observed is a silt loam throughout the three soil series/landscape positions with the exception of the HT 30-90 cm and MS 60-90 depths where an accumulation of clay has resulted in a silty clay loam textural class. Cation exchange capacity (CEC) is similar between the HT and MS locations and somewhat increased at the TS position with all samples being within 14.4 – 21.2 meq/100 g soil. Higher CEC values are accounted for through increased soil organic matter (SOM) content and/or clay content. The soil

organic matter (SOM) content is similar between the three landscape positions, reducing with increasing depth in the soil profiles, however, at the TS position the SOM content increases from 1.0 % at the 30-60 cm depth to 2.1 % at the 60-90 cm depth.

The three soil series/landscape positions follow a similar trend of increasing pH units with depth up to about 60 cm beyond which the pH stays relatively consistent or slightly decreases. Although pH vs. depth relationships are similar between landscape positions the overall pH increases moving down the landscape (HT pH<MS pH<TS pH), with the HT and MS positions having strongly to moderately acidic conditions (HT: 5.2 – 6.0 pH and MS: 5.7– 6.4 pH), whereas, the TS position is near neutral (6.8- 7. 4 pH). The base saturation (BS) of the cation exchange sites shows the same trends as the pH. The BS is between 38 – 58.4 %, 52.7 – 70.9 %, and 69.2- 81.1 % at the HT, MS, and TS positions, respectively, increasing from the HT to the TS position. Additionally, sharp drops in pH and base saturation are realized in soils adjacent to the post compared to similar depth background samples.

The background concentrations of Mehlich III extractable phosphorus (Meh-P) are higher in the TS position than in the MS and HT positions. For example, at the 0-15 cm soil depth HT, MS, and TS positions have 77, 70, 111 mg/dm^3 of Meh-P respectively, at depth this effect is even more pronounced as the HT, MS, and TS positions have 55, 75, and 134 mg/dm^3 of Meh-P respectively (Table 2.2). Although, background meh-P concentrations are higher at the TS position in soils adjacent to the post Meh-P is increased with respect to background in both the HT and MS positions; the alternative being true for Meh-Ca adjacent to the post in that Meh-Ca is reduced with respect to background. At the TS position the concentrations of Meh-Ca are 39% - 132% higher

(2012 - 3056 mg/dm^3), compared to the corresponding depths at the HT and MS positions. The exception to this is the 30- 60 cm depth were all Meh-Ca concentrations are within 15% of each other. The increasing pH, base saturation, and % Ca while moving down the topographic sequence are all consistent with general soil properties as influenced by landscape position (Brubaker et al., 1993; Seibert et al., 2007). All landscape positions are rich in Al and Fe total metal concentrations (Appendix 4).

Table 2.2: Basic Soil Properties*

Depth	Soil Texture Class	Silt %	Clay %	SOM % B	SOM % A	pH B	pH A	CEC (meq/100g) B	CEC (meq/100g) A	Base Saturation % B	Base Saturation % A	MehP B	MehP A	MehCa B	MehCa A
Hilltop															
0 to 15	Silt Loam	71	15	4.11	3.47	5.2	4.4	19.6	16.9	38.0	18.3	77	155	1173	475
15 to 30	Silt Loam	71	18	1.77	1.91	5.9	5.1	14.6	15.1	54.8	39.9	31	87	1443	1090
30 to 60	Silty Clay Loam	60	29	0.88	1.07	6.0	5.7	15.7	16.3	58.4	54.5	36	76	1729	1584
60 to 90	Silty Clay Loam	48	36	0.40	0.40	5.5	5.4	18.2	19.6	49.0	47.7	55	60	1591	1691
BP: 75 to 80 cm	Silty Clay Loam	50	34	0.86		5.6		19.6		51.1		72		1804	
Midslope															
0 to 15	Silt Loam	75	14	3.46	3.82	5.7	5.1	16.9	16.9	52.7	27.3	70	118	1311	559
15 to 30	Silt Loam	76	16	2.20	2.51	6.1	5.2	15.6	15.6	57.2	38.6	36	90	1604	900
30 to 60	Silt Loam	65	26	1.03	1.31	6.4	6.0	14.4	15.0	70.9	60.7	44	70	1887	1598
60 to 90	Silty Clay Loam	53	31	0.57	0.58	6.3	6.2	17.6	18.3	67.8	64.0	75	97	2195	2116
BP: 80 to 90 cm	Silty Clay Loam	52	34	0.76		6.3		18.3		68.6		91		2208	
Toeslope															
0 to 15	Silt Loam	78	12	4.09	6.55	6.8	6.6	21.2	22.3	74.2	75.1	111	91	2725	2456
15 to 30	Silt Loam	81	13	3.04	3.11	7.1	7.1	21.1	19.8	69.2	71.1	55	56	2737	2712
30 to 60	Silt Loam	79	16	1.03	1.15	7.4	7.1	14.4	12.8	75.1	79.8	77	61	2012	1997
60 to 90	Silt Loam	65	24	2.13	2.18	7.3	7.1	21.1	20.3	81.1	81.4	134	130	3056	3127
BP: 90-105	Silt Loam	56	27	2.15	2.61	7.3	7.1	25.6	23.7	84.4	77.2	159	148	3979	3283

* Below Post (BP), B indicates Background samples, A indicates soil adjacent to CCA post (0-5 cm)

2.2.3 Iron Characterization

There were no statistical differences in the total ammonium oxalate extractable iron (AO-Fe) between the landscape positions, however, when taking into account the total metal digest iron (T-Fe) the proportion of AO-Fe/T-Fe is higher at the TS position than the HT position with the MS position being at an intermediate level. A similar trend is observed with the total ammonium oxalate extractable Fe(II) (AO-Fe(II)), in that the proportion of AO-Fe(II)/T-Fe is larger in the TS position than in the MS and HT positions. Regardless, the significant amount of AO-Fe indicates the presence of amorphous iron oxides. Water extractable Fe (W-Fe) and water extractable Fe(II) (W-Fe(II)) where significantly higher at the TS position than the MS and HT position at 60 – 90 cm, and the TS position was statistically higher in W-Fe and W-Fe(II) than the HT at 90 -120 cm depth.

Table 2.3: Iron Analyses of Soil after Rain Event [a]

Location	Depth	Total Metal Digest		Ammonium Oxalate Extractable				Water Extractable			
	cm	Fe		Fe		Fe(II)		Fe		Fe(II)	
		Mean	St.Dev.	Mean	St.Dev	Mean	St.Dev	Mean	St.Dev.	Mean	St.Dev.
Hilltop											
	60-90	48836	6207	9623	2992	193.83	45.66	–	–	0.12	0.04
	90-120	57794	2910	10474	3996	330.27	103.11	0.518	0.168	0.14	0.18
Midslope											
	60-90	37880	4787	13113	1694	147.70	6.83	1.69	1.09	0.54	0.18
	90-120	45941	4837	13309	1321	318.91	119.62	1.30	0.75	1.18	0.68
Toeslope											
	60-90	21490	3242	9232	780	177.62	11.15	16.29	2.83	1.40	0.25
	90-120	30960	4781	8315	761	234.29	50.05	21.76	2.72	1.58	0.19

Units: mg kg^{-1}

[a] n=10 for total metal digest, else n=3

2.2.4 As Speciation via μ-SXRF

The spatial distribution of elements within soil samples was probed using synchrotron x-ray fluorescence mapping (SXRF) which allows for the determination of correlations between multiple elements. Multiple X-ray fluorescence maps were collected for the surface soil samples (0-15 cm) directly next to (0-5 cm) the HT,MS and TS fence posts which were determined to have total As concentrations of 758, 496, and 132 mg kg^{-1}, respectively. Multiple maps were also collected from subsoil samples directly beneath the HT, MS and TS posts each containing 268, 204, and 94 mg kg^{-1} of As, respectively. Micro-XAFS spectra were collected at areas of interest (AOI) within the μ-SXRF maps to facilitate the determination of As species present. Figure 2.3, is a map from the hilltop surface soil, the separate images showing the fluorescence signals for As, Cr, Cu, Fe, Zn, and Mn, the warmer colors, with white being highest and indicating regions of elevated counts while the cooler colors(black being lowest), indicating regions of low/no counts. As-metal associations were confirmed by the similarities in fluorescence maps, for instance, in Figure 2.3 fluorescence map of As and fluorescence map of Fe, look similar. The fluorescence signals for Fe and Mn, not only show correlation with As, but also indicate the structure of soil particles, often indicating discrete Fe and/or Mn containing particles. As can be seen from the map and multiple channel analysis (MCA) in Figure 2.3, spot 1 contains the highest counts of arsenic and corresponds to an area that is concentrated in Fe, Mn and Al, as well as, Cu, Zn, and Cr. Spot 2 and 3 are different showing high As counts colocalized with Fe and Al. In general, regions of high As counts correlate better with Fe than the other metals analyzed, as assessed with Pearson correlation coefficients on the maps (data not shown). Unfortunately, As-Al correlations

cannot be exhibited with this technique because Al is a component in many soil minerals, however, the MCA exhibits that Al is located at these AOI. Arsenic concentrations are more diffuse in surface soils SXRF maps whereas, subsurface SXRF maps indicate more discreet regions of elevated As (Appendix 5).

Only qualitative data of As speciation can be address via SXRF mapping techniques. To illicit quantitative data on the bonding environment of As a μ-XAFS analysis was conducted over many discreet spots on multiple maps in order to probe and characterize the As species present. The predominant species present was As(V) based on the edge energy of the bulk spectra at ~11.874 keV (Figure A7.1). The arrows with numbers on the XRF maps correspond to locations in which μ-XAFS spectra were taken. In total 6 bulk XAFS (Figure A7.1-2) and 20 μ-XAFS spectra (Figure A7.3-4) were taken from the Maury, Newark, and Donerail Silt Loam soils. Overall, surface and subsurface soils were examined in the three soil series.
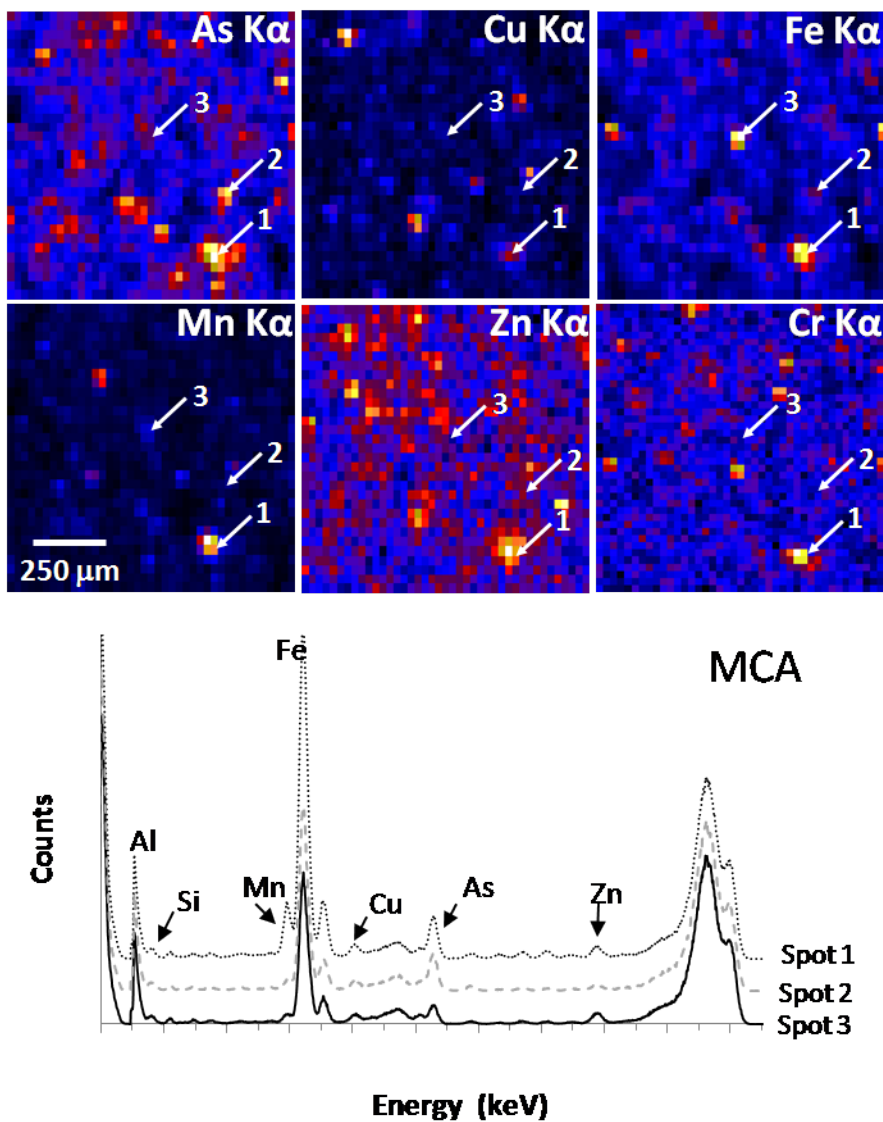
Figure 2.1: Hilltop surface soil µSXRF maps of As, Cu, Fe, Mn, Zn, and Cr localization. Warmer colors correspond to regions of elevated metal concentrations. Multiple Channel Analysis (MCA) indicating element counts at various areas of interest (AOI). Arrows are spots in which MCA and µ -EXAFS spectra were taken.

2.2.5 Principal Component Analysis and Linear Least Squares Fitting of μ and bulk XAFS

The principal component analysis (PCA) procedure was performed over the combination of all μ-EXAFS and bulk EXAFS spectra, as well as, with sets of these spectra with the noisiest spectra successively removed. In all cases the PCA analysis shows a minimum in Malinowski Indicator value (IND) at 3-4 components (Figure A8.1), indicating the data set is best represented with 3-4 unique components, the removal of the noisiest spectra cleans up the principal component set (Figure A8.2). The species that most statistically constitute the unknown spectra as determined through target transformation (TT) analysis through the calculation of a SPOIL value consist of As(V)Zn(II)-Goethite (SPOIL~0.92), Mansfieldite ($AlAsO_4 \cdot H_2O$) (SPOIL ~0.73) , As(V)-Gibbsite (SPOIL ~.83), the addition of a 4th component is As(V)-Goethite or As(V)Zn(II)-Gibbsite. Overall, the principal component analysis highlights the importance of iron and aluminum complexes in controlling arsenic speciation in the soils observed. The principal component analysis indicates the spectral set is principally made up of As(V) adsorbed and/or As(V) Zn(II) coprecipitated on iron and aluminum minerals.

With the principal components indicated above linear least squares fitting was used to determine the percent of each constituent in all μ– and bulk- EXAFS spectra (Table 2.4). Micro-EXAFS spectra were averaged at each soil location, the percent gibbsite and percent Mansfieldite species do not exhibit a correlation between the average μ– and bulk-EXAFS spectra possibly due to the similarity between these Al-As spectra. In some cases the species identified via LLSF of the μ -EXAFS spectra tend to over or

underestimate the bulk- EXAFS spectra, likely due to the selection of the spots in which

μ–EXAFS were taken. The noise in the μ–EXAFS spectra tends to lead to higher

normalized sum square (NSS) values than their bulk counter parts. Although, the bulk

and μ -EXAFS spectra show some deviations from one another, a correlation plot with

μ vs. bulk EXAFS spectra show slopes at ~ 1, although the R^2 is low (Figure A9.1). The

results indicate higher concentrations of As(V) coprecipitated with Zn(II) on Goethite in

subsoil samples compared to the surface soil counter parts. Also, there are increased

concentrations of As sorbed to goethite moving from the HT to the TS position. When %

As sorbed by iron species and % As sorbed by aluminum species is plotted vs. soil pH

(Figure 2.4), a trend arises which indicates that at low pH and high As concentration Al

species hold a more predominant role in controlling As speciation whereas as pH

increases the iron phases become more important in controlling As speciation.

Table 2.4: Linear Least Squares Fitting with 3 Principal Components

Location	Soil	Type	As(V)-Gibbsite	As(V)Zn(II)-Goethite	Mansfieldite*	Sum	NSS	ΔE	Aluminum Species	Iron Species	pH
Hilltop	Surface	Bulk	64%	15%	27%	107%	0.1150	0.4600	91%	15%	4.4
Hilltop	Surface	Average μ	15%	23%	76%	114%	0.6433	1.4700	91%	23%	4.4
Hilltop	Subsurface	Bulk	13%	32%	51%	96%	0.1230	1.2900	64%	32%	5.6
Hilltop	Subsurface	Average μ	11%	28%	69%	108%	0.3255	0.1050	79%	28%	5.6
Midslope	Surface	Bulk	43%	31%	31%	105%	0.0274	0.1000	74%	31%	5.1
Midslope	Surface	Average μ	51%	16%	37%	104%	0.0873	0.5567	88%	16%	5.1
Midslope	Subsurface	Bulk	38%	58%	0%	96%	0.0507	0.7500	38%	58%	6.3
Midslope	Subsurface	Average μ	23%	52%	17%	92%	0.2188	0.7825	40%	52%	6.3
Toeslope	Surface	Bulk	55%	47%	0%	102%	0.0449	0.3800	55%	47%	6.6
Toeslope	Surface	Average μ	0%	35%	52%	87%	0.5633	-2.3400	52%	35%	6.6
Toeslope	Subsurface	Bulk	28%	45%	22%	95%	0.1330	0.5100	50%	45%	7.1
Toeslope	Subsurface	Average μ	34%	79%	16%	128%	0.4410	-0.2300	49%	79%	7.1

*thought to be mansfieldite XRD revealed amorphous aluminum phase, NSS-Normalized Sum Squares

Figure 2.2: The percent As bound to Fe and Al vs. pH. It was determined by linear least squares fitting of the bulk and μ-XAFS spectra from the HT(Diamonds),MS(X) and TS(circles) positions plotted vs. soil pH .

2.3 Discussion and Conclusion

Moving down the topographic gradient a slight trend of increased mass (Figure 2.2, Table 2.1) and concentration (Figure 2.1) of arsenic in the surrounding post soil was observed at depth possibly indicating higher potential for As leaching from posts moving down the toposequence. Lebow et al. (2004) found that As release from CCA wood by rain water was largest during longer periods of exposure to water (Lebow et al., 2004a) .

Due to the drainage characteristics of the soil in this study, increased periods of time with water contact to the fence posts occurs moving to more poorly drained conditions which is likely enhancing the leaching of As from the wood surfaces. In the surface soils a decreasing trend in the ratio of As in the 0 – 5 cm sampling distance to that in the 10-15 cm sample going from the HT position to the poorly drained TS location (Figure 2.1) once again alluding to the increased mobility of As in these soils. Potentially accelerating the loss of As from the TS locations is the increased pH compared to soils at the MS and HT. Poor drainage provides the anoxic conditions favorable for the release of As into solution; the increase in pH lowers the adsorption capacity of various soil constituents. Several researchers have shown that increases in pH result in a decrease of arsenate adsorption potential to amorphous aluminum oxide, aluminum oxides, clays, and iron oxides (Dixit and Hering, 2003; Goldberg, 1986; Goldberg, 2002). As shown in Figure 2.2, the radial extent of As mobilization is occurring to the greatest degree in surface soils which likely has to do with increased As leaching from the post, biological activity, bioturbation, and lower bulk density in surface soil horizons as opposed to subsurface horizons. The organic matter profile in these soils follow the same trends as the total mass of As, and the radial extent of leaching is highest at the surface soils; indicating that biological activity or organic matter competition for As sorption sites (Bauer and Blodau, 2006; Bauer and Blodau, 2009; Redman et al., 2002) is likely influencing the mobilization of As.

Although, the SXRF map correlations and colocalization are stronger for As and Fe compared with other elements, the results from the PCA analysis and subsequent target transformation indicates that Al-species are playing a predominant role in the

sequestration of As, especially in acidic soils. Unfortunately, Al species are not easily mapped through SXRF mapping, because Al is a major constituent in most soil minerals, thus the predominant Al-As relationship is not decipherable through SXFR mapping. Multiple channel analysis (MCA) scans at select AOI indicate Al is colocalized along with As. The goethite species, gibbsite species and the amorphous Al-As complex, originally believed to be Mansfieldite, fit the PC's best. The aluminum species play the main role in As speciation at the HT surface soil location, the most acid location evaluated at a pH of 4.4, and previous mineralogical analysis conducted by Karathanasis et al. (2002, 2006a) indicate significant quantities of Al oxides and amorphous Al oxides in the Bluegrass Maury silt loam soil. The LLSF of the select standards indicates the Al-As complexes (Mansfieldite, As(V)-Gibbsite) predominate in the HT surface soil, indicating the probable mode of adsorption is with aluminum bearing minerals in which Fe, Zn, Cu, etc. are all colocalized together. This mechanism of sorption is likely true throughout all landscape positions; however, the surface charge on Al and Fe functional groups shifts with the pH, thus causing Fe to play more of a role in As sorption when soils become more basic. This trend is clearly shown in Figure 2.4 and the apparent crossover point at which Fe begins to play a more predominant roll is near the pH in which Al function groups gain net negative charges (Sadiq, 1997). This could explain the increase in meh- P in soils adjacent to the post is attributed to As out competing with phosphorus on Al surfaces (a predominant sorption mechanism for phosphorus) and thus causing P to be mobilized to less strongly sorbed sites. The meh- P increase is most apparent in the acidic soils with the highest concentrations of As, the same locations in

which As-Al species predominate; as the concentration of arsenic decreases and soils shift towards more basic pH, the meh-P is drastically reduced.

The lower retention of As at the TS soil location can be explained by a confluence of factors, first the affinity for soil particles is less due to the pH being at near neutral conditions, the lower affinity is accompanied by a higher concentration of meh- P at the TS than at the HT and MS position, which can strongly compete with As for sorption sites. This, accompanied with an increase in water allowing these interactions to take place more frequently, allows arsenic to be mobilized more readily. The landscape position of the TS also experiences extended periods of time during the year in reduced conditions due to its location near an intermittent stream. It is shown that Fe plays a greater role in the speciation of arsenic at this landscape position in comparison to the HT and MS landscape positions, since iron is a redox sensitive element, the reduction of Fe may release As. The results of the Fe analysis indicate both higher concentration of W-Fe(II) and W-Fe, the increase in W-Fe(II) is an indication of redox conditions favorable for reductive dissolution of Fe- minerals and the subsequent mobilization of As bound to this fraction. The higher degree of W- Fe in solution may indicate a possible mobile pathway through colloidal iron. The same TS soils exhibit increased SOM at depth which is attributed to a higher water table causing reducing conditions in which less energy efficient microbial anaerobic respiration processes predominate thus limiting SOM decomposition rates and resulting in a net increase in SOM (Sylvia, 2005). Additionally, at conditions conducive to Fe reduction, As reduction is also thermodynamically favorable (As(V) to more mobile As(III)) (Kocar and Fendorf, 2009), another mode of mobilization in this TS position.

Overall, Fe and Al bearing minerals are the principal sorption mechanisms for As in the soil studied with Al controlling As sorption at low pH conditions and Fe playing an increased role at higher pH conditions. The pH of the soil, which is increasing while moving down the topographic gradient, is resulting in a higher degree of As mobilization while moving down the toposequence. Although a measurement of remaining As in the posts was not taken, all geochemical indices may be a sign of the low concentrations of As remaining in soils at the TS position is likely a result of mobilization through competition (meh-P, SOM), increased pH conditions, and redox conditions favorable for As mobilization (higher Fe(II) and total-Fe concentrations in water extracts).

Chapter 3: Speciation and Spatial Distribution of Copper and Chromium from CCA Treated Fences Across a Toposequence

3.0 Introduction

Copper and chromium speciation and spatial distribution were assessed adjacent to Chromated Copper Arsenate (CCA) fence posts along a toposequence. Metal distribution was evaluated on both macroscopic (soil profile contour maps) and microscopic scales (XRF images), speciation of Cu was conducted using extended x-ray absorption fine structure (EXAFS) and a myriad of basic soil properties probed to determine which soil properties (pH, soil texture, CEC, etc) most influence Cu spatial distribution and speciation. This study indicates Cu speciation is controlled through organic matter complexes in surface soils and Cu-Mn complexes in subsoil horizons. Also, Pearson correlation coefficients on SXRF maps indicate Cr-Mn/Fe are highly correlated with each other, especially in subsoil's. Finally, the study highlights the influence of somewhat poorly drained condition causing a large loss of Cu over the 20 yrs. of use.

Copper and chromium are essential micronutrients; copper serves as a cofactor for many proteins, while, chromium is required for a properly functioning glucose metabolism (Valko et al., 2005). In excessive quantities heavy metals in soils have been shown to decrease microbial biomass, alter utilization of C substrates, decreasing the mineralization rate, and decrease microbial symbiotic N_2-fixation (Giller et al., 1998). Due to the widespread use of copper it can be highly elevated in surface soils as a result of mining and related activities, waste emissions, biosolids, fertilizer and fungicide

applications (Flemming and Trevors, 1989). Likewise, Cr concentration in soils have been increased through the application of biosolids (Kabata-Pendias, 2001), as well as, in areas surrounding mining and smelter heaps (Uminska, 1988). To gain further understanding of Cu and Cr chemistry in soil an analysis was conducted using soil adjacent to chromated copper arsenate (CCA) treated lumber fence posts. Fences transect a wide array of soil series and landscape positions, thus it is possible to use this consistent metal source to evaluate which soil properties influence Cr and Cu mobility and speciation.

Chromated copper arsenate (CCA) is a pesticide treatment introduced under pressure to timbers in order to preserve the integrity of wooden structures. CCA works through arsenic acting as an insecticide and copper acting as a fungicide (Warner and Solomon, 1990). Chromium acts to aid in the fixation of the other elements within the wooden matrix, particularly As (Chirenje et al., 2003). The most common CCA treatment is form C consisting of 47.5% CrO_3 , 18.5% CuO, 35% As_2O_5 applied at rates of 4.0 to 40.0 kg/m^3 depending on use (Association, 2005; AWPA, 2005). Copper is fixed in the wood by the formation of carboxylate-copper(II) complexes (Bull, 2001), while Cr is complexed with lignin or cellulose (Hingston et al., 2001). Copper has been shown to leach into the environment from CCA treated lumber however, the extent of Cr leaching is not as substantial because of the strong Cr- lignin/cellulose complexes (Cooper, 1991; Khan et al., 2004; Kim et al., 2007; Lebow et al., 2004b; Robinson et al., 2006; Stilwell et al., 2003; Stilwell and Gorny, 1997; Stilwell and Graetz, 2001). It is speculated that Cu and Cr are principally being leached as individual ions or organometallic complexes (Lebow, 1996). This manuscript will address how a variety of soil physicochemical

70

properties influence Cu and Cr speciation from fence posts along a toposequence by employing a variety of macroscopic and spectroscopic tools to assess their speciation and mobility. The specific objectives of the study are (1) to determine the amount and distribution of Cu and Cr around CCA treated fence posts along a toposequence; (2) determine the speciation of Cu and Cr (and therefore, the potential mobility, and bioavailability) in these soils and (3) determine which soil properties most strongly influenced the observed speciation. Because of the widespread use of CCA treated lumber and concern for the adverse effects these metal constituents may have in the soil and water environment, an evaluation of these metals in the Kentucky soil environment needs to be addressed.

3.1 Materials and Methods

3.1.1 Soil Sample Collection, Description and Preparation

The field site is located in the Inner Bluegrass region of Kentucky on the University of Kentucky Spindletop Research farm. Sampling was conducted along a Chromated-Copper-Arsenate (CCA) treated fence line which had been in place for ~20 years surrounding a mixed grass pasture. The fence line was chosen because it transects a Bluegrass-Maury silt loam (fine, mixed, semiactive, mesic Typic Paleudalfs), a Donerail silt loam (fine, mixed, active, mesic Oxyaquic Argiudolls), and a Newark silt loam (fine-silty, mixed, active, nonacid, mesic Fluventic Endoaquepts), each having different pH, drainage class and slope. Additional information regarding the site location and soil series specification can be found in Appendix 1.Soil pits were dug by backhoe to a depth of ~1m alongside a fence post at the hill top (HT), a midslope (MS), and a toeslope (TS)

position corresponding to the Maury, Donerail, and Newark silt loam soils respectively. A grid pattern was established on the face of the pit containing the fence post from which about 60 soils samples were collected into Whirl-Pak® (Nasco, Fort Atkinson, Wisconsin) bags and stored on ice (See Appendix 2 for sampling plan schematic). Upon returning to the lab, soils were sieved past 2 mm, placed in new whirl-pack® bags and stored at 4^oC until analysis. Additionally, soil samples were collect every 8 posts (~20m) along the toposequence from the HT position to the TS position at distances 0-5 cm and 10-15 cm away and depths 0-15 cm and 15-30 cm (See Appendix 10 for additional details).

3.1.2 Soil chemical properties

In preparation for analysis, sieved soils were dried at 60° C. Soil pH was determined by a glass electrode in a 1:1 soil/water ratio which was stirred manually and allowed to set for ≥15 min. Mehlich III -P, K, Ca, Mg, Zn, Cd, Cr, Ni, Pb, Cu, and Mo (Meh-P, Meh-K, etc.) were determined by inductively couples plasma mass spectroscopy (ICP-MS) after 2 cm^3 soil mixed with 20 ml of Mehlich III solution (0.2 N acetic acid, 0.25 N NH_4NO_3, 0.015 N NH_4F, 0.013 N HNO_3, and 0.001 N EDTA), shaken for 5 min. and filtered through Whatman #2 filter paper (Mehlich, 1984). Soil carbon and nitrogen determined by dry combustion with 0.5 g soil. Cation exchange capacity (CEC) and base saturation determined with 10 g soil by saturation with 1 N ammonium acetate. Soil texture was determined by the micropipette method. Analysis, with the exception of pH, was performed by the University of Kentucky's Division of Regulatory Services.

3.1.3 Total Metal Determination

Total metal content of the soil samples was determined using a modification of EPA method 3052. Briefly, 9 ml of nitric acid and 5 ml hydrofluoric acid were added to 250 mg of dry soil in Teflon pressurized/sealed vessels and rapidly digested in a 1600W MARS (CEM, Matthews, North Carolina) microwave digestion unit. Samples were brought up to 180° C and kept at this temperature for 10 min., after which they were allowed to cool, transferred to 50mL falcon tubes, and brought up to final volume of 50 mL using ultrapure water. Samples were then analyzed on an Agilent 7500 series (Santa Clara, Ca) Inductively Coupled Plasma- Mass Spectrometer (ICP-MS). All reagents used were ultra-pure trace-metal grade.

3.1.4 Metal Speciation via Synchrotron X-ray Absorption Fine Structure Spectroscopy (XAFS)

3.1.4.1 Sample Preparation and Data Collection

Data collection was performed at beamline 13-BM-D [Advanced Photon Source (APS), Argonne National Laboratory, Argonne, IL] and beamline 10.3.2 [Advanced Light Source (ALS), Lawrence Berkeley National Laboratories, Berkeley, CA](Marcus et al., 2004). μ-X-ray Absorption Fine Structure Spectroscopy (μXAFS) and μ-Synchrotron X-ray Fluorescence (μSXRF) mapping data were collected on beam lines 13-BM-D at APS and 10.3.2 at ALS, while, bulk XAFS data was collected at beamline 13-BM-D at APS. Soil samples were dried at 60° C for 24 hrs and ground with an agate mortar and pedestal. Samples for bulk X-ray analysis were retained in a 20 mm by 5 mm by 3mm hole between two pieces of non-adhesive Kapton film in an acrylic sample holder. For μSXRF and μXAFS data collection an even layer of soil was adhered to

Kapton film using a thin layer of silicone based vacuum grease. Samples were mounted at 45° to the incident beam and data collected in fluorescence mode by a 16- element and 7- element Ge detector at beamlines 13-BM-D and 10.3.2, respectively.

At beamline 13-BM-D, μ–SXRF mapping was conducted over an area of 1 mm^2 at 14 keV using a beam size of 10 μm by 20 μm with 20 μm steps, and a 2 s dwell time while, μSXRF mapping conducted at beamline 10.3.2 was over an area of 1 mm^2 to 4 mm^2 at 13 keV using a beam size of 6 μm by 6 μm using a continuously scanning stage with 6 μm steps. At 13-BM-D multiple (≥5) extended X-ray absorption fine structure spectra (EXAFS) were collected in fluorescence mode from 150 below to 650 above the Cu K-edge (8.979 keV), from each area of interest (AOI) found in the μSXRF maps. At beamline 10.3.2 (ALS), a quick scanning x-ray adsorption spectroscopy (Q-XAS) technique was used to probe the speciation of Cu in order to account for any changes that may occur as a result of beam induced damage. This technique continually scans the monochromator from low to high energy, over the energy envelope of interest. In this study consecutive scans of ~45 s each where conducted and could then be visualized in order to determine any apparent beam induced damage. To limit radiation damage samples were cooled to – 30 C with a Peltier cooler .The beam size was set to 6 mm by 0.9mm for all bulk EXAFS data collected. For μSXRF mapping and μEXAFS spectra collection a beam size of 10 μm by 20 μm was used at 13-BM-D while, a beam size of 4 μm by 3 μm was used at beam line 10.3.2.

3.1.4.2 Data Analysis

All data reduction was performed using WinXAS 2.1 (Ressler, 1997). Individual spectra were calibrated for shifts in edge energy using the 2nd derivative of the adsorption edge and setting the edge energy equal to 8.988 keV. Q-XAS data collected at 10.3.2 (ALS) were calibrated based on the monochromatic glitches and spectra showing no signs of beam induced radiation damage were averaged. Then, spectra were background corrected using 1st order polynomials for the pre-edge and post-edge region and then normalized. After normalization, multiple scans per AOI were averaged and converted from energy (keV) to photo-electron wave units k ($\mathring{A}^{-1}$) by setting the edge energy origin at ~8.988 keV. A single atomic spectra with the absence of back scattering was estimated using a cubic-spline function of 7 knots over an average k space of 2.0 to 12.5 $\mathring{A}^{-1}$ and subtracted from the spectra to obtain raw $\chi(k)$ data. The $\chi(k)$ was weighted by a factor of k^3 to amplify oscillations at higher k values. Fourier transformation of the $\chi(k)k^3$ was performed over the k ranges of 3.4 – 10.8 $\mathring{A}^{-1}$ to obtain radial structure functions using a Bessel window with a smoothing parameter of 4.

3.2 Results

3.2.1 Total Metal Concentration and Spatial Distribution

Geostatistical constructions of the total copper concentrations into contour maps show significant enrichment of Cu adjacent to the HT and MS posts (Figure 3.1). The maximum concentrations of copper (HT: 309 ppm, MS: 580 ppm, and TS: 41 ppm) are located directly adjacent to the post and fan out toward the surface soil which exhibit elevated concentrations (50 – 100 ppm) up to 30 – 35 cm from the post. At depth

increased concentrations of copper are confined to the 0-10 cm region adjacent to the CCA post, otherwise copper concentrations approach background. For the hilltop and midslope positions the highest copper concentrations are located at the 15-30 cm depth sampling point directly adjacent to the post. The midslope position shows a higher mass of copper throughout all depths (Table 3.1, Figure 3.1). The sum of copper in the soils surrounding posts at the HT, MS and TS is 15.8 g, 24.2 g, and 1.93 g, respectively. The toeslope position has copper concentrations on average that are much lower than the HT and MS positions with elevated Cu concentrations only occurring in surface soil samples and directly beneath the post. The Cu distribution is similar to that of As which showed enrichment in the topsoil where it emanated further from the post, compared to the subsoil where it generally remain within 0-10 cm from the post (see Figure 2.1 Chapter 2). As one moves down the topographic gradient a slight trend of increased mass and concentration of copper is occurring in the surrounding post soil, this trend can be observed in Figure 3.2 and also in Figure 3.1 /Table 3.1. In the surface soils a decreasing trend in the ratio of the adjacent to the post (0 – 5cm) soil Cu concentration: away from post (10-15 cm) soil Cu concentration is exhibited while moving to more poorly drained conditions Figure 3.1.
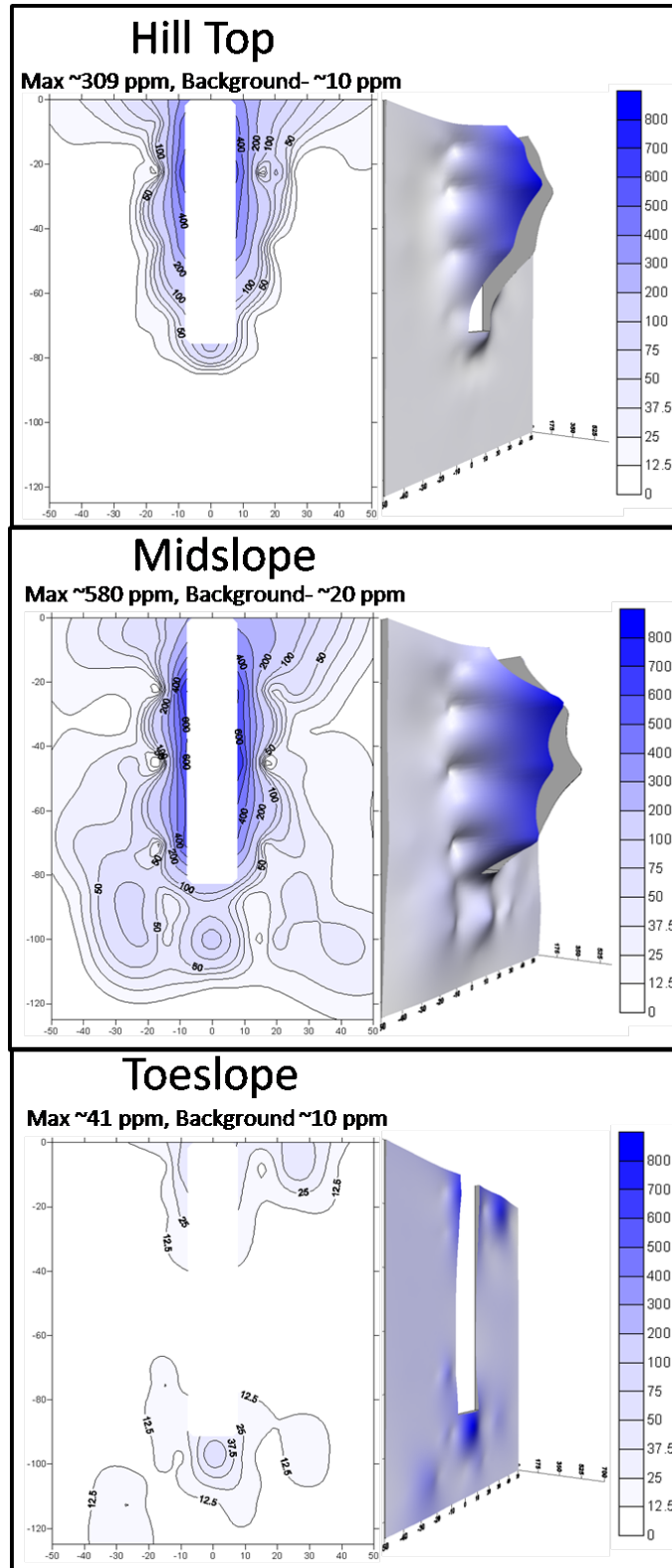
Figure 3. 1: Soil profile contour map of copper concentrations (ppm) in soils along the toposequence. The blanked section indicates regions where post enters the soil.

Table 3.1: Total mass and normalized enrichment factor (NEF) of arsenic at specific depths in the soil profile. Detailed explanation of the calculations is provided in the Appendix 6.

| Depth	Mass per unit depth (g/cm)	Normalized Enrichment Factor (NEF)
Hilltop		
0 to 15 cm	0.376	13
15 to 30 cm	0.268	9
30 to 60 cm	0.186	8
60 to 90cm	0.016	1
90 to 105 cm	0.007	1
Total g (0-105cm)	15.827	
Midslope		
0 to 15 cm	0.366	14
15 to 30 cm	0.266	15
30 to 60 cm	0.243	15
60 to 90cm	0.191	11
90 to 110 cm	0.109	5
Total g (0-105cm)	24.162	
Toeslope		
0 to 15 cm	0.046	2
15 to 30 cm	0.009	1
30 to 60 cm	0.004	1
60 to 90cm	0.020	1
90 to 120 cm	0.026	2
Total g (0-105cm)	1.932	
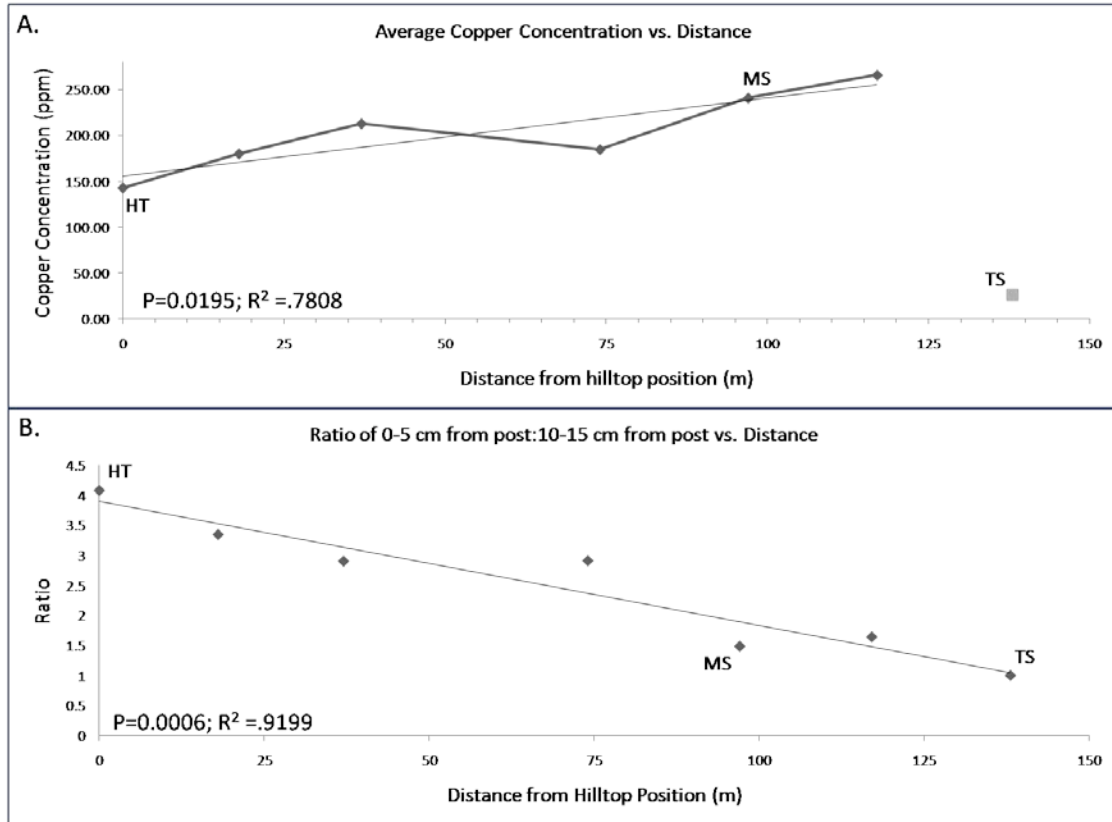
Figure 3. 2 Concentration and mobilization of copper across the topographic gradient. A) Average copper concentration of samples collected along the toposequence and B.)ratio of 0-5 cm from post: 10-15 cm from post at 0-15 cm depth along the toposequence. Hilltop (HT), Midslope (MS), Toeslope (TS)

3.2.2 Basic Soil Properties

Basic soil properties are exhibited in Table 3.2, principally, the soil texture class observed is a silt loam throughout the three soil series/landscape positions with the exception of the HT 30-90 cm and MS 60-90 depths where an accumulation of clay has resulted a silty clay loam textural class. Cation exchange capacity (CEC) is similar between the HT and MS sampling locations and somewhat increased at the TS position, all samples being within 14.4 – 21.2 meq/100 g soil. The soil organic matter (SOM)

content is similar between the three landscape positions, reducing with increasing depth in the soil profiles, however, at the TS position the SOM content increases from 1.0 % at the 30-60 cm depth to 2.1 % at the 60-90 cm depth.

The three soil series/landscape positions follow a similar trend of increasing pH units with depth up to about 60 cm beyond which the pH stays relatively consistent or slightly decreases. Although pH vs. depth relationships are similar between landscape positions the overall pH increases moving down the landscape (HT pH<MS pH<TS pH), with the HT and MS positions having strongly to moderately acidic conditions (HT: 5.2 – 6.0 pH and MS: 5.7– 6.4 pH), whereas, the TS position is near neutral (6.8- 7. 4 pH). The base saturation (BS) of the cation exchange sites shows the same trends as the pH. The BS is between 38 – 58.4 %, 52.7 – 70.9 %, and 69.2- 81.1 % at the HT, MS, and TS positions, respectively, increasing from the HT to the TS position. Additionally, sharp drops in pH and base saturation are realized in soils adjacent to the post compared to similar depth background samples. Although total metal acid digest chromium concentrations were similar at all landscape positions and chromium was not suspected to be leaching to a high degree from CCA treated posts, there were detectable Meh-Cr concentrations at the TS position. The soil adjacent to the CCA treat post showed highly elevated levels(105 – 355 mg/dm^3) of meh-Cu while the TS position showed just slightly elevated levels(7.8-20.3 mg/dm^3) of meh-Cu.

Table 3.2: Basic Soil Properties*

Depth	Soil Texture Class	Silt %	Clay %	SOM % B	SOM % A	pH B	pH A	CEC (meq/100g) B	CEC (meq/100g) A	Base Saturation % B	Base Saturation % A	MehP B	MehP A	MehCa B	MehCa A	MehCr B	MehCr A	MehCu B	MehCu A
Hilltop																			
0 to 15	Silt Loam	71	15	4.11	3.47	5.2	4.4	19.6	16.9	38.0	18.3	77	155	1173	475	BDL	BDL	9.3	188.7
15 to 30	Silt Loam	71	18	1.77	1.91	5.9	5.1	14.6	15.1	54.8	39.9	31	87	1443	1090	BDL	BDL	3.8	258.1
30 to 60	Silty Clay Loam	60	29	0.88	1.07	6.0	5.7	15.7	16.3	58.4	54.5	36	76	1729	1584	BDL	BDL	3.1	203.0
60 to 90	Silty Clay Loam	48	36	0.40	0.40	5.5	5.4	18.2	19.6	49.0	47.7	55	60	1591	1691	BDL	BDL	2.0	11.4
BP: 75 to 80 cm	Silty Clay Loam	50	34	0.86		5.6		19.6		51.1		72		1804		BDL		30.1	
Midslope																			
0 to 15	Silt Loam	75	14	3.46	3.82	5.7	5.1	16.9	16.9	52.7	27.3	70	118	1311	559	BDL	BDL	9.6	123.8
15 to 30	Silt Loam	76	16	2.20	2.51	6.1	5.2	15.6	15.6	57.2	38.6	36	90	1604	900	BDL	BDL	4.1	354.9
30 to 60	Silt Loam	65	26	1.03	1.31	6.4	6.0	14.4	15.0	70.9	60.7	44	70	1887	1598	BDL	BDL	9.6	267.6
60 to 90	Silty Clay Loam	53	31	0.57	0.58	6.3	6.2	17.6	18.3	67.8	64.0	75	97	2195	2116	BDL	BDL	9.6	105.5
BP: 80 to 90 cm	Silty Clay Loam	52	34	0.76		6.3		18.3		68.6		91		2208		BDL		40.2	
Toeslope																			
0 to 15	Silt Loam	78	12	4.09	6.55	6.8	6.6	21.2	22.3	74.2	75.1	111	91	2775	2456	0.09	0.67	4.5	20.3
15 to 30	Silt Loam	81	13	3.04	3.11	7.1	7.1	21.1	19.8	69.2	71.1	55	56	2737	2712	0.06	0.44	4.4	16.0
30 to 60	Silt Loam	79	16	1.03	1.15	7.4	7.1	14.4	12.8	75.1	79.8	77	61	2012	1997	0.05	0.16	2.3	7.9
60 to 90	Silt Loam	65	24	2.13	2.18	7.3	7.1	21.1	20.3	81.1	81.4	134	130	3056	3127	0.07	0.09	3.8	7.8
BP: 90 to 105	Silt Loam	56	27	2.15	2.61	7.3	7.1	25.6	23.7	84.4	77.2	159	148	3979	3283	0.1	0.28	7.7	30.1

MehCa, MehCr, MehCu columns are under Mehlich III Extractable (mg/dm3)

* Below Post(BP), B indicates Background samples, A indicates soil adjacent to CCA post (0-5 cm)

81

3.2.3 Copper and Chromium Speciation via μ-SXRF Mapping

Select x-ray fluorescence maps of surface and subsurface soils are shown in Figure 3.3. In general, μ-SXRF mapping does not indicate a strong correlation between Cu and the other metals analyzed, however, the maps reveal the greatest correlations, though still low (ρ ~0.4 to ~0.65), with Mn followed by As. An exception to this is the hilltop subsurface soil (Figure 3.3) which exhibits a strong Cu-Mn correlation (ρ = 0.879). In contrast, Cr is strongly correlated with Fe and Mn in subsurface soils (ρ >0.8) at the HT and MS position as well as in HT, MS, and TS surface and TS subsurface soils (~0.6 to ~ 0.8).

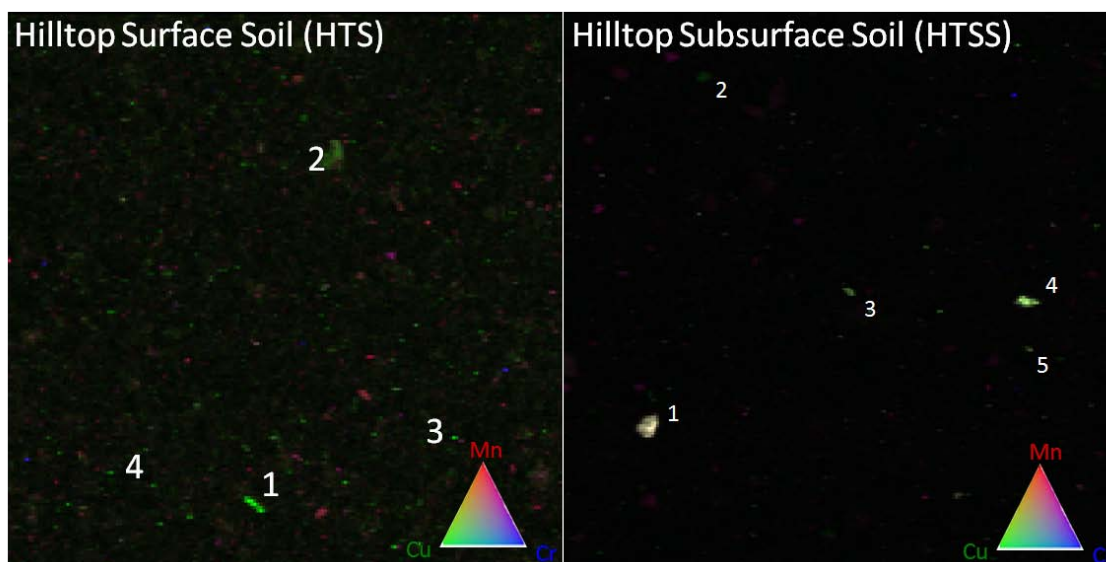**Figure 3. 1:** Images of contrasting surface and subsurface SXRF maps of Copper (green), Chromium (blue), and Mn (red). Pearson correlation coefficients were .562 and .822 for Cu/Mn and Cr/Mn respectively in the hilltop surface soil. In the subsoil horizon Pearson correlation coefficients were .879 and .951 for Cu/Mn and Cr/Mn, respectively. Numbers correspond to points in which m-XAFS spectra were collected.

3.2.4 Copper Speciation via Synchrotron X-ray Spectroscopy

The Q-EXAFS scans show signs of rapid change in copper coordination as a result of beam induced reduction (Figure 3.4). When graphing the $\chi(k)$xk^3-spectra and radial structure function (RSF) of the average of the initial scans (0 – 5) against the average of scans 5-10, 10-20, 20-60 and 60 – 120 the changes are drastic and obvious. New peaks evolve in the raw data at ~9.03 keV, 9.08 keV, and 9.14 keV, and in the $\chi(k)$xk^3-spectra at 4.9, 6.3, 7.8, and 9 Å^{-1} . The damage resulted in a shift from copper coordinated with oxygen at R_{Cu-O}= ~1.5 Å in what was similar to that of Cu bound to humic acid to copper coordinated with another Cu atom at R_{Cu-Cu} = ~2.2 Å, (uncorrected for phase shift) resembling copper metal (Figure 3.4). The transition from Cu-O to Cu-Cu coordination was quick and observable within the first 10 quick scans (~3-8 min.) with the copper metal bond dominating the spectral signal. Because, this damage occurred so quickly it highlights the importance of the Q-EXAFS technique in evaluating radiation damage unobservable using traditional scanning techniques.
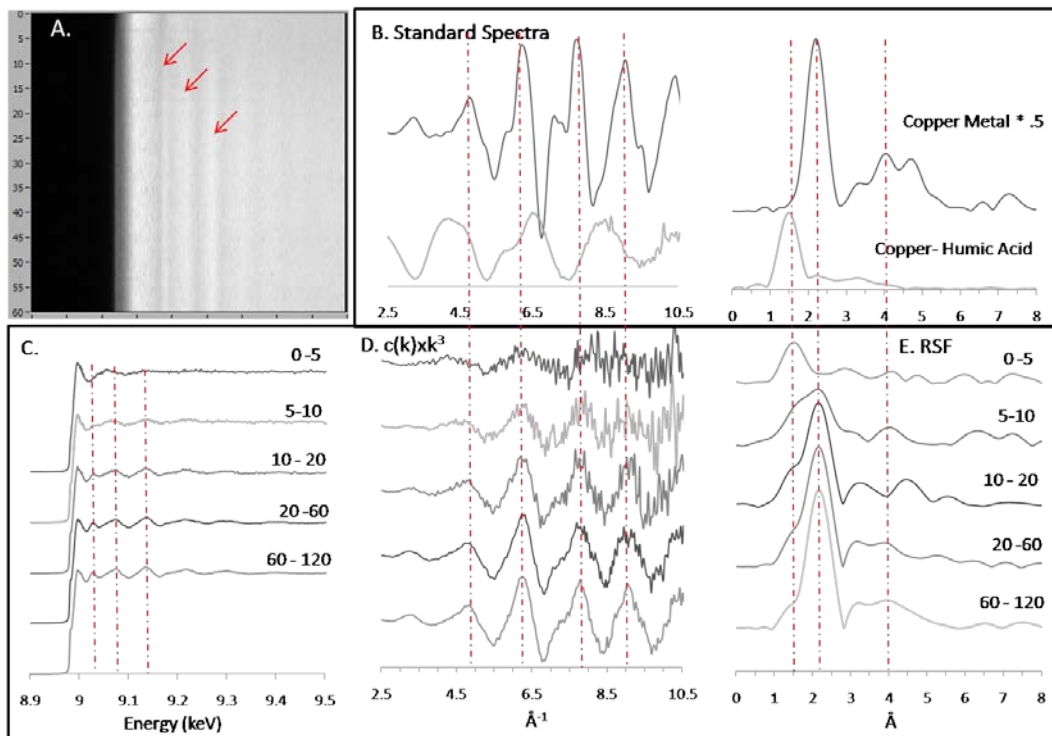
Figure 3. 2: Radiation damage to Cu-Soil Organic Matter complex. A. Q-XAFS scan image, arrows indicating development of radiation induced peaks over time. B. Standard -$\chi(k)xk^3$ and Radial Structure Function (RSF). C. Normalized Raw spectra D. $\chi(k)xk^3$ and E. RSF showing beam induced damage to a presumable Cu-SOM complex.

3.2.5 EXAFS Analysis

Unfortunately, due to poor signal to noise ratio and/or radiation induced damage the amount of spectra capable of being analyzed was severely limited. Spectra showing no signs of radiation induced damage (HTSS-1, HTSS-3, and HTSS-5 in Figure 3.5) were located in subsoil samples at locations in which strong Cu-Mn colocalization was apparent in the μ-SXRF maps. Scans MSS-2, MSS-3, MSS-4, HTS-3, and HTS-4 in Figure 3.5 were the result of radiation induced damage. Initial scans at these locations exhibited a first RSF peak corresponding to R_{Cu-O} at ~1.5 Å (uncorrected for phase shift), however, as time/scans progressed the development of Cu(I)-S (HTS-3, HTS-4) and

84

Cu(0)-Cu(0) (MSS-2, MSS-3, MSS-4) bonds developed at ~1.85 Å and ~2.2 Å, respectively. Due to the radiation damage at the surface horizons the exact bonding environment of Cu complexes in these samples is unattainable however, it is quite clear that Cu(II) is in a complex with organic matter as is indicated by the first scans in the series of Q-EXAFS spectra.

Figure 3. 3: Raw, $\chi(k) \times k^3$, and Radial Structure Function Copper in surface and subsurface soils.
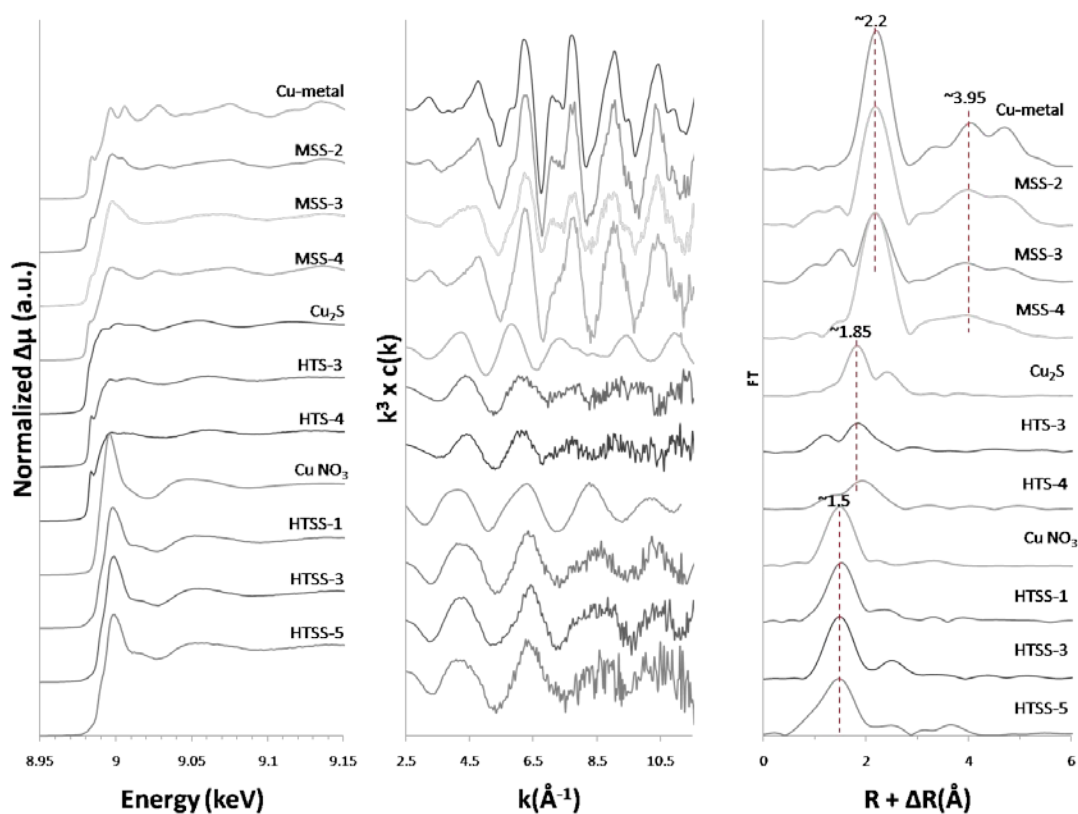
3.3 Discussion and Conclusion

Although significant radiation damage had occurred in the study of Cu through the synchrotron based techniques, it is likely this is a cause of Cu strongly being absorbed by organic matter constituents, which is widely observed in Cu studies (Korshin et al.,

1998; Strawn and Baker, 2008). This is especially true in the surface soil samples analyzed(all surface soil spectra exhibited radiation damage) in the study which indicate radiation damage resulting in Cu(I)-S or Cu(0)-Cu(0) bond formation at 1.85 Å and 2.2 Å. Similar radiation induced damage on Cu- natural organic matter complexes is exhibited by (Manceau, 2010) showing radiation induced damage resulting in Cu(I)-S and Cu(0)-Cu(0) bond formation. Likely, depending on the total Cu concentration and organic matter substrate various differences and degrees of radiation damage occur. The radiation damage is not exhibited, or exhibited to a lesser extent, in subsoil samples in which Cu-Mn correlations are substantial and organic matter contents are low. Fe/Mn oxide have been found to control Cu distribution in soils low in organic matter (Yu et al., 2004). Likely, copper is strongly bound to organic matter in surface horizons, however, having a higher percentage of inorganic bonds (Cu-Mn) in subsurface soil horizons. The radiation induced damage results in surface soil horizons revealing the importance of Q-EXAFS techniques in assessing damage to redox sensitive organic bound metals. The fact that the damage occurred so quickly shows that traditional scanning techniques where it may take 30-40 min to collect one spectra may result in misinterpretation of the actual binding environment of Cu . For example, Manceau et. al, (2006) showed what they believed to be the formation of Cu-metal nanoparticles in rhizosphere soils using EXAFS methods at the same X-ray beamline used in this study (ALS 10.3.2) except in conventional scanning mode. Our findings call into question the results obtained by Manceau et. al. (2006), indicating that the thermodynamically unfavorable formation of Cu metal nanoparticles was probably the result of photo reduction of organic bound copper by the X-ray beam.

Chromium exhibited no clear patterns of soil enrichment directly correlated to the presence of the post; instead, the Cr distribution increased uniformly with depth (See Appendix 4 Figures A4.7-9), which is similar to Fe distribution (See Appendix 4 Figures A 13-15). The μ-SXRF maps (Appendix 5, Figure A5.1) show a clear correlation of Cr with Fe and Mn and taken together with the aforementioned observation, indicates that most of what was detected was geogenic in origin (e.g. chromite ($FeCr_2O_4$), isomorphically substituted for Fe(III) in spinel minerals or as sorption complexes on Mn and Fe containing minerals). The absence of Cr in the soils around the posts is not surprising in light of its intended role in the pressure treating process to form strong complexes with lignin and cellulous (Bull, 2001; Hingston et al., 2001). Additionally, in the TS position, with higher pH conditions, meh-Cr concentrations are observed although low. This may indicate a slight difference in Cr speciation at the TS position. A possible species under these pH conditions that is thermodynamically favorable is the formation of $Cr(OH)_3$ precipitates (Kotas and Stasicka, 2000), which may be solubilized under a Mehlich III extraction. Also, the fact that these concentrations are higher in the adjacent to post soil sample, although still low (<0.64 mg/dm^3), may indicate a small quantity of Cr enrichment adjacent to the post. Unfortunately, the bonding environment of Cr was not investigated due to the low concentrations.

The similar distribution of Cu at all locations is a good indication that the source is indeed the post (and not geogenic) and since it mimics the distribution of organic matter may possibly be due to the influence of SOM concentrations in these positions. The elevated concentrations of meh-Cu (100-350 mg dm^{-1}) in soil samples adjacent to the posts indicate a large fraction of Cu is phytoavailable. Increased concentrations of Cu are

occurring in the surrounding post soil while moving down the topographic gradient. Likely, a result of the drainage characteristics of the soil, increased periods of time with water contact to the wood surfaces occurs while moving down the toposequence and enhancing the leaching of Cu from the wood surface. Surface soils exhibit a decreasing trend in the ratio of the adjacent to the post (0 – 5cm) soil Cu concentration: away from post (10-15 cm) soil Cu concentration while moving to more poorly drained conditions. This trend is likely related to the mobility of Cu in these soils, indicating that the mobility of these constituents increases while moving down the topographic gradient. The drainage characteristics may provide the medium for movement, while the increase in meh-Ca induces increased competition for Cu. Although, competition of Cu and Ca on SOM has generally been attributed to be low, decreases in Cu complexation have been found as a result of Ca competition on humic and fulvic acid, especially at high Cu loading rates (Cao et al., 1995; Iglesias et al., 2003). Interestingly, Cu adsorption and solubility is expected to increase with pH on many soil constituents (Cavallaro and McBride, 1980; McBride and Bouldin, 1984; McLaren and Crawford, 1973a; Sanders and Bloomfield, 1980); in contrast to the lower mobility of Cu observed in the low pH conditions in this study. However, since copper is largely bound to organic matter in solution (McBride and Bouldin, 1984) and increased dissolved organic matter (DOM) concentrations occur with increasing pH (Kalbitz et al., 2000), the possible mechanism of Cu mobilization is through Cu bound to DOM. Similarly, the radial extent of Cu mobilization is occurring to the greatest degree in surface soils compared to subsurface soils and the organic matter profile in these soils follow the similar trends to the total

mass of Cu likely indicating that biological activity and SOM is likely influencing the mobilization of Cu in surface soil horizons.

Chapter 4: Overall Conclusion and Future Directions

In general, As and Cu concentrations are enriched to a high degree in soils adjacent to CCA treated fence posts while Cr is not, which is attributed to the complexes these metals form in the CCA treated fence posts. Mobilization of Cu and As are occurring to a higher degree in surface soils and in more poorly drained/higher pH conditions. Overall, Fe and Al bearing minerals are the principal sorption mechanisms for As in the soil, with Al controlling As sorption at low pH conditions and Fe playing an increased role at higher pH conditions. Copper is strongly complexed with SOM in surface horizons with a higher degree of inorganic (Cu-Mn) bonds occurring in subsurface horizons. Chromium is likely complexed as chromite ($FeCr_2O_4$), isomorphically substituted for Fe(III) in spinel minerals or as sorption complexes on Mn / Fe containing minerals due to the strong Fe/Mn correlations in the soils exhibited through SXRF mapping. The pH of the soil, which is increasing while moving down the topographic gradient, is resulting in a higher degree of As mobilization likely a result of increases in negative charges on both As and soil minerals. Additionally, pH is influencing Cu mobility possibly through the formation of Cu-DOC complexes. The results indicate metal mobilization occurs to a much greater degree in surface soil horizons as found in contour maps, indicating biologically - mediated processes are likely influencing mobility of Cu and As. Additionally, the low concentrations of Cu and As at the TS position, although fence post concentrations weren't measured, may indicate that poor drainage conditions and the resultant soil physicochemical properties (increased pH, meh-P, meh-Ca, reducing conditions etc.) results in conditions that favor Cu and As mobilization .

To aid in the study of the speciation and mobility of these constituents future investigations should include a detailed soil mineralogical investigation to determine trends occurring along the toposequence. Specifically, an in depth assessment of iron and aluminum containing minerals occurring in these soils should be addressed. Additionally, the detection of Chromite ($FeCr_2O_4$) could support the case that Cr is of geogenic origin. Other toposequences may be sampled in order to assess if field conditions at other sites conform to the findings in this study, whether sites with differing land uses (e.g. forests) show the same trends, and if other poorly drained soils exhibit low As and Cu concentrations. Additionally, investigating the SOM makeup of these soils including DOC and metal concentrations in SOM fractions would be beneficial in understand Cu speciation and mobility. The proportion of Cu complexed to DOC can be tested to confirm or weaken the hypothesis that Cu mobilization is occurring in higher pH conditions as a result of increased concentrations of Cu-DOC complexes. Biologic soil parameters (e.g. As and Fe reducing microorganisms, soil mineralization rate, microbial community profiling) can be assessed to determine which biological indicators may aid in controlling the speciation and mobility of As and Cu, and an assessment of rhizosphere soils and plant biomass can be conducted to assess what role plants are playing in the speciation and mobility of As and Cu.

Appendix 1: Site Location/ Soil Series Specification
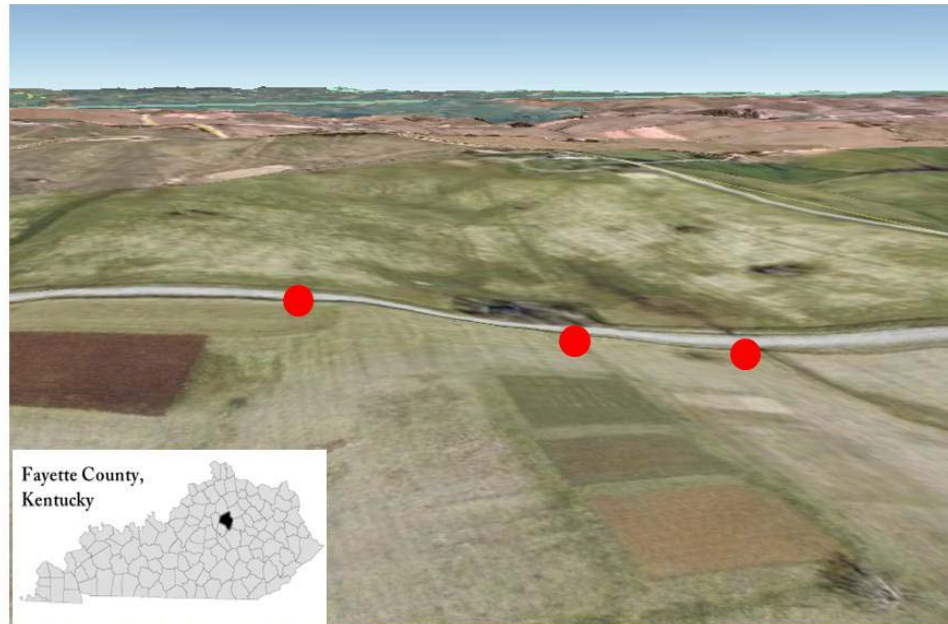
Figure A1. 1: Soil profile sample location adjacent to Iron Works Pike (1973) on the north side of the University of Kentucky Spindletop Farm

The study is located in Fayette County, Kentucky in the Inner Bluegrass region of Kentucky as can be seen in Figure A-1. The average rainfall in this area is ~117 cm (46 inches) with an annual average temperature of ~13 °C (55 °F) (University of Kentucky Agricultural Weather Center). This region is known for its Karst Landscape which causes the gentle rolling topography. A karst landscape occurs where soluble bedrock such as limestone is near the earth's surface. As water weathers the underlying rock it dissolves and creates fractures, thus forming sinkholes and underground streams. The underlying geologic material of the inner bluegrass consists of Lexington limestone, limestone particularly rich in phosphate of the Late Ordovician age. This area is of low relief resulting in the development of deep, phosphate rich soils which have aided the development of this region as the "Horse Capitol of the World".

The sampling site is located adjacent to Iron Works pike (1973) between Newtown Pike (922) and the north entrance to the University of Kentucky's Spindletop Farm. Samples were taken from the fence line adjacent to Iron Works Pike (1973) on Spindletop farm. The topography can be seen in Figure A1-2, from east to west (left to right on paper) the slope consists of a slightly sloping (2-6 percent) area near the left arrow. This area stays slightly sloping for a bit and then slopes at approximately 6-12 percent. The topography levels off near the right arrow where the last sample is taken near an intermittent stream. The total drop in elevation in the sample area is ~10 m over ~140 m (length between arrows) approximate a 4 percent slope through the complete drop. The CCA treated fence had been in place for ~20 years under tall fescue pasture conditions.
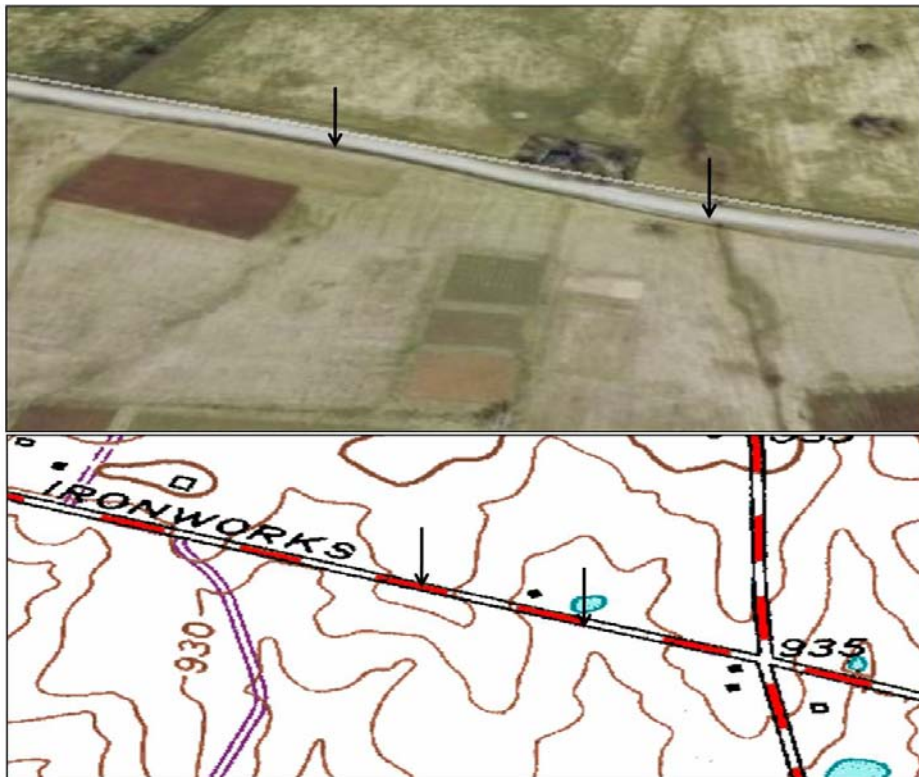

Figure A1. 2: Aerial image of sample site along with the site topographic characteristics. The arrows represent the same areas on both maps and exhibit the extent of sample collection.

Although the accuracy of the web soil survey can be questioned the information provided gave valuable information on the changes of the soil along the fence line. This data, which can be seen in Figure A1-3, along with the topographic data was used to select specific soil sample sites along the fence line. The fence line transects three soil series the Maury silt loam, Donerail silt loam, and Newark silt loam. These soil series have differing pH, drainage class and slope characteristics therefore samples were acquired for each soil series along the fence line. This allows for an analysis of metal mobility and speciation along the toposequence. The Maury silt loam is a Fine, mixed, semiactive, mesic Typic Paleudalfs, the Donerail silt loam a Fine, mixed, active, mesic Oxyaquic Argiudolls, and the Newark silt loam a Fine-silty, mixed, active, nonacid, mesic Fluventic Endoaquepts.

 "The Maury series consists of deep, well drained, moderately permeable soils formed in silty material and weathered limestone, or old alluvium. These soils are on uplands. The Donerail series consists of deep, moderately well drained soils formed in residuum or slope alluvium from limestone. These soils are in slight depressions on uplands or along small drainage ways. The Newark series consists of very deep, somewhat poorly drained soils formed in mixed alluvium from limestone, shale, siltstone, sandstone, and loess. The soil is on nearly level flood plains and in depressions." as stated by the Official Soil Series descriptions.
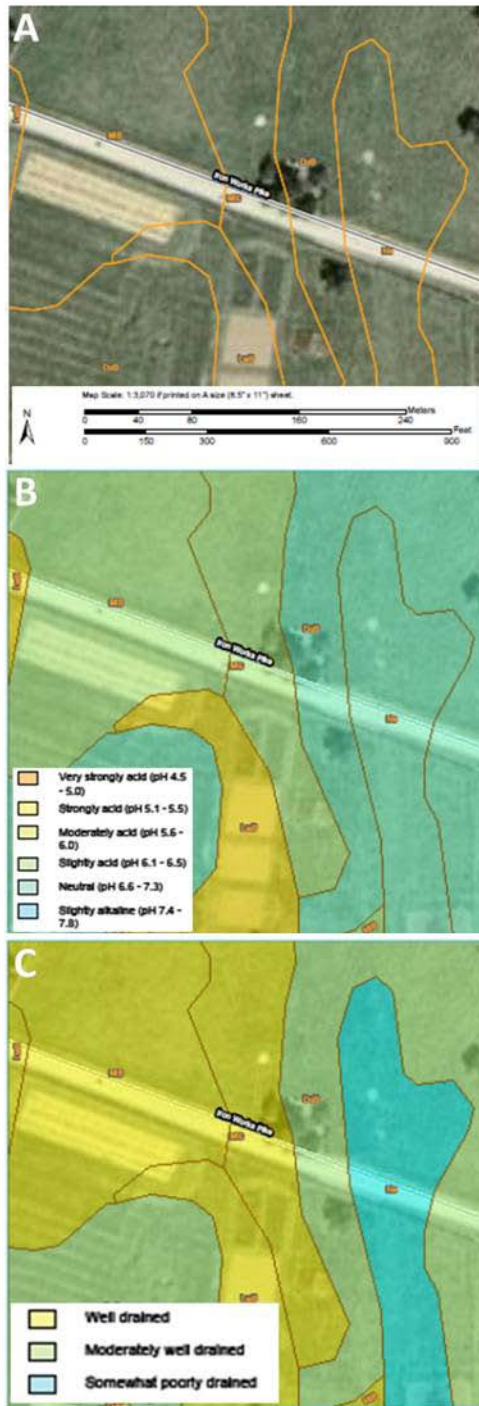
Figure A1. 3: NRCS/USDA Web Soil Survey Images of a) general soil series map, b) soil pH, and c) soil drainage classification.

Soil profile samples were pulled from the hilltop(HT), midslope(MS), and toeslope(TS) position as indicated in Figure A2.1. The sampling along these profiles can be seen in Figures A2.2 to A2.4.

Figure A2. 1: Soil profile sampling locations along Iron Works Pike on the University of Kentucky Spindletop Farm. Hilltop (HT), midslope (MS), toeslope (TS).

cm	30.0-35.0	15.0-20.0	10.0-15.0	5.0-10.0	0.0-5.0	cm	0.0-5.0	5.0-10.0	10.0-15.0	15.0-20.0	30.0-35.0	cm
0-15												0-15
	A1	B1	C1	D1	E1		G1	H1	I1	J1	K1	5
												10
15.0-30.0												15.0-30.0
	A2	B2	C2	D2	E2		G2	H2	I2	J2	K2	20
												25
30.0-60.0												30.0-60.0
												35
	A3	B3	C3	D3	E3		G3	H3	I3	J3	K3	40
						POST						45
												50
												55
60.0-75.0												60.0-75.0
	A4	B4	C4	D4	E4		G4	H4	I4	J4	K4	65
												70
75.0-90.0						F4						75.0-90.0
	A5	B5	C5	D5	E5		G5	H5	I5	J5	K5	80
						F5						85
90.0-105.0												90.0-105.0
	A6	B6	C6	D6	E6	F6	G6	H6	I6	J6	K6	105-110
												100
105-110						F7						105

Figure A2. 2: Sampling Scheme for the Hilltop (HT) soil.

cm	30.0-35.0	15.0-20.0	10.0-15.0	5.0-10.0	0.0-5.0	cm	0.0-5.0	5.0-10.0	10.0-15.0	15.0-20.0	30.0-35.0	cm
0-15	A1	B1	C1	D1	E1		G1	H1	I1	J1	K1	0-15
15.0-30.0	A2	B2	C2	D2	E2		G2	H2	I2	J2	K2	15.0-30.0
30.0-60.0	A3	B3	C3	D3	E3	POST	G3	H3	I3	J3	K3	30.0-60.0
60.0-81.0	A4	B4	C4	D4	E4		G4	H4	I4	J4	K4	60.0-81.0
81-90	A5	B5	C5	D5	E5	F5	G5	H5	I5	J5	K5	81-90
90-110	A6	B6	C6	D6	E6	F6	G6	H6	I6	J6	K6	90-110
110-115						F7						110-115

Figure A2. 3: Sampling scheme for the Midslope (MS) soil.

cm	30.0-35.0	15.0-20.0	10.0-15.0	5.0-10.0	0.0-5.0	cm	0.0-5.0	5.0-10.0	10.0-15.0	15.0-20.0	30.0-35.0	cm
0-15	A1	B1	C1	D1	E1		G1	H1	I1	J1	K1	0-15
												5
												10
15.0-30.0	A2	B2	C2	D2	E2		G2	H2	I2	J2	K2	15.0-30.0
												20
												25
30.0-60.0	A3	B3	C3	D3	E3	POST	G3	H3	I3	J3	K3	30.0-60.0
												35
												40
												45
												50
												55
60.0-90.0	A4	B4	C4	D4	E4		G4	H4	I4	J4	K4	60.0-90.0
												65
												70
												75
												80
												85
90-105	A5	B5	C5	D5	E5	F5	G5	H5	I5	J5	K5	90-105
												95
												100
105-120	A6	B6	C6	D6	E6	F6	G6	H6	I6	J6	K6	105-120
												110
												115
120-125						F7						120-125

Figure A2. 4: Sampling scheme for the Toeslope (TS) soil.

97

Appendix 3: Soil Physicochemical Properties

Table A3-1: Basic Soil Properties*

Depth	Soil Texture Class	Sand %	Silt %	Clay %	SOM % B	SOM % A	Total N% B	Total N% A
Hilltop								
0 to 15	Silt Loam	14	71	15	4.11	3.47	0.23	0.20
15 to 30	Silt Loam	11	71	18	1.77	1.91	0.12	0.12
30 to 60	Silty Clay Loam	12	60	29	0.88	1.07	0.07	0.08
60 to 90	Silty Clay Loam	16	48	36	0.40	0.40	0.06	0.05
BP: 75 to 80 cm	Silty Clay Loam	15	50	34	0.86		0.08	
Midslope								
0 to 15	Silt Loam	11	75	14	3.46	3.82	0.22	0.23
15 to 30	Silt Loam	9	76	16	2.20	2.51	0.16	0.17
30 to 60	Silt Loam	9	65	26	1.03	1.31	0.09	0.10
60 to 90	Silty Clay Loam	15	53	31	0.57	0.58	0.06	0.07
BP: 80 to 90 cm	Silty Clay Loam	14	52	34	0.76		0.07	
Toeslope								
0 to 15	Silt Loam	10	78	12	4.09	6.55	0.24	0.29
15 to 30	Silt Loam	6	81	13	3.04	3.11	0.20	0.21
30 to 60	Silt Loam	5	79	16	1.03	1.15	0.07	0.08
60 to 90	Silt Loam	11	65	24	2.13	2.18	0.12	0.13
90–105	Silt Loam	17	56	27	2.15	2.61	0.12	0.16
BP: 90–105 cm	Silt Loam	14	62	24	2.61		0.16	

Soil Texture spans Soil Texture Class, Sand %, Silt %, Clay %. *Carbon and Nitrogen* spans SOM % (B, A) and Total N% (B, A).

* Below Post(BP), B indicates Background samples, A indicates soil adjacent to CCA post (0–5 cm)

Table A3-2: Basic Soil Properties*

Depth	pH B	pH A	bufpH B	bufpH A	CEC (meq/100g) B	CEC (meq/100g) A	ExchK B	ExchK A	ExchCa B	ExchCa A	ExchMg B	ExchMg A	ExchNa B	ExchNa A	Base Saturation % B	Base Saturation % A
Hilltop																
0 to 15	5.2	4.4	6.2	5.6	19.6	16.9	0.16	0.30	5.85	2.24	1.38	0.50	0.08	0.06	38.0	18.3
15 to 30	5.9	5.1	6.7	6.2	14.6	15.1	0.09	0.20	7.15	5.21	0.68	0.54	0.08	0.09	54.8	39.9
30 to 60	6.0	5.7	6.6	6.4	15.7	16.3	0.14	0.16	8.27	7.92	0.65	0.69	0.12	0.11	58.4	54.5
60 to 90	5.5	5.4	6.2	6.2	18.2	19.6	0.11	0.13	7.81	8.03	0.92	1.12	0.09	0.09	49.0	47.7
BP: 75 to 80 cm	5.6		6.3		19.6		0.14		8.59		1.22		0.08		51.1	
Midslope																
0 to 15	5.7	5.1	6.6	6.0	16.9	16.9	0.25	0.27	7.01	3.00	1.27	0.50	0.38	0.86	52.7	27.3
15 to 30	6.1	5.2	6.7	6.1	15.6	15.6	0.10	0.18	7.77	5.02	0.83	0.55	0.23	0.28	57.2	38.6
30 to 60	6.4	6.0	6.8	6.6	14.4	15.0	0.12	0.14	9.15	8.05	0.85	0.72	0.12	0.19	70.9	60.7
60 to 90	6.3	6.2	6.7	6.6	17.6	18.3	0.15	0.16	10.60	10.34	1.02	1.02	0.15	0.19	67.8	64.0
BP: 80 to 90 cm	6.3		6.8		18.3		0.17		11.18		1.07		0.13		68.6	
Toeslope																
0 to 15	6.8	6.6	7.1	7.0	21.2	22.3	0.34	0.30	13.22	14.05	2.06	2.31	0.08	0.08	74.2	75.1
15 to 30	7.1	7.1	7.2	7.1	21.1	19.8	0.11	0.13	13.18	12.33	1.23	1.53	0.11	0.09	69.2	71.1
30 to 60	7.4	7.1	7.2	7.1	14.4	12.8	0.08	0.08	9.68	9.30	0.76	0.61	0.26	0.21	75.1	79.8
60 to 90	7.3	7.1	7.1	7.1	21.1	20.3	0.19	0.17	15.22	14.76	1.29	1.15	0.44	0.47	81.1	81.4
90-105	7.3	7.1	7.0	7.1	25.6	23.7	0.29	0.22	19.15	16.28	1.66	1.33	0.53	0.49	84.4	77.2
BP: 90-105 cm	7.1		7.1		23.7		0.22		16.28		1.33		0.49		77.2	

* Below Post(BP), B indicates Background samples, A indicates soil adjacent to CCA post (0-5 cm)

Table A3-3: Basic Soil Properties*

Mehlich III Extractable (mg/dm³) and Select Total Exchangeable Cations (mg/kg)

Depth	MehP B	MehP A	MehK B	MehK A	ExchK B	ExchK A	MehCa B	MehCa A	ExchCa B	ExchCa A	MehMg B	MehMg A	ExchMg B	ExchMg A	MehZn B	MehZn A	MehCd B	MehCd A	MehCr B	MehCr A	MehNi B	MehNi A	MehPb B	MehPb A	MehZn B	MehZn A	MehCu B	MehCu A
Hilltop																												
0 to 15 cm	77	155	60	112	63	117	1173	475	1172	449	161	60	168	61	3.10	2.25	0.04	0.08	BDL	BDL	0.46	0.32	2.64	2.47	3.08	2.25	9.3	188.7
15 to 30 cm	31	87	38	78	35	78	1443	1090	1433	1044	83	68	83	66	0.85	2.45	BDL	0.10	BDL	BDL	0.76	0.34	1.37	1.58	0.85	2.43	3.8	258.1
30 to 60 cm	36	76	54	63	55	63	1729	1584	1657	1587	85	85	79	84	0.60	1.20	BDL	0.07	BDL	BDL	0.74	0.24	0.88	1.25	0.59	1.21	3.1	203.0
60 to 90 cm	55	60	45	48	43	51	1591	1691	1565	1609	111	142	112	136	0.45	0.90	BDL	BDL	BDL	BDL	BDL	0.45	0.44	0.41	0.44	0.91	2.0	11.4
BP:75 to 80 cm	72		54		55		1804		1721		155		148		0.70		BDL		BDL		0.20		1.33		0.72		30.1	
Midslope																												
0 to 15 cm	70	118	93	95	98	106	1311	559	1405	601	138	54	154	61	3.45	4.50	0.05	0.07	BDL	BDL	0.42	0.49	3.52	3.63	3.43	4.47	9.6	123.8
15 to 30 cm	36	90	40	66	39	70	1604	900	1557	1006	100	62	101	67	1.30	4.00	0.03	0.11	BDL	BDL	0.36	0.40	2.17	1.92	1.30	3.93	4.1	354.9
30 to 60 cm	44	70	48	55	47	55	1887	1598	1834	1613	106	86	103	87	2.10	7.45	BDL	0.09	BDL	BDL	BDL	BDL	1.18	1.30	2.11	7.15	9.6	267.6
60 to 90 cm	75	97	61	62	59	63	2195	2116	2124	2072	126	124	124	124	2.45	6.40	BDL	0.05	BDL	BDL	BDL	BDL	0.83	0.98	2.38	6.31	9.6	105.5
BP:80 to 90 cm	91		64		66		2208		2240		124		130		7.00		BDL		BDL		0.78		1.43		6.82		40.2	
Toeslope																												
0 to 15 cm	111	91	121	92	133	117	2725	2456	2649	2815	248	235	250	281	7.55	8.65	0.06	0.05	0.09	0.67	0.34	0.32	5.64	5.05	7.27	8.45	4.5	20.3
15 to 30 cm	55	56	40	51	43	51	2737	2712	2641	2471	154	196	149	186	4.50	5.10	0.06	0.05	0.06	0.44	0.31	0.32	5.20	5.36	4.28	5.01	4.4	16.0
30 to 60 cm	77	61	33	36	31	31	2012	1997	1940	1864	98	83	92	74	0.70	0.80	BDL	BDL	0.05	0.16	0.23	0.27	2.51	2.64	0.71	0.79	2.3	7.9
60 to 90 cm	134	130	68	65	74	66	3056	3177	3050	2958	156	146	157	140	1.60	2.15	BDL	BDL	0.07	0.09	0.30	0.32	3.35	3.92	1.59	2.12	3.8	7.8
90-105 cm	159	148	107	77	113	86	3979	3283	3837	3262	203	157	202	162	2.35	3.25	BDL	BDL	0.1	0.28	0.26	0.83	2.38	5.91	2.35	3.20	7.7	30.1

* Below Post (BP), B indicates Background samples, A indicates soil adjacent to CCA post (0-5 cm)

Statistical Differences in Background Soil Properties

	pH	CEC	meh-Ca	meh-P	SOM*
Hilltop	5.34[a]	16.5[a]	1548[a]	55[a]	0.69[a]
Midslope	6.30[b]	17.3[a]	1841[a]	63[a]	0.87[a]
Toeslope	6.85[c]	20.2[b]	2902[b]	107[b]	1.62[b]

*at 30-105 cm depth

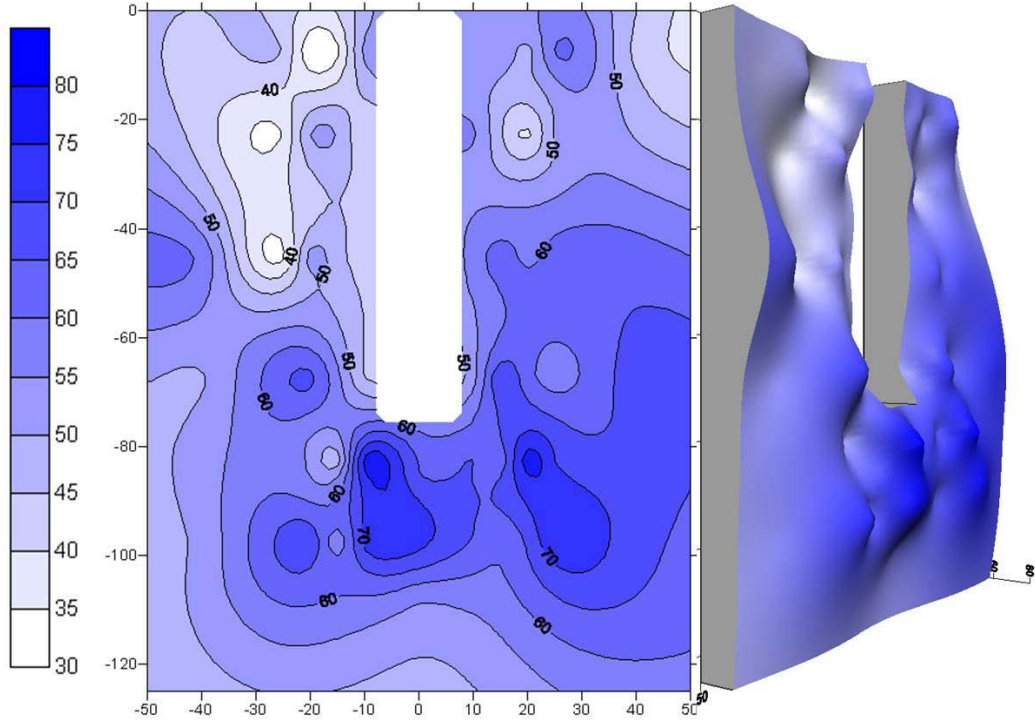**Appendix 4: Geostatistical Profile Metal Concentration Mapping**
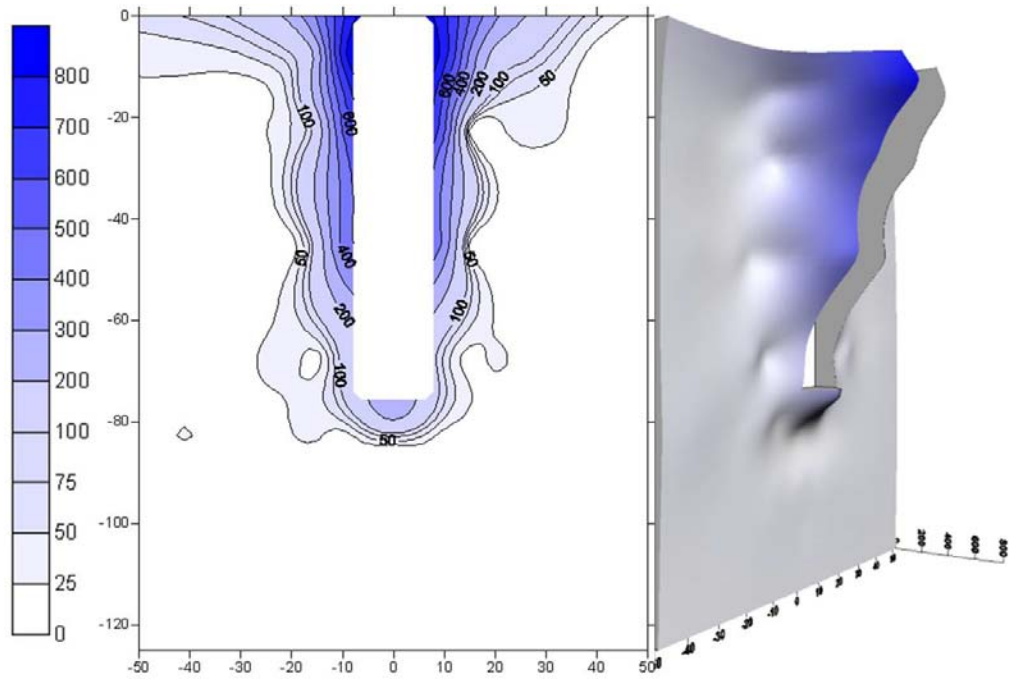
Figure A4. 1: Hilltop soil profile contour map of Arsenic concentration (ppm). The blanked section indicates region where post enters the soil.
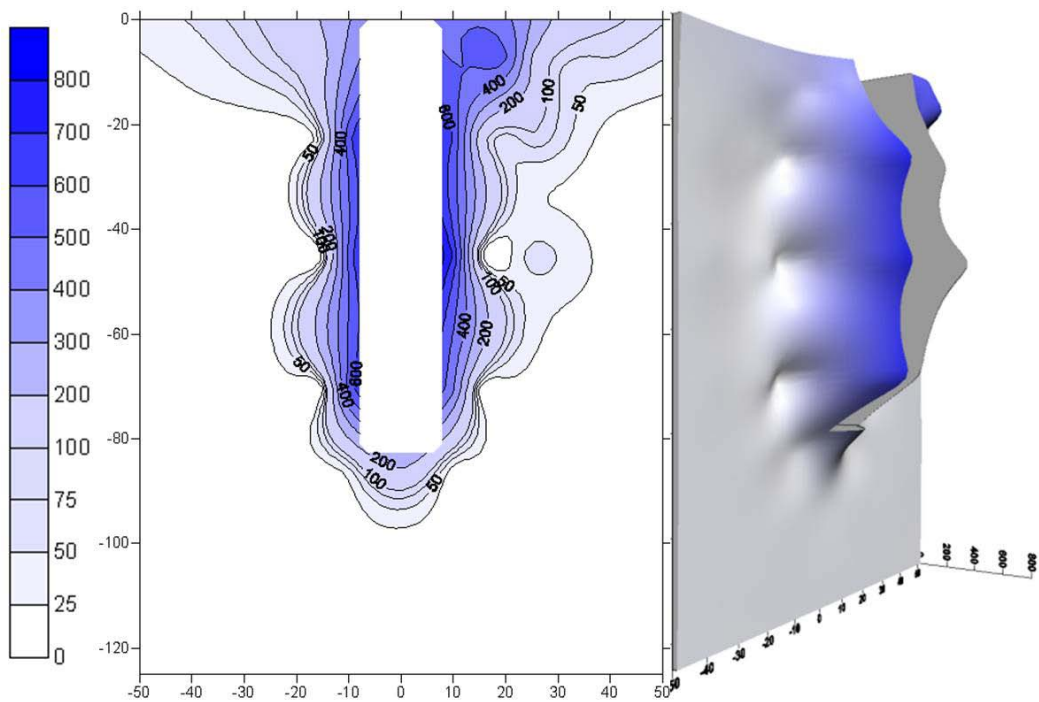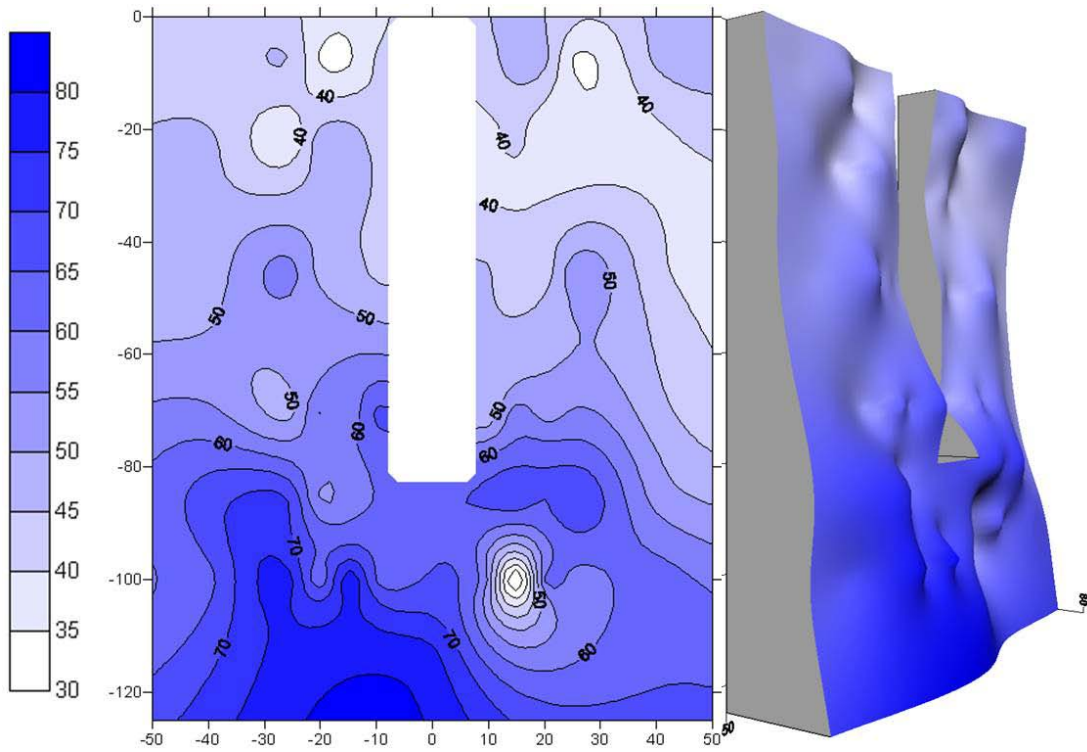

Figure A4. 2: Midslope soil profile contour map of Arsenic concentration (ppm). The blanked section indicates region where post enters the soil.
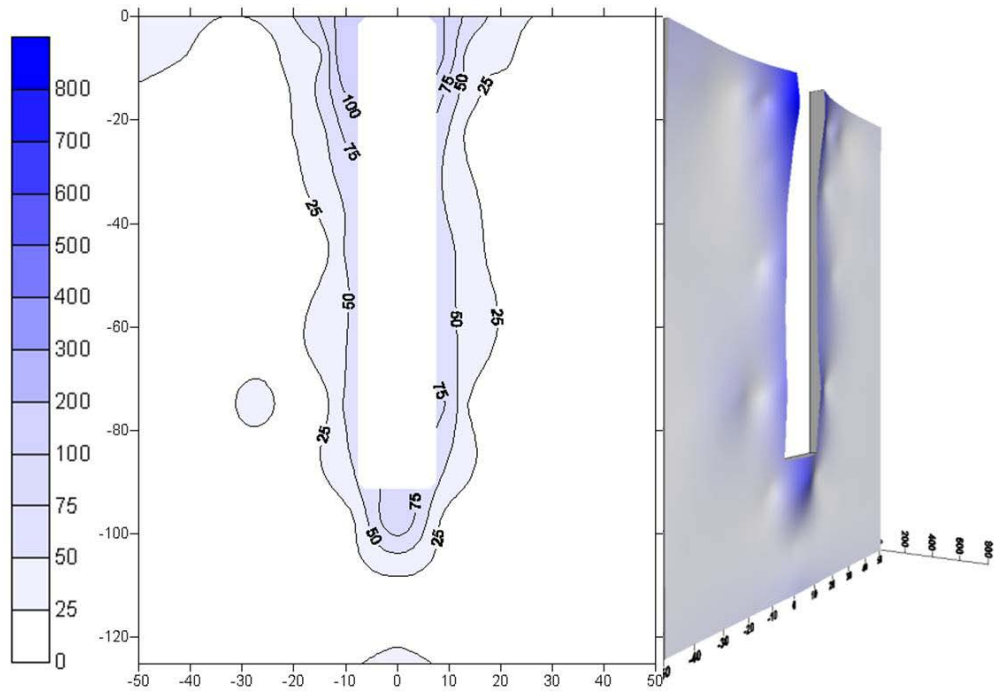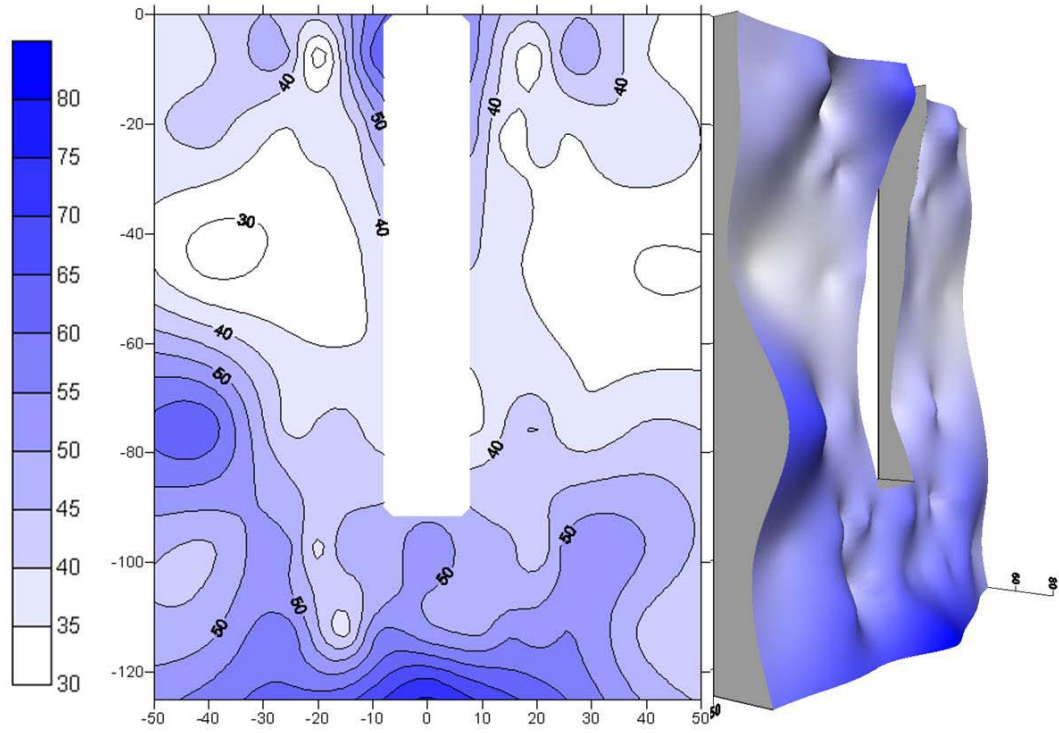
Figure A4. 3: Toeslope soil profile contour map of Arsenic concentration (ppm). The blanked section indicates region where post enters the soil.
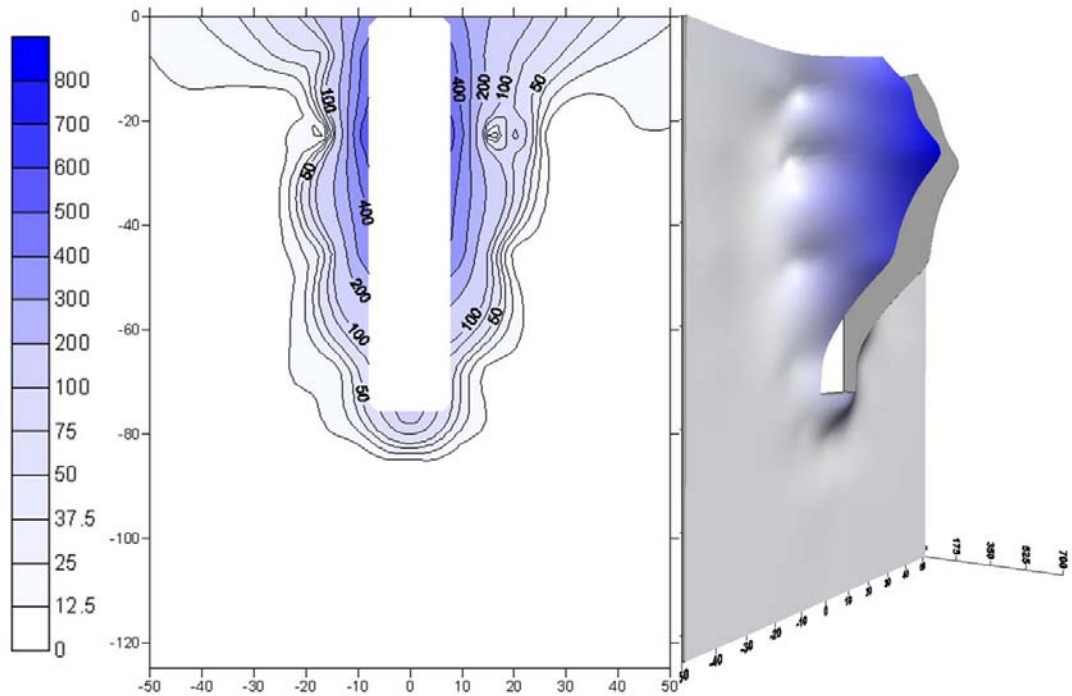
Figure A4. 4: Hilltop soil profile contour map of Copper concentration (ppm). The blanked section indicates region where post enters the soil.
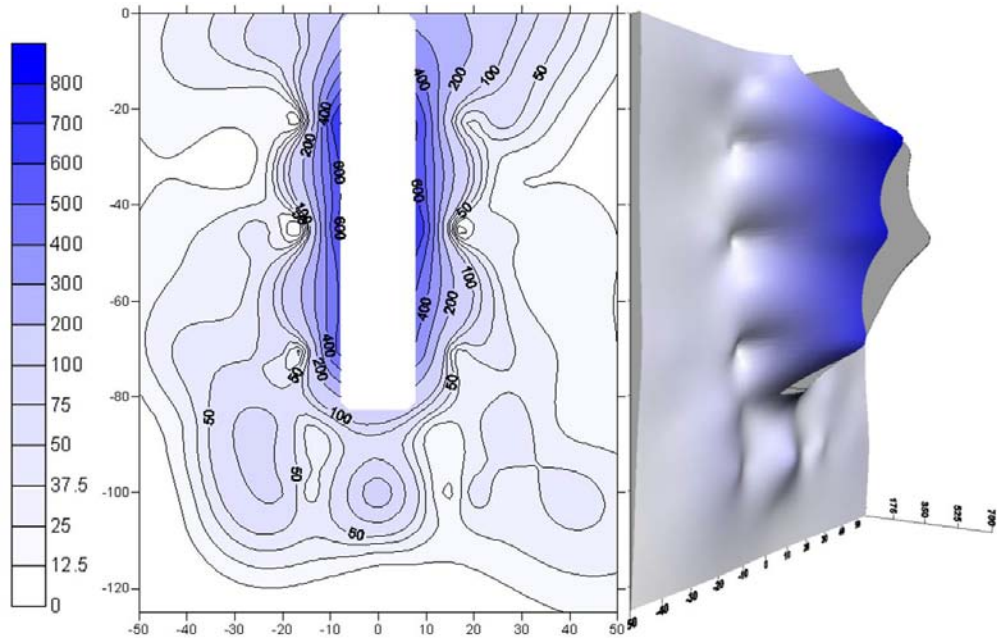
Figure A4. 5: Midslope soil profile contour map of Copper concentration (ppm). The blanked section indicates region where post enters the soil.
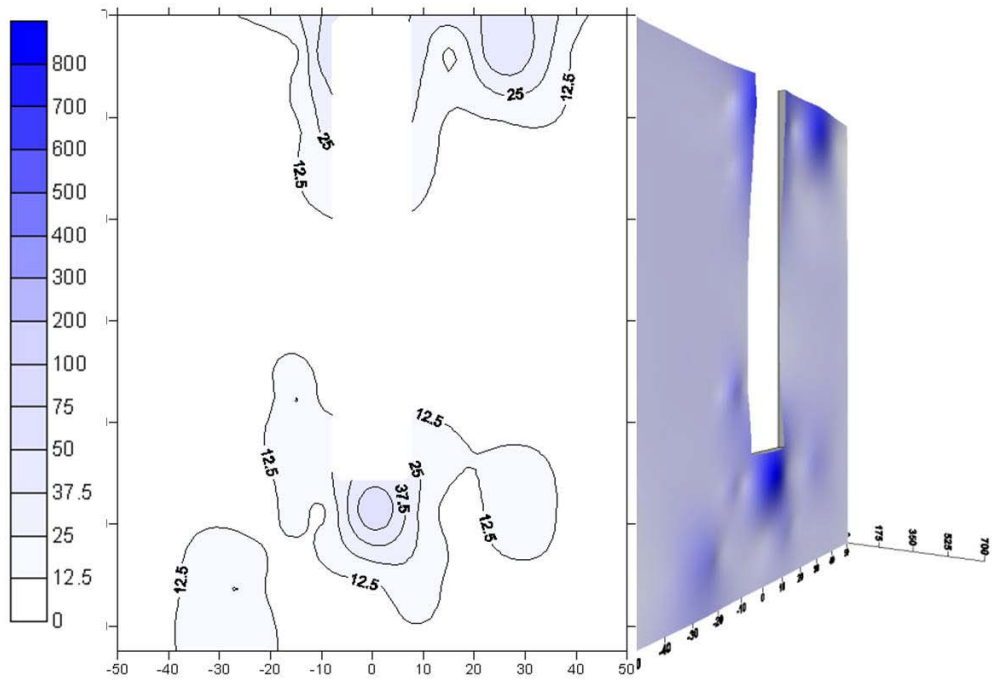
Figure A4. 6: Toeslope soil profile contour map of Copper concentration (ppm). The blanked section indicates region where post enters the soil.
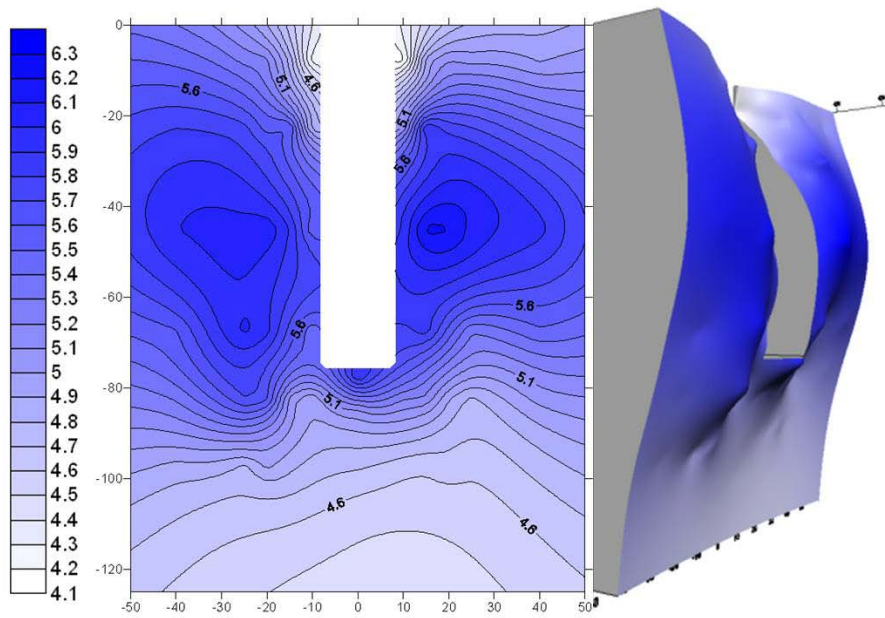
Figure A4. 7: Hilltop soil profile contour map of Chromium concentration (ppm). The blanked section indicates region where post enters the soil.

Figure A4. 8: Midslope soil profile contour map of Chromium concentration (ppm). The blanked section indicates region where post enters the soil.

Figure A4. 9: Toeslope soil profile contour map of Chromium concentration (ppm). The blanked section indicates region where post enters the soil.

Figure A4. 10: Hilltop soil profile contour map of pH. The blanked section indicates region where post enters the soil. The pH range in the soil was from 4.2 to 6.2.
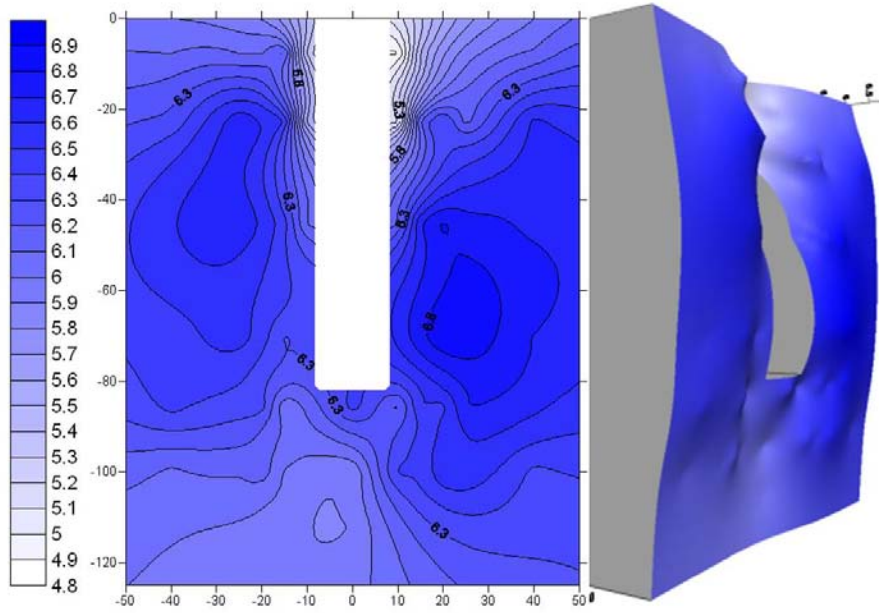
Figure A4. 11: Midslope soil profile contour map of pH. The blanked section indicates region where post enters the soil. The pH range in the soil was from 4.9 to 6.9.
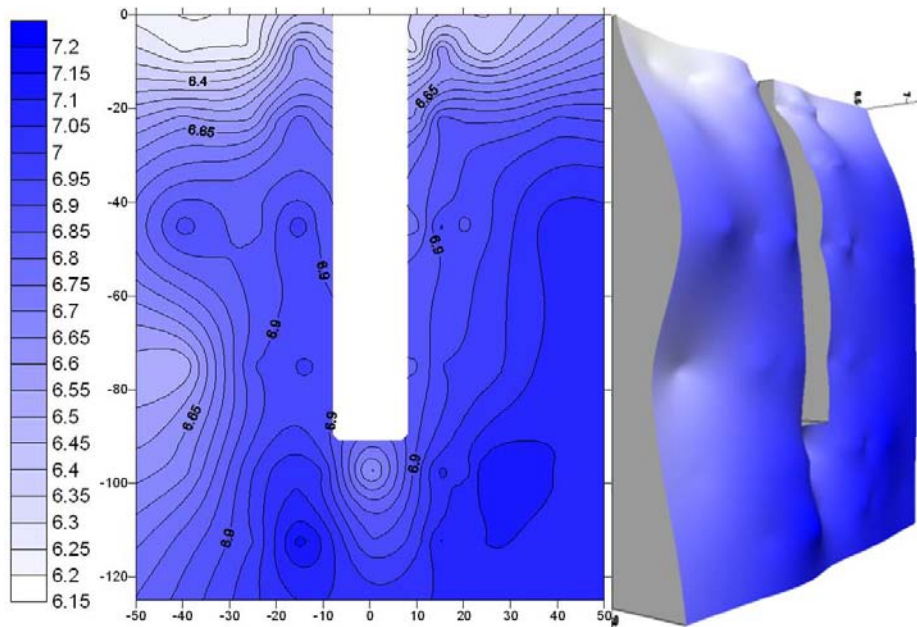

Figure A4. 12: Toeslope soil profile contour map of pH. The blanked section indicates region where post enters the soil. The pH range in the soil was from 6.2 to 7.2.
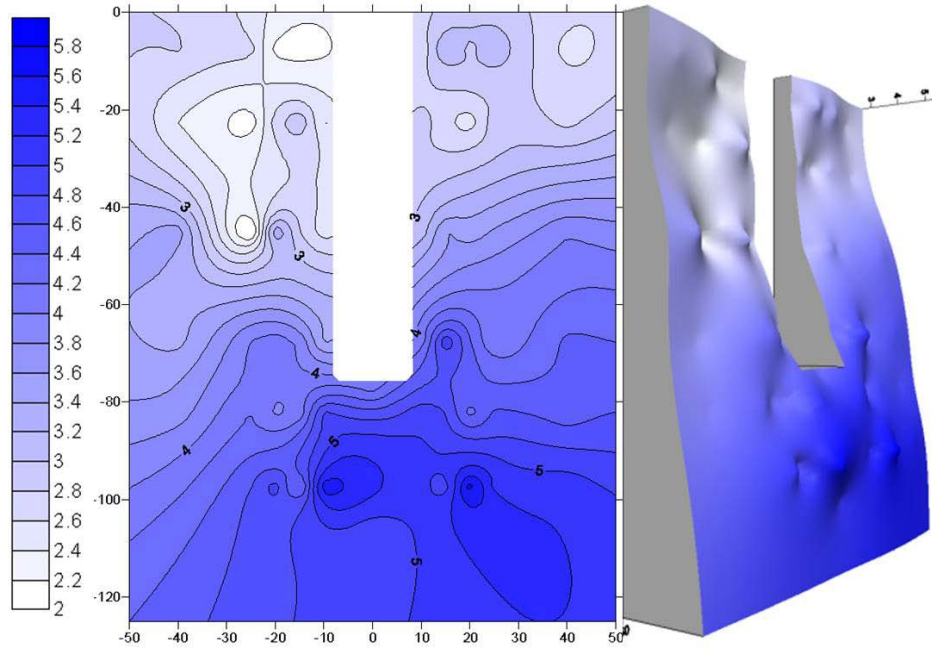
Figure A4. 13: Hilltop soil profile contour map of Iron %. The blanked section indicates region where post enters the soil.
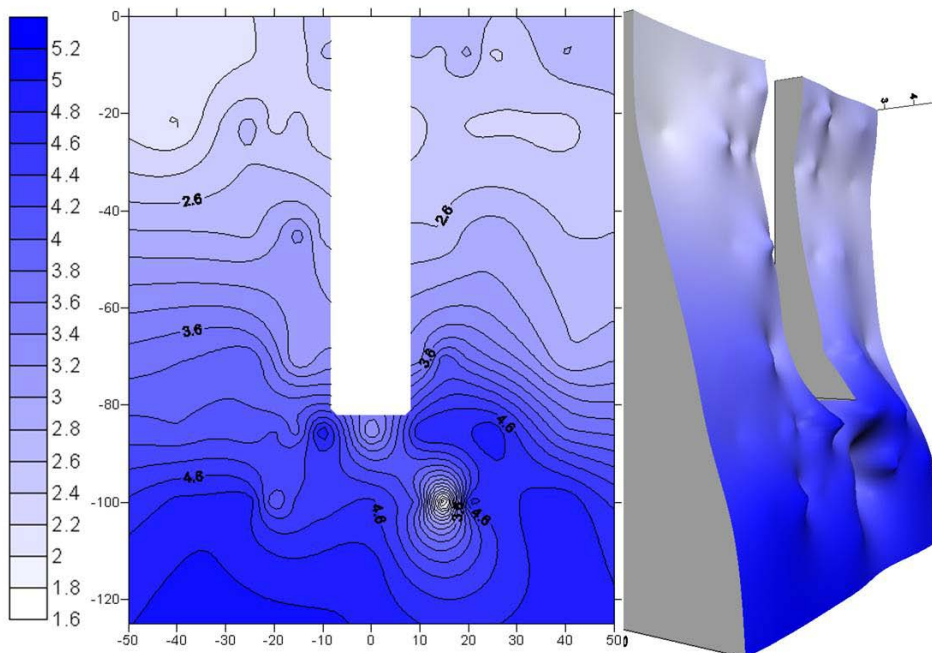

Figure A4. 14: Midslope soil profile contour map of Iron %. The blanked section indicates region where post enters the soil.
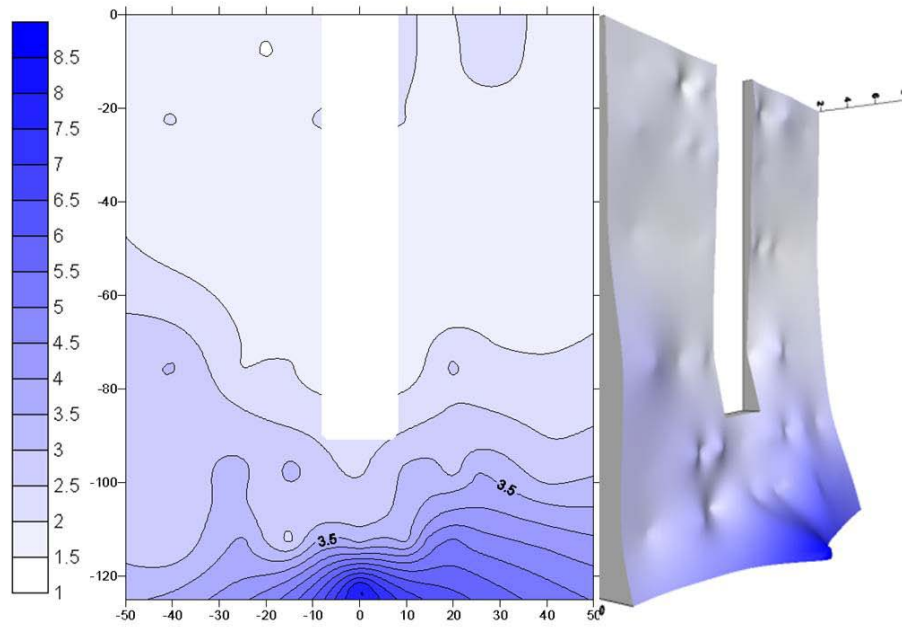
Figure A4. 15: Toeslope soil profile contour map of Iron %. The blanked section indicates region where post enters the soil.
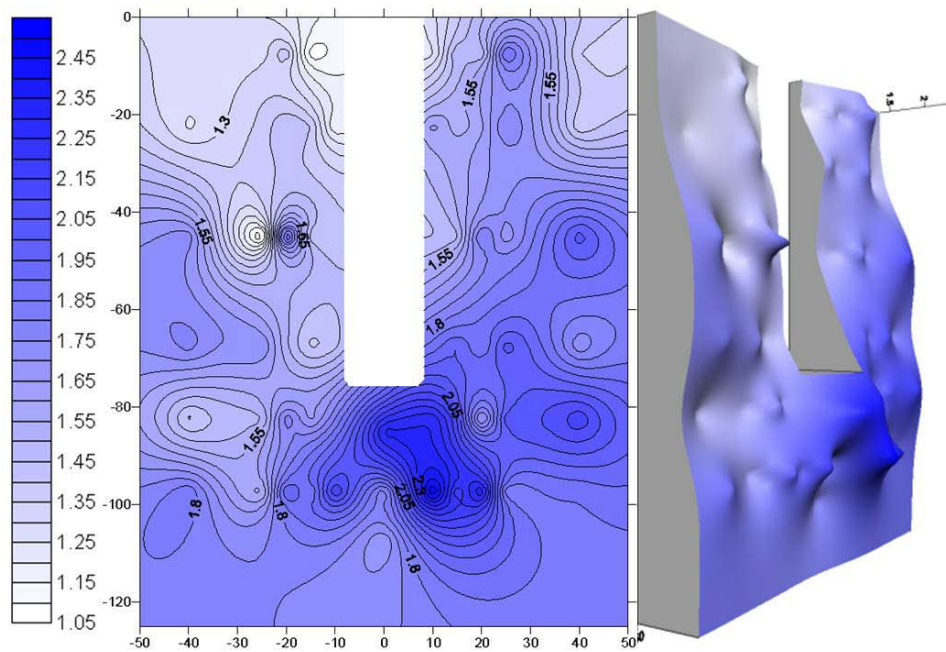

Figure A4. 16: Hilltop soil profile contour map of Aluminum %. The blanked section indicates region where post enters the soil.
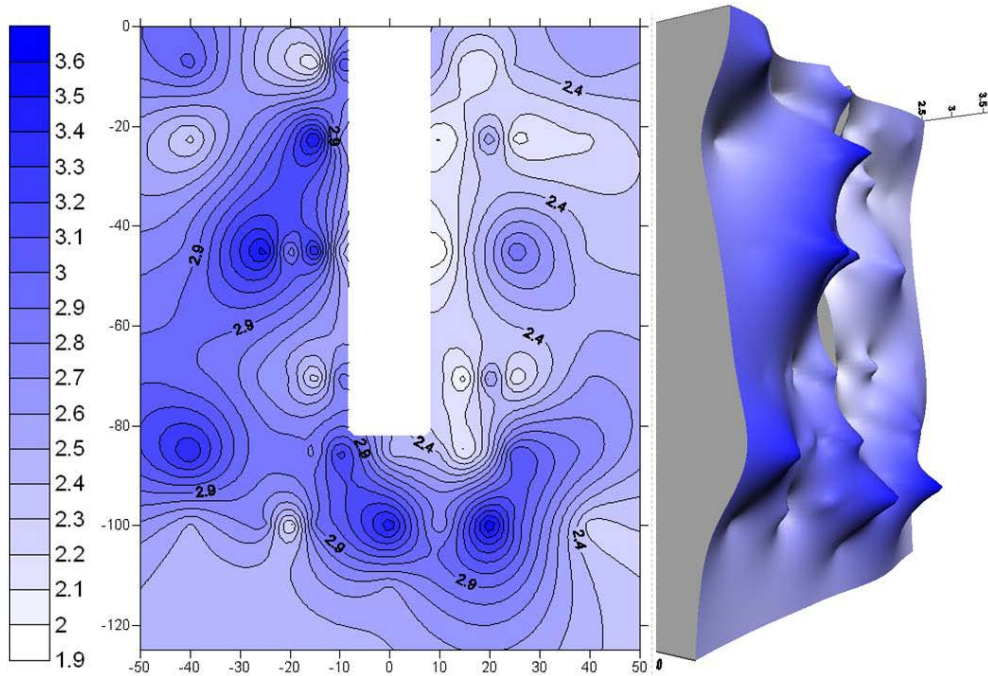
Figure A4. 17: Midslope soil profile contour map of Aluminum %. The blanked section indicates region where post enters the soil.
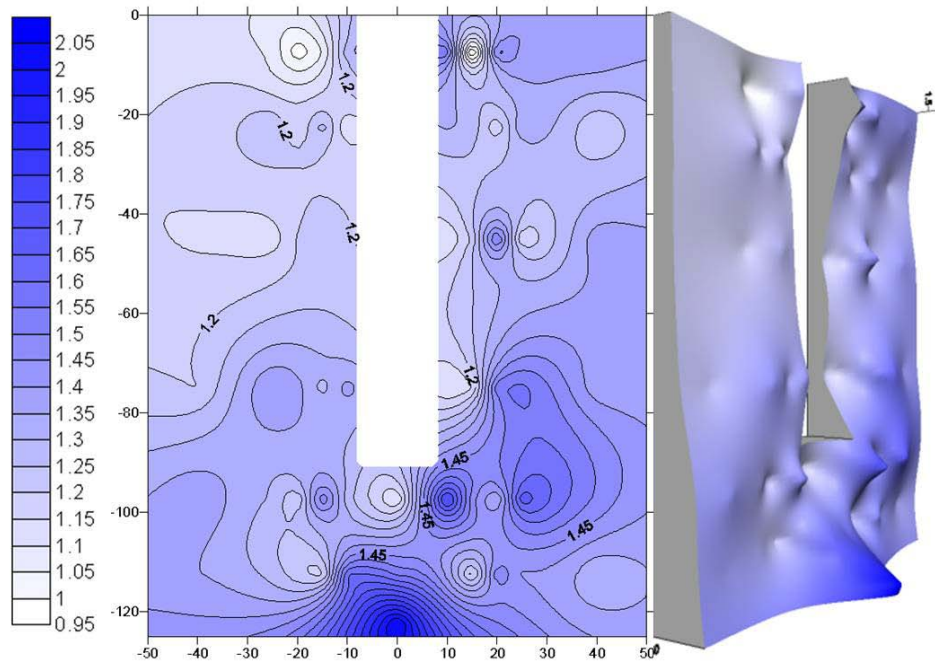

Figure A4. 18: Toeslope soil profile contour map of Aluminum %. The blanked section indicates region where post enters the soil.

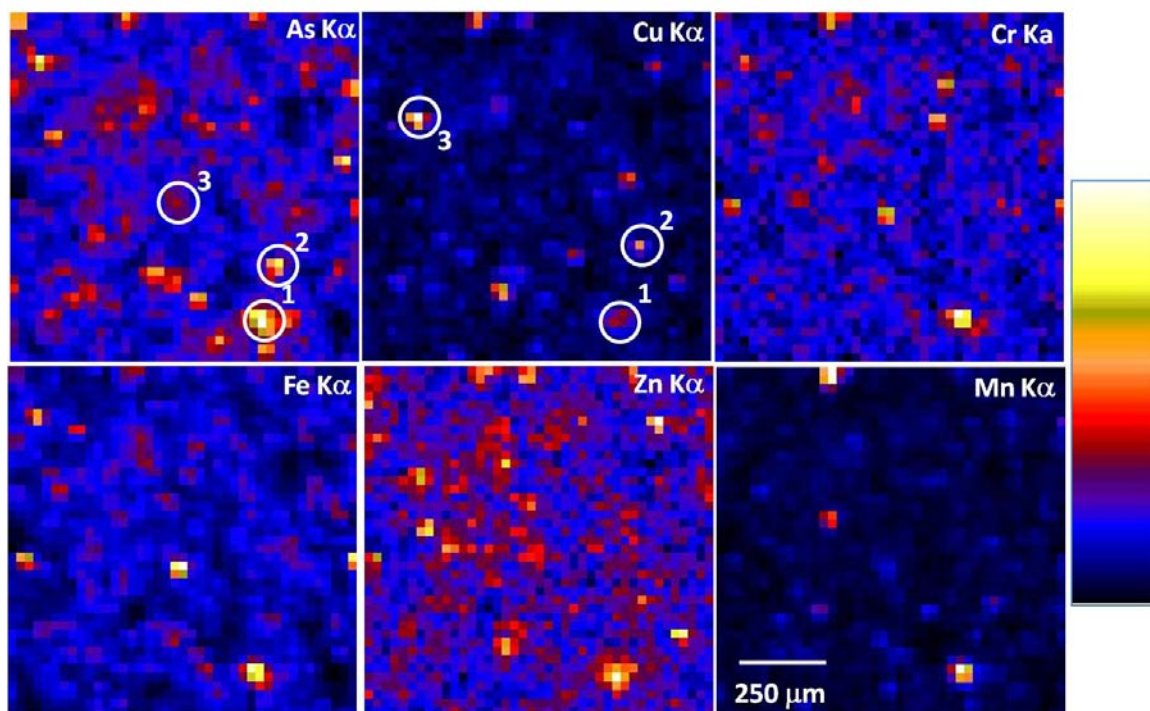**Appendix 5: μ-SXRF Images and Elemental Correlations**

Figure A5. 1: Hilltop surface soil (0-5 cm from post, 0-15 cm depth, file AE1 Map1) XRF elemental mapping. Minimum values correspond to black and maximum to white.

Arsenic 479 – 2098 counts, copper 136 – 1137 counts, chromium 42-223 counts, iron 3338 – 19244 counts, zinc 43 – 203 counts, manganese 171 – 3113 counts. Spots indicate regions where μXAFS data taken. Arsenic map spot 1, (40.708, 39.920) counts As-1895, Cu- 396, Cr- 178, Fe- 15314, Zn- 144, Mn- 2280. Arsenic map spot 2, (40.758,40.070), counts As- 1759, Cu- 251 , Cr- 95, Fe- 8510 , Zn- 95 , Mn- 463. Arsenic map spot 3,(40.458, 40.250), counts As- 1093, Cu- 251 , Cr- 107, Fe- 7787 , Zn- 116 , Mn- 475. Copper map spot 1, (40.733, 39.920), counts As- 1292, Cu- 504 , Cr- 78, Fe- 8391 , Zn- 125 , Mn- 731. Copper map spot 2, (40.782, 40.120), counts As- 1086, Cu- 688 , Cr- 94, Fe- 6165 , Zn- 128 , Mn- 1055. Copper map spot 3, (40.133, 40.490), counts As- 872, Cu- 1137 , Cr- 96, Fe- 6267 , Zn- 149 , Mn- 353. Maps generated at the Advanced Photon source beamline 13-BM-D Argonne National Laboratory, IL.

111

Figure A5. 2: Hilltop subsurface soil (beneath post, file AF4 map1) XRF elemental mapping. Minimum values correspond to black and maximum to white.

Arsenic 112 – 1666 counts, copper 47 – 1476 counts, chromium 35-284 counts, iron 2647 – 36155 counts, zinc 48 – 1375 counts, manganese 98 – 2761 counts. Spots indicate regions where μXAFS data was taken. Arsenic map spot 1, (40.808, 40.045), counts As- 1666, Cu- 182 , Cr- 182 , Fe- 16749, Zn- 226 , Mn- 530. Arsenic map spot 2, (41.083, 39.870), counts As- 809, Cu- 257 , Cr- 257, Fe- 10918 , Zn- 105 , Mn- 2021. Maps generated at the Advanced Photon source beamline 13-BM-D Argonne National Laboratory, IL.
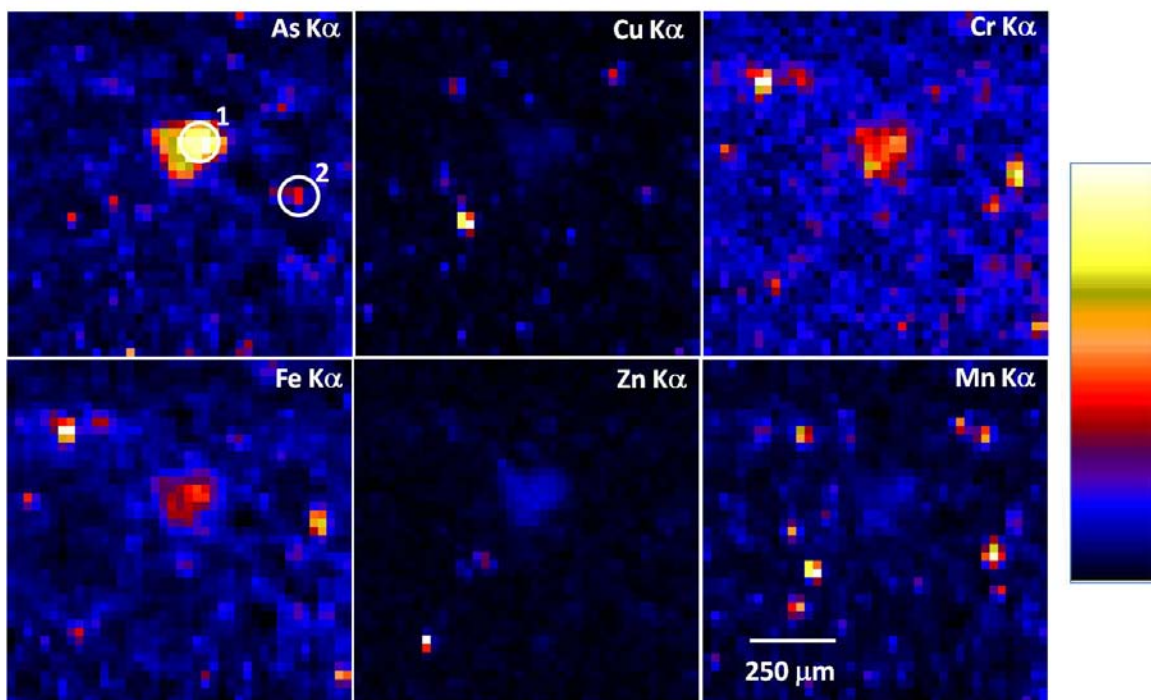
Figure A5. 3: Hilltop subsurface soil (beneath post, file AF4 map 2) XRF elemental mapping. Minimum values correspond to black and maximum to white.

Arsenic 117 – 3590 counts, copper 42 – 1542 counts, chromium 38-450 counts, iron 2451 – 31238 counts, zinc 46 – 461 counts, manganese 105 – 5569 counts. Spots indicate regions where μXAFS data was taken. Arsenic map spot 1, (41.283, 38.745), As- 2771, Cu- 408 , Cr- 267 , Fe- 27140 , Zn- 301, Mn- 828. Arsenic map spot 2, (41.458, 39.270), As- 1582, Cu- 291, Cr- 87, Fe- 6478, Zn- 103, Mn- 285. Arsenic map spot 3, (41.953, 38.600), As- 3590, Cu- 190, Cr- 111, Fe- 7572, Zn- 74, Mn- 423. Copper map spot 1, (41.528, 38.920), As- 741 , Cu- 728 , Cr- 190 , Fe- 14432, Zn- 240, Mn- 2983. Copper map spot 2, (41.083, 38.890), location not on this map incorrect data entry? Maps generated at the Advanced Photon source beamline 13-BM-D Argonne National Laboratory, IL.

Figure A5. 4: Toeslope surface soil (0-5 cm from post, 0-15 cm depth, and file BE1 map 1) XRF elemental mapping. Minimum values correspond to black and maximum to white.

Arsenic 159 – 1660 counts, copper 67 – 271 counts, chromium 37-291 counts, iron 1671 – 34791 counts, zinc 66 – 302 counts, manganese 89 – 1733 counts. Spots indicate regions where μXAFS data was taken. Arsenic map spot 1, (36.653, 40.745), As- 1660, Cu- 134, Cr- 270, Fe- 34791, Zn- 215, Mn- 939. Arsenic map spot 2, (35.608, 40.170), As- 1191, Cu- 235, Cr- 113, Fe- 12194, Zn- 302, Mn- 453. Arsenic map spot 3, (35.958, 40.420), As- 973, Cu- 148, Cr- 94, Fe- 5150, Zn- 128, Mn- 231. Copper map spot 1, (35.608, 40.155), As- 1191, Cu- 235, Cr- 113, Fe- 12194, Zn- 302, Mn- 453. Maps generated at the Advanced Photon source beamline 13-BM-D Argonne National Laboratory, IL.
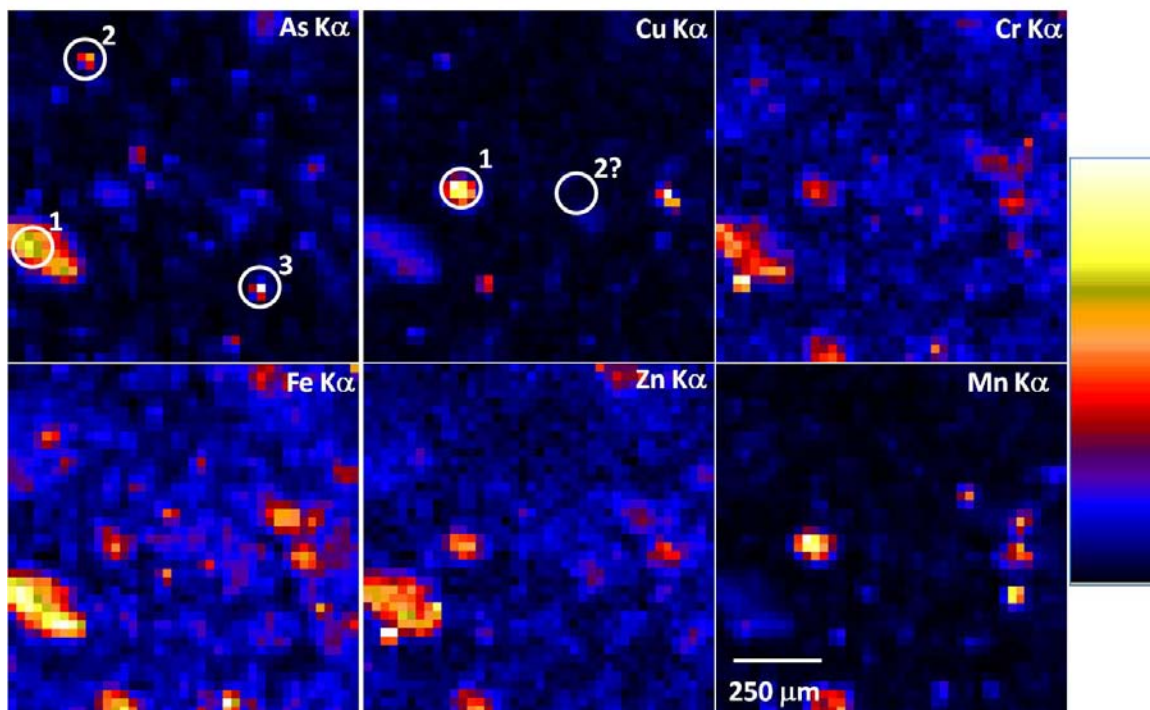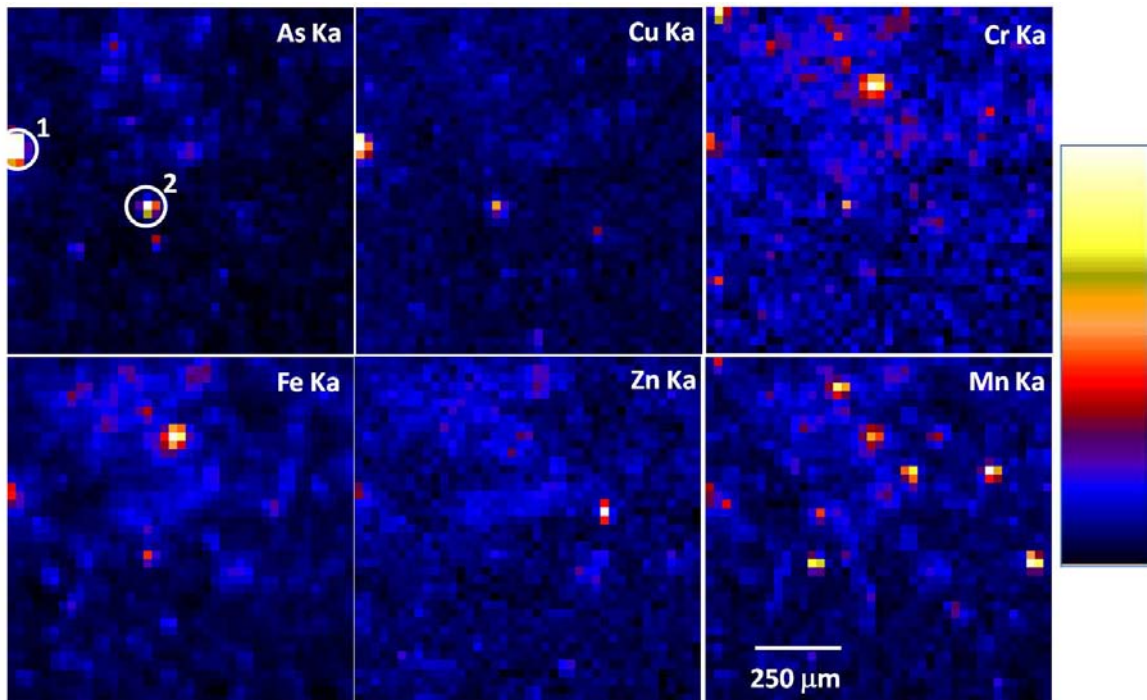
Figure A5. 5: Toeslope subsurface soil (beneath post, file BF5 map 2) XRF elemental mapping. Minimum values correspond to black and maximum to white.

Arsenic 88 – 6172 counts, copper 38 – 596 counts, chromium 28-203 counts, iron 1217 – 22248 counts, zinc 41 – 426 counts, manganese 51 – 782 counts. Spots indicate regions where μXAFS data was taken. Arsenic map spot 1, (36.390,39.670), As- 5878 , Cu- 596 , Cr- 113 , Fe- 10710 , Zn- 178, Mn- 296. Arsenic map spot 2, (36.785, 39.480), As- 1878, Cu- 379 , Cr- 127 , Fe- 11243 , Zn- 120 , Mn- 178. Maps generated at the Advanced Photon source beamline 13-BM-D Argonne National Laboratory, IL.

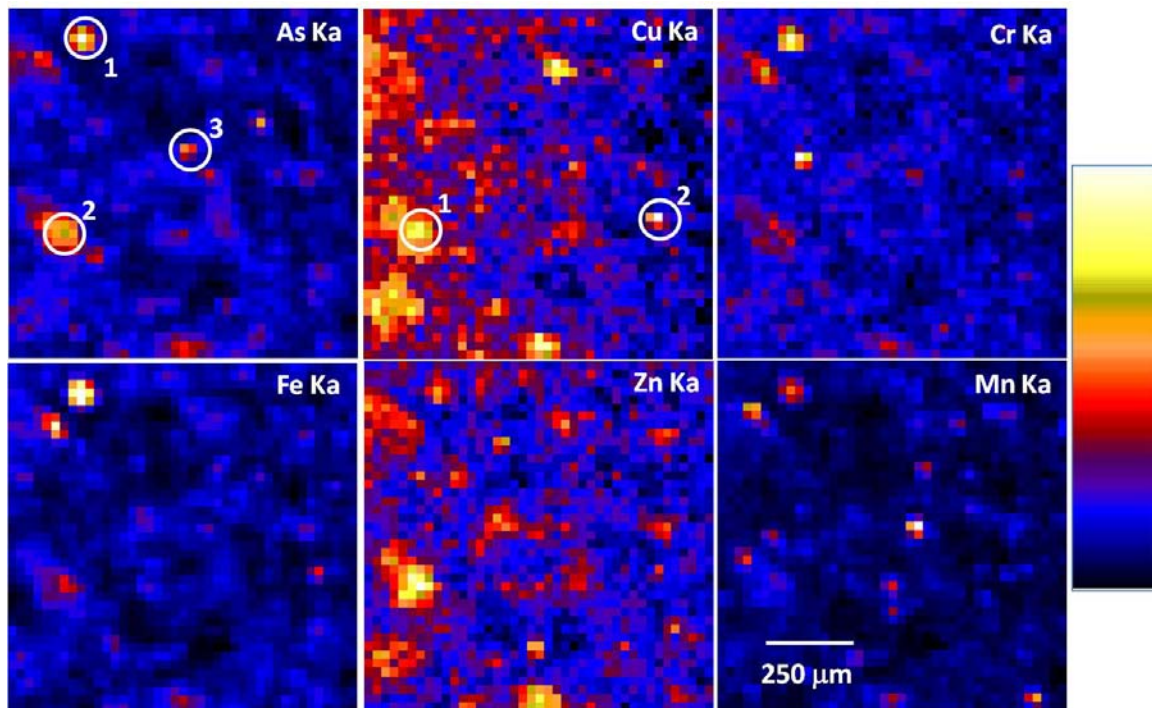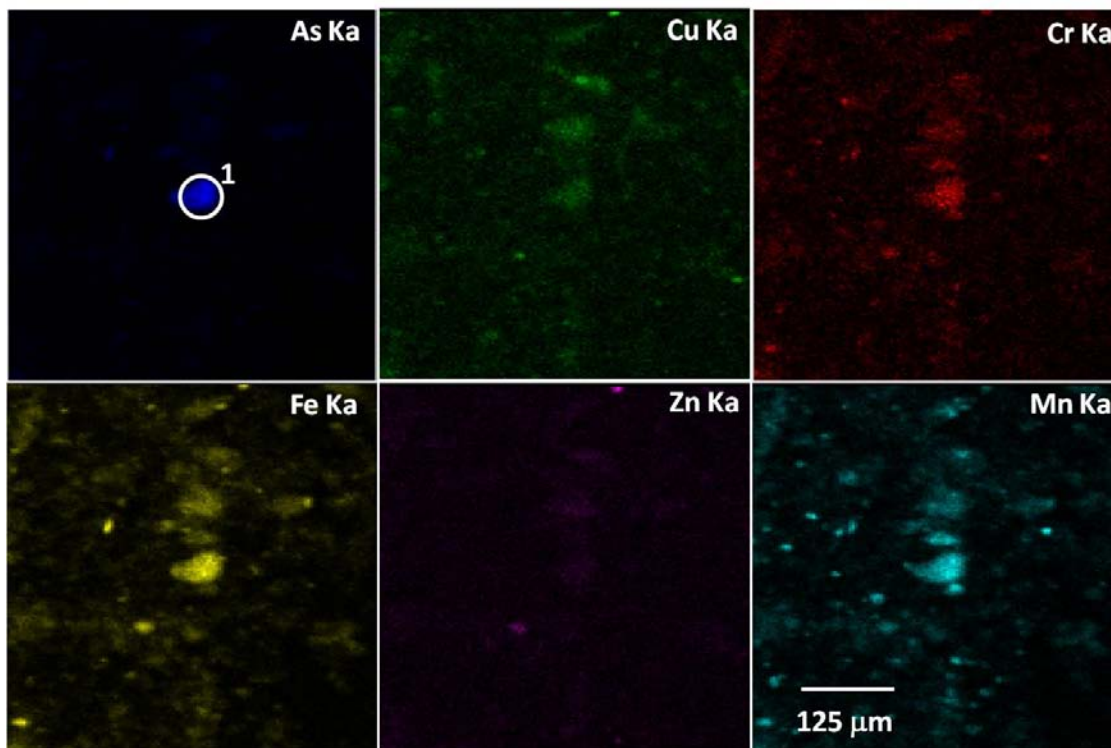**Figure A5. 6: Midslope surface soil (0-5 cm adjacent, 0-15 cm depth, file CE1 map 3) XRF elemental mapping. Minimum values correspond to black and maximum to bright.**

Arsenic 0 – 88756 counts, copper 0 – 33536 counts, chromium 0-12170 counts, iron 0 – 103684 counts, zinc 0 – 34001 counts, manganese 0 – 84295 counts. Spots indicate regions where µXAFS data was taken. Maps generated at the Advanced light source beamline 10.3.2 Berkeley National Laboratory, Ca.

Figure A5. 7: Midslope surface soil (0-5 cm adjacent, 0-15 cm depth, file CE1 map 5) XRF elemental mapping. Minimum values correspond to black and maximum to white.

Arsenic 0 – 3308 counts, copper 0 – 1903 counts, chromium 0-2988 counts, iron 0 – 73956 counts, zinc 0 – 649 counts, manganese 0 – 6123 counts. Spots indicate regions where μXAFS data was taken. Maps generated at the Advanced light source beamline 10.3.2 Berkeley National Laboratory, Ca.
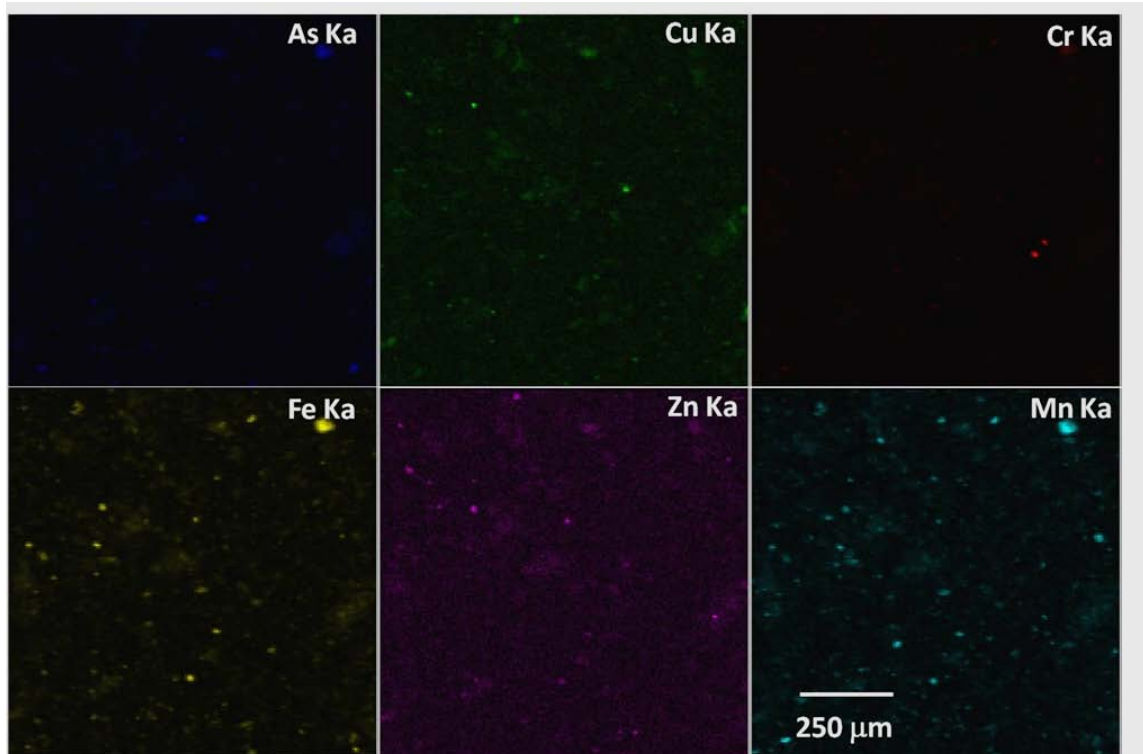
Appendix 6: Mass and Normalized Enrichment Factor of Arsenic and Copper

To check for overall enrichment of the metal(loid)s in the soil at different depths a calculation was conducted to establish the total mass of metal per depth increment. The method consists of revolving the boundaries of the sample around the post and calculating the subsequent volume of soil enriched (eq. A6.1). The expected mass of the metal could be determined by multiplying this volume of enrichment by the estimated soil bulk density (1.25 g cm^{-3}) and the concentration of the sample (eq. A6.2). The mass per depth increment was then estimated through the summation of samples with the same depth profiles (eq. A6.3). This estimation allows one to compare overall leaching at different depth increments in order to postulate on how profile depth/soil properties are influencing total leaching and leaching patterns. Because samples were pulled from both sides of posts the summation of the total enrichment was averaged between both sides.

Volume of enrichment

$$V = \pi \cdot (x_2^2 - x_1^2) \cdot (\Delta y) \qquad\qquad \text{eq. A6.1}$$

  V=volume of enrichment (cm^3)

  x_2=sample's farthest vertical position from center of post (cm)

  x_1=sample's closest vertical position from center of post (cm)

  Δy= range in sample depth (cm)

Mass of Metal per sample

$$M = V \cdot D_b \cdot (C_s - C_b) \cdot 10^{-6} \qquad\qquad \text{eq. A6.2}$$

  M=mass of metal (g)

  V=volume of enrichment (cm^3)

  D_b=Bulk density (1.25 g cm^{-3})

C_s= Sample Concentration (mg/kg)

C_b= Background concentration (mg/kg)

Mass per Unit Depth Increment

$$m = \frac{M}{\Delta y}$$ eq. A6.3

m= mass per unit depth (g/cm)

Total Mass of Metal

$$\sum M_i$$ eq. A6.4

M=mass of metal (g) depth

Additionally, to account for sample heterogeneity because of changes in soil properties throughout the profile a technique of normalization of the enrichment factor is conducted. The normalization approach uses aluminum as the normalizer, which has been shown to be appropriate for normalizing the enrichment factor in sediments (Loring and Rantala, 1992). A recent paper that uses this approach is (Liu et al., 2010).

Normalized Enrichment Factor

$$EF = \left(\frac{M}{X}\right)_{sample} / \left(\frac{M}{X}\right)_{background}$$

M=metal concentration

X= normalize concentration (Aluminum)

Table A6-1: Mass and Normalized Enrichment Factor of Cr, Cu and As

Position	Depth	Mass per unit depth (g/cm)		Normalized Enrichment Factor (NEF)		
		Copper	Arsenic	Chromium	Copper	Arsenic
Hilltop						
	0 to 15 cm	0.376	0.662	1	13	15
	15 to 30 cm	0.268	0.268	1	9	8
	30 to 60 cm	0.186	0.200	1	8	6
	60 to 90cm	0.016	0.046	1	1	2
	90 to 105 cm	0.007	0.009	1	1	2
	Total (0-105cm)	15.827	21.463			
Midslope						
	0 to 15 cm	0.366	0.771	1	14	16
	15 to 30 cm	0.266	0.347	1	15	10
	30 to 60 cm	0.243	0.268	1	15	10
	60 to 90cm	0.191	0.148	1	11	6
	90 to 110 cm	0.109	0.003	1	5	2
	Total (0- 105 cm)	24.162	29.269			
Toeslope						
	0 to 15 cm	0.046	0.100	1	2	4
	15 to 30 cm	0.009	0.049	1	1	2
	30 to 60 cm	0.004	0.030	1	1	2
	60 to 90cm	0.020	0.033	1	1	2
	90 to 120 cm	0.026	0.017	1	2	2
	Total (0-105 cm)	1.932	4.363			

NEF = $(M/X)_{sample}$ / $(M/X)_{background}$ see text (NEF=1 is no enrichment), the mass using a volume revolved around the post

Appendix 7: Arsenic Bulk and μ XAFS spectra
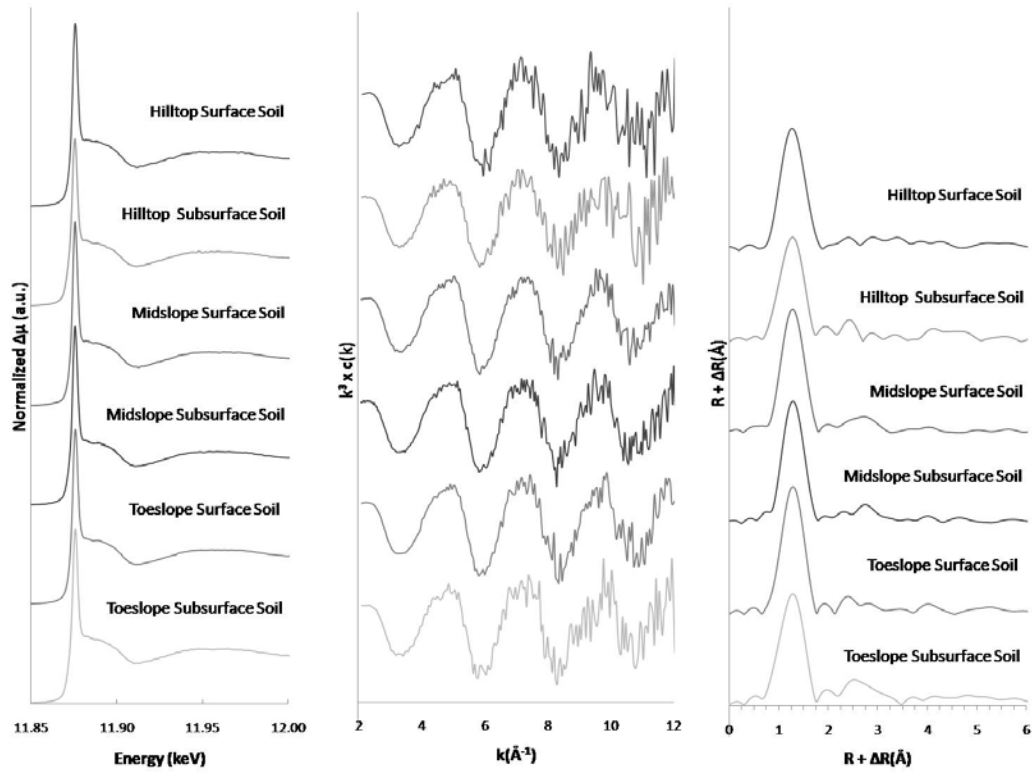
Figure A7. 1: XANES, CHI*k^3, and radial structure function (RSF) data of bulk XAFS data.
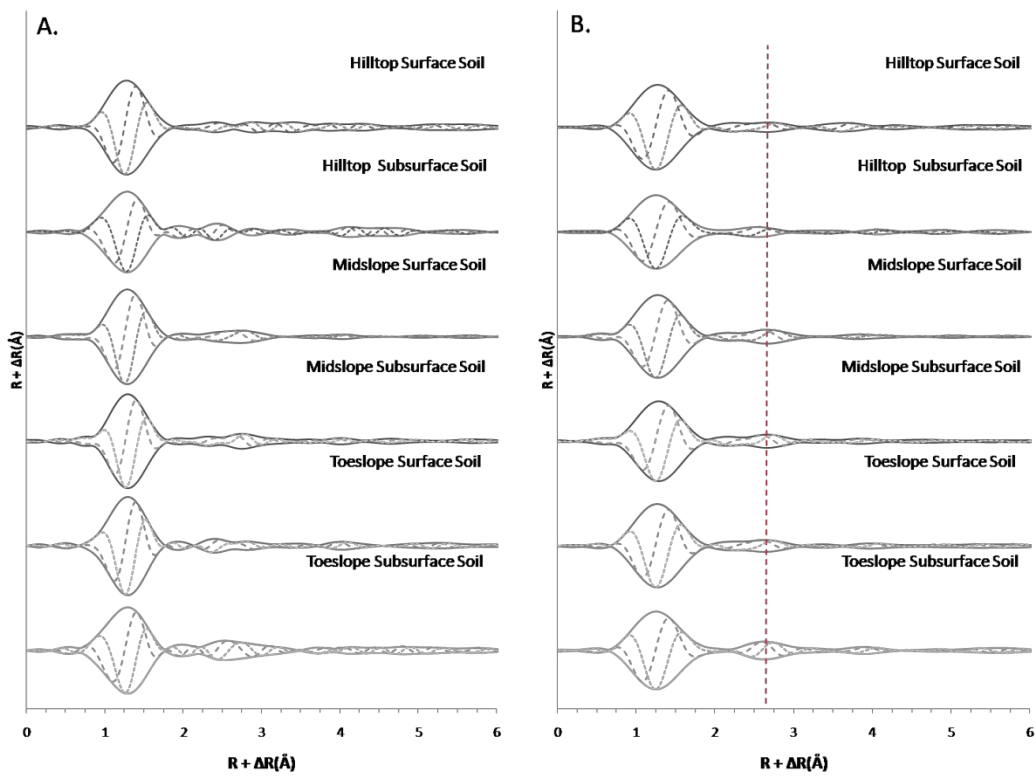
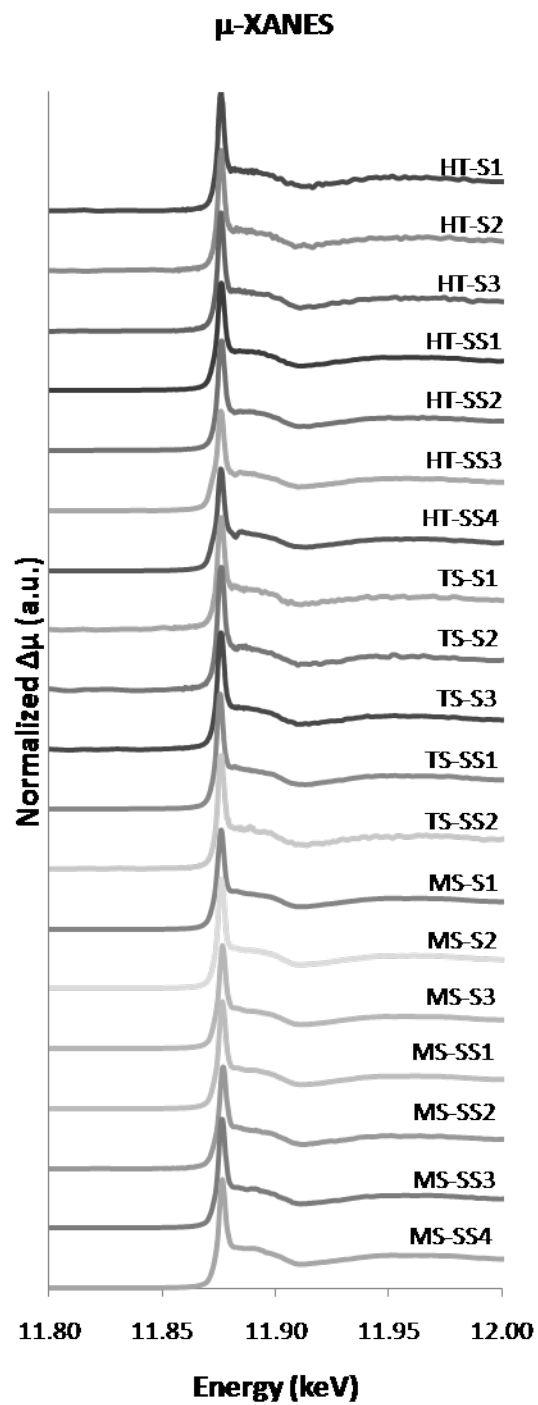**Figure A7. 2: Radial structure function (RSF) with imaginary data of the bulk XAFS spectra.**

Figure A7. 3: μ XANES arsenic spectra. Hilltop (HT), Midslope (MS), Toeslope (TS), Surface Soil (S), and Subsurface Soil (SS)
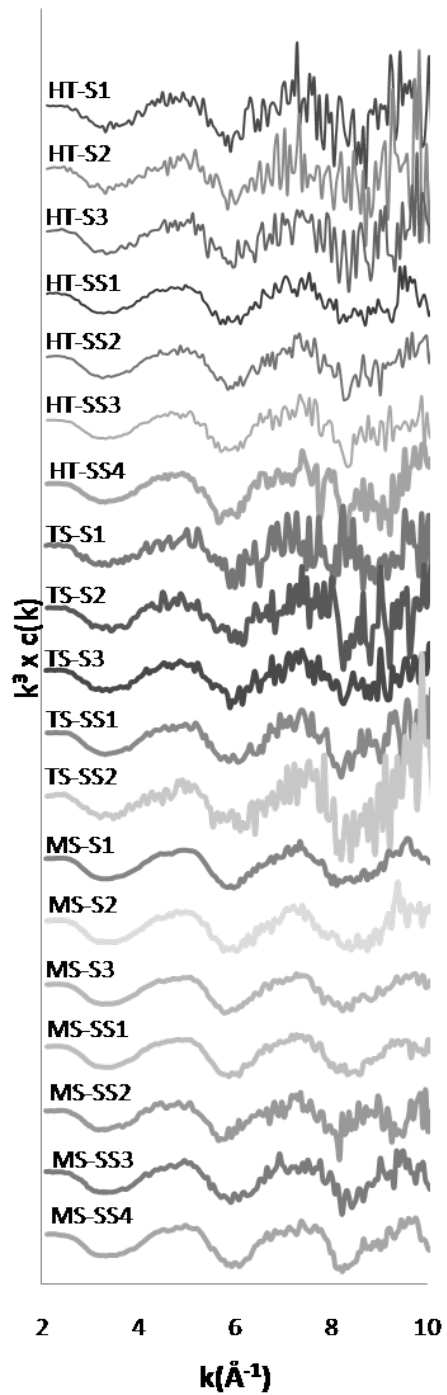
Figure A7. 4: Chi*k3 arsenic spectra. Hilltop (HT), Midslope (MS), Toeslope (TS), Surface Soil (S), and Subsurface Soil (SS)

Appendix 8: Arsenic Principle Component Analysis

Traditional single shell fitting of EXAFS data in heterogeneous systems, such as soil, is often difficult to ascertain because of the complexity and quantity of overlapping atomic shells. Therefore, a principle component analysis (PCA) is conducted with Labview[TM] based software developed at beamline 10.3.2 at the ALS (http://xraysweb.lbl.gov/uxas/Index.htm) using all bulk and μ EXAFS spectra. The PCA analysis accompanied with target transformation (TT) analysis can be used to identified the standard spectra that are the most probably components of the spectral data set. In PCA analysis the number of dominant species present must be equal to or less than the total number sample spectra taken.

The methodology of PCA analysis is reviewed in (Ressler et al., 2000) or (Manceau et al., 2002). Provided here is a brief reiteration of the theory provided by Manceau et al. (2002), PCA takes a set of X spectra (the sample set) and represents the X spectra through a linear combination of Y spectra in which Y ≤ X components. Using linear algebra a rectangular matrix A can be treated as follows

$$A_{ia} = E_{ib} \lambda_b W_{ba} \qquad \qquad \text{eq. A8.1}$$

where A is an N ×M matrix, E is a column- orthogonal N×M matrix, and W is a square, M ×M orthonormal matrix. Roughly, E is the set of decomposed components, λ_b are scale factors and W is a table of weights. The $\lambda_b{}^2$ are the eigenvalues of A*A and indicate the contributions of various components, generally λ_b is only of any significant magnitude for only some components. Therefore the data set can be represented as

$$\chi_i^b \approx E_{i\alpha}\lambda_\alpha W_{b\alpha} \qquad\qquad\qquad\qquad\qquad \text{eq. A8.2}$$

in which α goes from 1… Y, Y being the number of components used, and b goes from 1…X. The resultant spectra the E components do not correspond to any single species and may not even look like EXAFS spectra when plotted and are thus referred to as abstract components.

To address the quality of the fit given by the principal components to the standard spectra during TT a SPOIL value is calculated which estimates the fit error, lower SPOIL values correspond to better fits. In general, SPOIL values < 1.5 are excellent, 1.5 – 3 good, 3-4.5 fair, 4.5 -6 poor, and >6 unacceptable (Malinowski, 1978). When fitting EXAFS data through linear least squares the fit can be improved simply by adding more components. Therefore, to determine the approximate number of components to use an indicator (IND) function must be constructed (Malinowski, 1977). The minimization of the IND value gives an indication of the # of principal components that accounts for a majority of the data set. The PCA analysis was performed using the $\chi(k) \times k^3$ (Å^{-3}) over a k range of 2 – 10 Å^{-1}. The results exhibited in Figure A8.1 show a minimization of the IND value at 3 or 4 which suggests there are 3 -4 significant components in our system. These 3-4 components are exhibited in Figure A8.2. Target transformation results are exhibited in Table A8.2 and Table A8.3 indicating that these 3-4 principal components are best represented by an amorphous aluminum oxide and arsenic complex originally believed to be mansfieldite, As sorbed to gibbsite, and As and Zn coprecipitated on Goethite.

Figure A8. 1: Indicator values vs. component #, a.) refers to PCA conduction with all spectra, b.) refers to the PCA conducted on all data except the 4 noisiest spectra, and c.) refers to the PCA conducted on all data except 5 noisiest spectra.
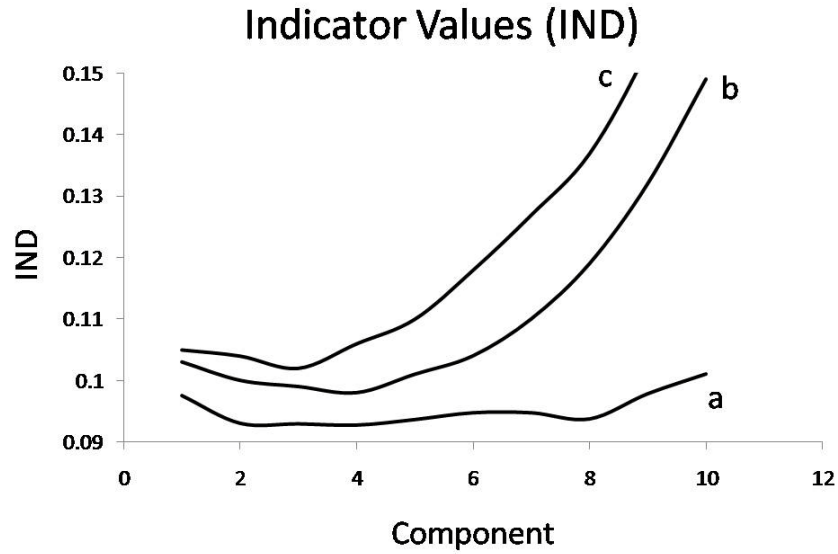

Figure A8. 2: Component 1, 2, 3 ,4 in which a.) refers to PCA conduction with all spectra, b.) refers to the PCA conducted on all data except the 4 noisiest spectra, and c.) refers to the PCA conducted on all data except 5 noisiest spectra.
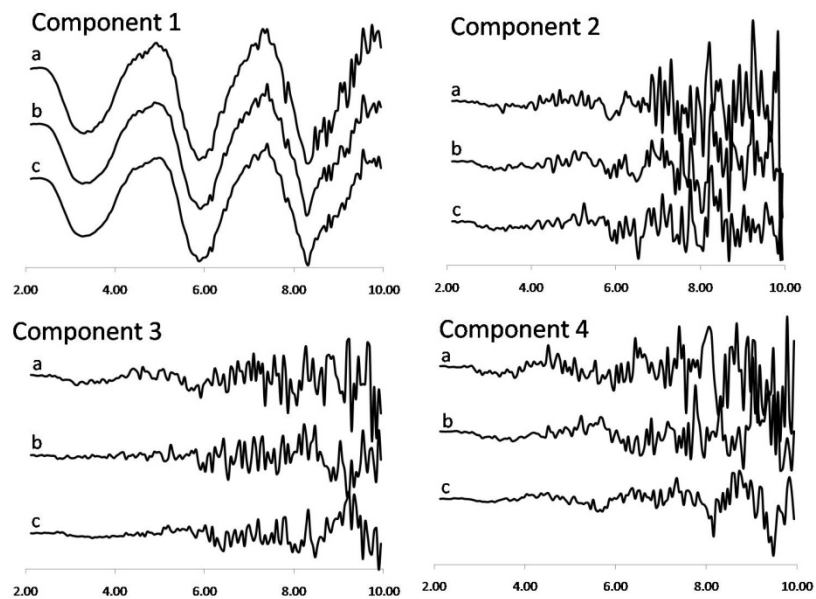
Table A8-1: Eigenvalues and Indicator values (IND) of Principal Component Analysis*

Component	A Eigenvalue	A IND	B Eigenvalue	B IND	C Eigenvalue	C IND
1	348	0.0975	306	0.103	298	0.105
2	141	0.093	96	0.1	84.1	0.104
3	106	0.0929	79.4	0.099	75.4	**0.102**
4	96.8	**0.0927**	69.9	**0.098**	54.7	0.106
5	84.2	0.0936	53.6	0.101	50.1	0.11
6	76.4	0.0947	50	0.104	42	0.118
7	72.4	0.0947	42	0.11	38.2	0.127
8	67	0.0937	35.8	0.119	35.8	0.137
9	49.3	0.0978	29.8	0.132	29.4	0.154
10	47.1	0.101	27.2	0.149	27.2	0.176

*A indicates PCA w/ all spectra, B indicates PCA w/ all but 4 nosiest spectra and C indicates PCA with all but 5 noisiest spectra

Table A8-2: Spoil values for Standards with Three Principle Components*

Standards	A Spoil	A Normalized Sum Sq	A Normalized Sum Abs	B Spoil	B Normalized Sum Sq	B Normalized Sum Abs	C Spoil	C Normalized Sum Sq	C Normalized Sum Abs
Adamite	3.05	0.178	0.351	3.08	0.165	0.355	4.33	0.173	0.360
Allactite	2.99	0.170	0.374	3.19	0.168	0.364	3.36	0.152	0.353
As(V)-Gibbsite	**0.83**	0.031	0.136	**0.88**	0.027	0.133	**1.00**	0.021	0.116
As(V)-Goethite	1.07	0.038	0.160	1.12	0.032	0.145	1.27	0.026	0.131
As(V)Zn(II)-Birnessite	6.33	0.750	0.818	9.65	0.801	0.868	5.19	0.682	0.801
As(V)Zn(II)-Gibbsite	0.98	0.035	0.154	1	0.030	0.148	1.26	0.027	0.137
As(V)Zn(II)-Goethite	**0.92**	0.033	0.146	**0.96**	0.028	0.132	**1.02**	0.021	0.119
As(V)Zn(II)-SilicaOxide	1.37	0.049	0.178	1.46	0.045	0.180	1.63	0.038	0.166
Chalcophyllite	2.32	0.113	0.290	2.35	0.101	0.278	3.16	0.104	0.284
Liquid As(V)	1.27	0.048	0.192	1.28	0.040	0.171	1.31	0.031	0.149
Mansfieldite	**0.73**	0.027	0.134	**0.66**	0.021	0.113	**0.91**	0.018	0.106
Ojuelaite	1.48	0.059	0.189	1.42	0.046	0.170	1.54	0.037	0.156
Olivenite	2.81	0.139	0.310	3.3	0.141	0.314	3.80	0.137	0.314
Scordite	2.33	0.110	0.283	2.47	0.108	0.293	3.30	0.110	0.297

*A indicates PCA w/ all spectra, B indicates PCA w/ all but 4 noisiest spectra and C indicates PCA with all but 5 noisiest spectra

Table A8-3: Spoil values for Standards with Four Principle Components*

Standards	4 Principle Components								
	A			B			C		
	Spoil	Normalized Sum Sq	Normalized Sum Abs	Spoil	Normalized Sum Sq	Normalized Sum Abs	Spoil	Normalized Sum Sq	Normalized Sum Abs
Adamite	3.07	0.167	0.346	3.92	0.162	0.350	4.36	0.168	0.359
Allactite	3.22	0.166	0.364	3.43	0.151	0.351	2.75	0.132	0.316
As(V)-Gibbsite	**1.02**	0.031	0.134	**1.06**	0.021	0.116	**0.87**	0.017	0.108
As(V)-Goethite	1.26	0.038	0.161	**1.33**	0.026	0.132	1.43	0.026	0.128
As(V)Zn(II)-Birnessite	6.99	0.750	0.818	5.34	0.668	0.788	5.53	0.678	0.793
As(V)Zn(II)-Gibbsite	**1.16**	0.034	0.153	1.34	0.027	0.137	**1.17**	0.023	0.125
As(V)Zn(II)-Goethite	**1.12**	0.033	0.147	**1.11**	0.022	0.120	**1.03**	0.019	0.114
As(V)Zn(II)-SilicaOxide	1.58	0.049	0.179	1.72	0.038	0.167	1.70	0.036	0.160
Chalcophyllite	2.51	0.110	0.284	3.11	0.101	0.278	3.14	0.099	0.283
Liquid As(V)	1.45	0.048	0.192	1.36	0.030	0.148	1.23	0.027	0.138
Mansfieldite	**0.93**	0.027	0.134	**1.01**	0.018	0.107	**0.90**	0.016	0.104
Ojuelaite	1.70	0.059	0.188	1.58	0.036	0.155	1.70	0.036	0.154
Olivenite	3.01	0.135	0.304	4	0.136	0.313	3.64	0.130	0.310
Scordite	2.47	0.105	0.282	3.27	0.108	0.292	3.10	0.102	0.293

*A indicates PCA w/ all spectra, B indicates PCA w/ all but 4 noisest spectra and C indicats PCA with all but 5 noisiest spectra

Appendix 9: Arsenic Linear Least Squares Fitting (LLSF)

Table A9.1: Linear Least Squares Fitting with 3 Principal Components

Location	Soil	Type	As(V)-Gibbsite	As(V)Zn(II)-Goethite	Mansfieldite*	Sum	Norm. Sum-Sq	Delta E
Hilltop	Surface 1.3	μ	0%	70%	39%	108%	0.5590	1.08
Hilltop	Surface 1.2	μ	0%	0%	110%	110%	0.7730	1.19
Hilltop	Surface 1.1	μ	46%	0%	79%	124%	0.5980	2.14
Hilltop	Surface	Average μ	15%	23%	76%	114%	0.6433	1.47
Hilltop	Surface	Bulk	64%	15%	27%	107%	0.1150	0.46
Hilltop	Subsurface 2.3	μ	0%	0%	124%	124%	0.4750	0.03
Hilltop	Subsurface 2.2	μ	0%	90%	0%	90%	0.3450	1.13
Hilltop	Subsurface 2.1	μ	10%	23%	79%	112%	0.2290	-0.92
Hilltop	Subsurface 1.1	μ	33%	0%	71%	104%	0.2530	0.18
Hilltop	Subsurface	Average μ	11%	28%	69%	108%	0.3255	0.11
Hilltop	Subsurface	Bulk	13%	32%	51%	96%	0.1230	1.29
Midslope	Surface 6.1	μ	0%	36%	59%	95%	0.0495	0.61
Midslope	Surface 5.1	μ	98%	12%	0%	110%	0.1480	0.34
Midslope	Surface 3.1	μ	55%	0%	53%	108%	0.0643	0.72
Midslope	Surface	Average μ	51%	16%	37%	104%	0.0873	0.56
Midslope	Surface	Bulk	43%	31%	31%	105%	0.0274	0.10
Midslope	Subsurface 2.2	μ	0%	95%	6%	101%	0.0983	-0.31
Midslope	Subsurface 2.1	μ	0%	92%	0%	92%	0.1820	0.03
Midslope	Subsurface 1.2	μ	0%	16%	60%	76%	0.5230	2.18
Midslope	Subsurface 1.1	μ	93%	5%	0%	98%	0.0717	1.23
Midslope	Subsurface	Average μ	23%	52%	17%	92%	0.2188	0.78
Midslope	Subsurface	Bulk	38%	58%	0%	96%	0.0507	0.75
Toeslope	Surface 1.3	μ	0%	13%	83%	96%	0.3510	-1.85
Toeslope	Surface 1.2	μ	0%	93%	0%	93%	0.6140	-3.48
Toeslope	Surface 1.1	μ	0%	0%	73%	73%	0.7250	-1.69
Toeslope	Surface	Average μ	0%	35%	52%	87%	0.5633	-2.34
Toeslope	Surface	Bulk	55%	47%	0%	102%	0.0449	0.38
Toeslope	Subsurface 2.2	μ	0%	143%	0%	143%	0.5490	-1.49
Toeslope	Subsurface 2.1	μ	67%	15%	32%	114%	0.3330	1.03
Toeslope	Subsurface	Average μ	34%	79%	16%	128%	0.4410	-0.23
Toeslope	Subsurface	Bulk	28%	45%	22%	95%	0.1330	0.51

*thought to be mansfieldite XRD revealed amorphous aluminum phase

Table A9.2: Linear Least Squares Fitting with 3 Principal Components Reduced

Location	Soil	Type	As(V)-Gibbsite	As(V)Zn(II)-Goethite	Mansfieldite*	Sum	NSS	ΔE	Aluminum Species	Iron Species	pH
Hilltop	Surface	Bulk	64%	15%	27%	107%	0.1150	0.4600	91%	15%	4.4
Hilltop	Surface	Average μ	15%	23%	76%	114%	0.6433	1.4700	91%	23%	4.4
Hilltop	Subsurface	Bulk	13%	32%	51%	96%	0.1230	1.2900	64%	32%	5.6
Hilltop	Subsurface	Average μ	11%	28%	69%	108%	0.3255	0.1050	79%	28%	5.6
Midslope	Surface	Bulk	43%	31%	31%	105%	0.0274	0.1000	74%	31%	5.1
Midslope	Surface	Average μ	51%	16%	37%	104%	0.0873	0.5567	88%	16%	5.1
Midslope	Subsurface	Bulk	38%	58%	0%	96%	0.0507	0.7500	38%	58%	6.3
Midslope	Subsurface	Average μ	23%	52%	17%	92%	0.2188	0.7825	40%	52%	6.3
Toeslope	Surface	Bulk	55%	47%	0%	102%	0.0449	0.3800	55%	47%	6.6
Toeslope	Surface	Average μ	0%	35%	52%	87%	0.5633	-2.3400	52%	35%	6.6
Toeslope	Subsurface	Bulk	28%	45%	22%	95%	0.1330	0.5100	50%	45%	7.1
Toeslope	Subsurface	Average μ	34%	79%	16%	128%	0.4410	-0.2300	49%	79%	7.1

*thought to be mansfieldite XRD revealed amorphous aluminum phase, NSS-Normalized Sum Squares
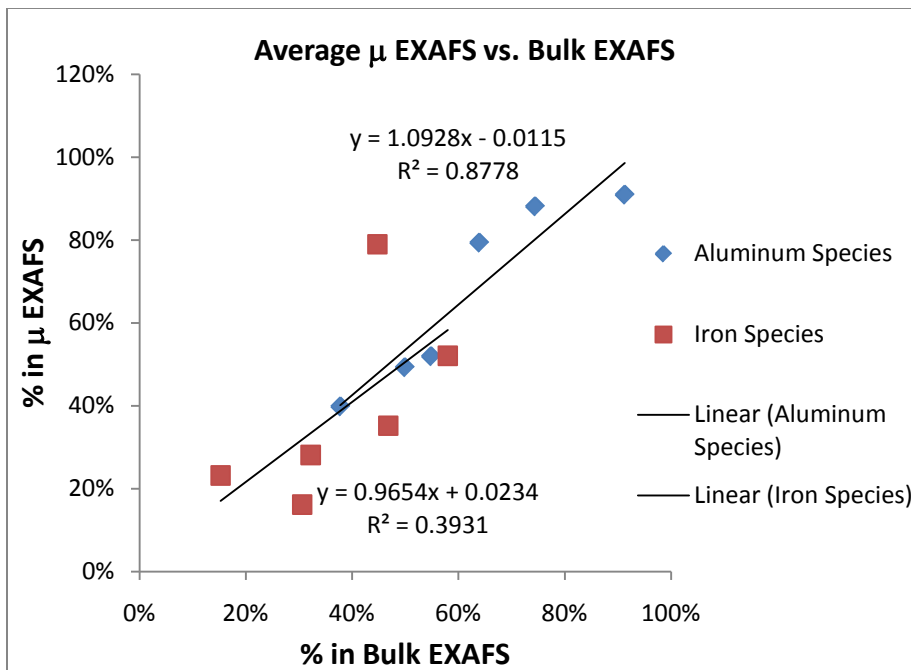
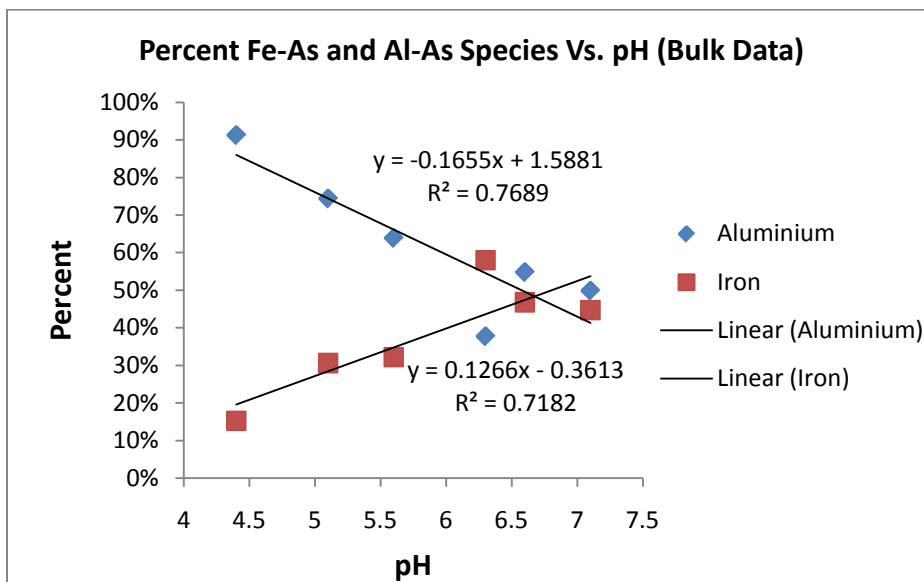**Figure A9. 1:** Correlation among the bulk and average μ EXAFS LLSF results.

Figure A9. 2: Percent Iron and Aluminum Arsenic Complexes vs. pH for bulk EXAFS data
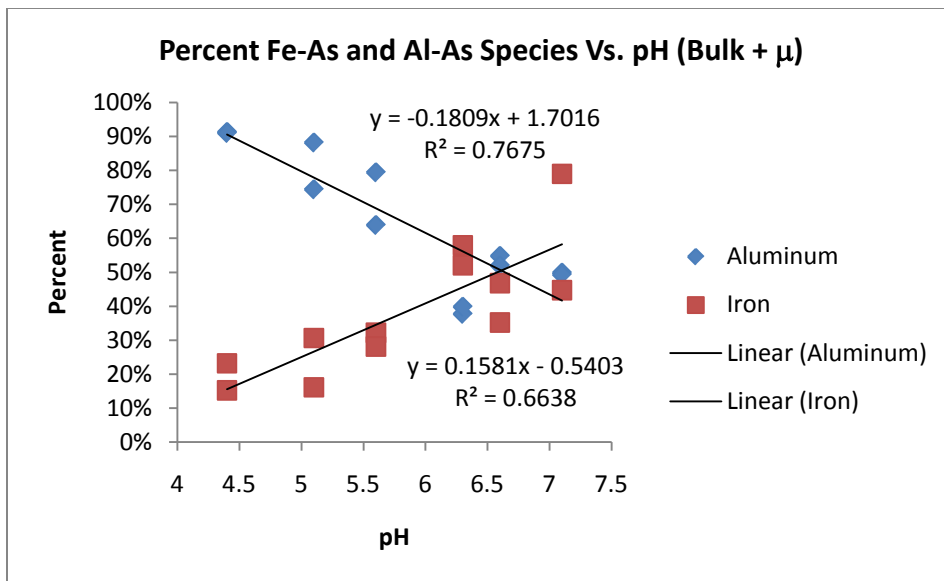
Figure A9. 3: Percent Iron and Aluminum Arsenic Complexes vs. pH for bulk and μ EXAFS data

Appendix 10: Spatial Distribution along the Toposequence

Samples were collected every 8 posts (~ 20 m) from the HT position to the TS position at two distances 0-5 cm (G) and 10-15 cm (I)away from the post and at two depths 0-15 cm (1)and 15-30 cm (2), corresponding to G1, G2, I1, and I2 in Figure A2 2-4. Samples were average to assess concentration differences and ratios were constructed to evaluate the extent of mobilization.

Figure A10. 1: Positions of Profile pits dug and approximate distance from Hilltop position.
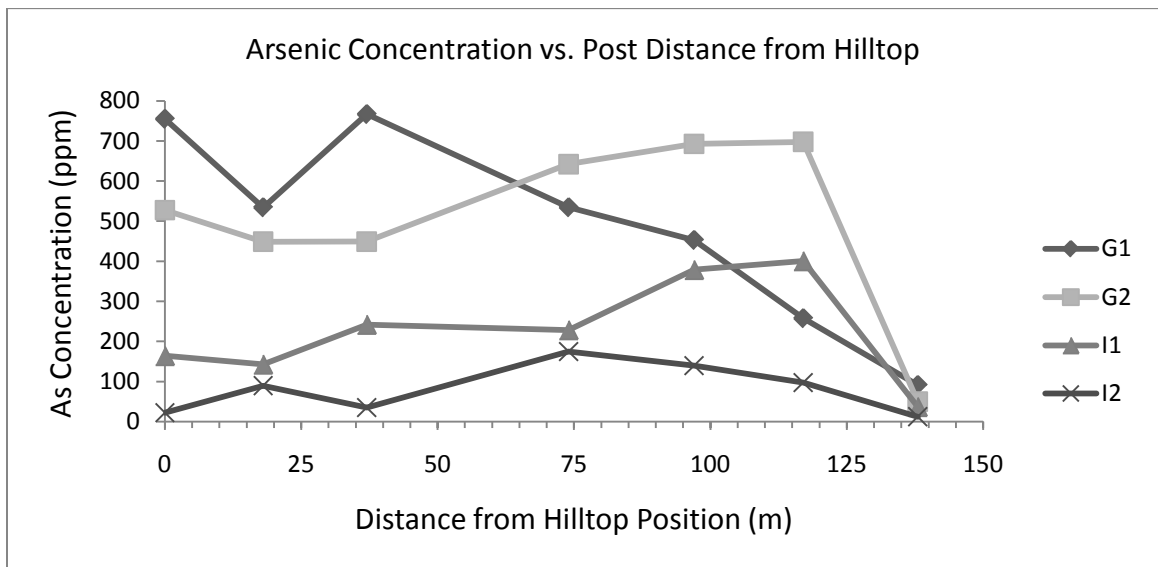

Figure A10. 2: Arsenic concentration vs. post distance from hilltop sampling location. Hilltop location corresponds to 0 m, midslope position corresponds to 97 m, and toeslope position corresponds to 138 m.

Figure A10. 3: Arsenic average concentration (Sample G1, G2, I1, I2) vs. post distance from hilltop sampling location. Hilltop location corresponds to 0 m, midslope position corresponds to 97 m, and toeslope position corresponds to 138 m.
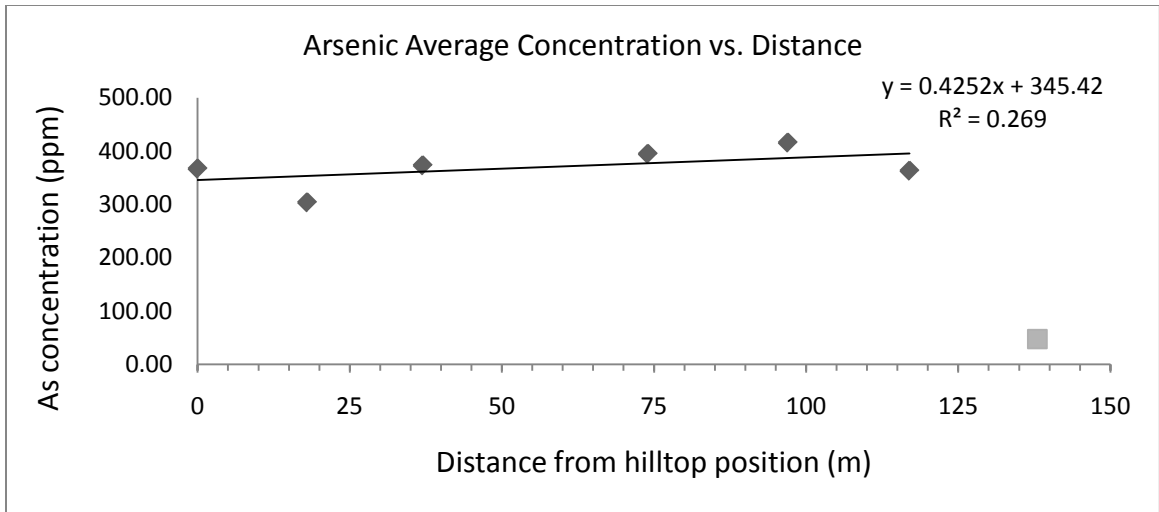

Figure A10. 4: Ratio of G1:I1 Arsenic Concentration vs. post distance from hilltop sampling location. Hilltop location corresponds to 0 m, midslope position corresponds to 97 m, and toeslope position corresponds to 138 m.
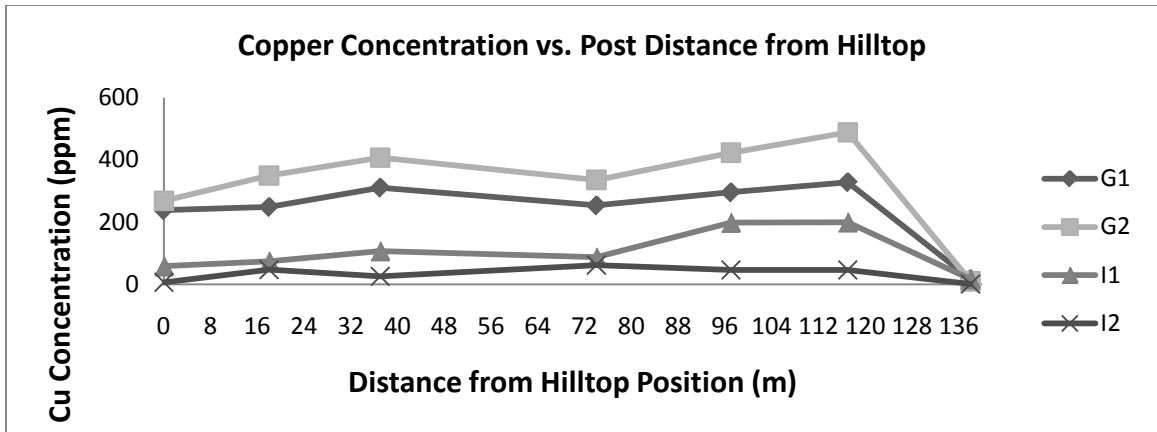
Figure A10. 5: Copper concentration vs. post distance from hilltop sampling location. Hilltop location corresponds to 0 m, midslope position corresponds to 97 m, and toeslope position corresponds to 138 m.
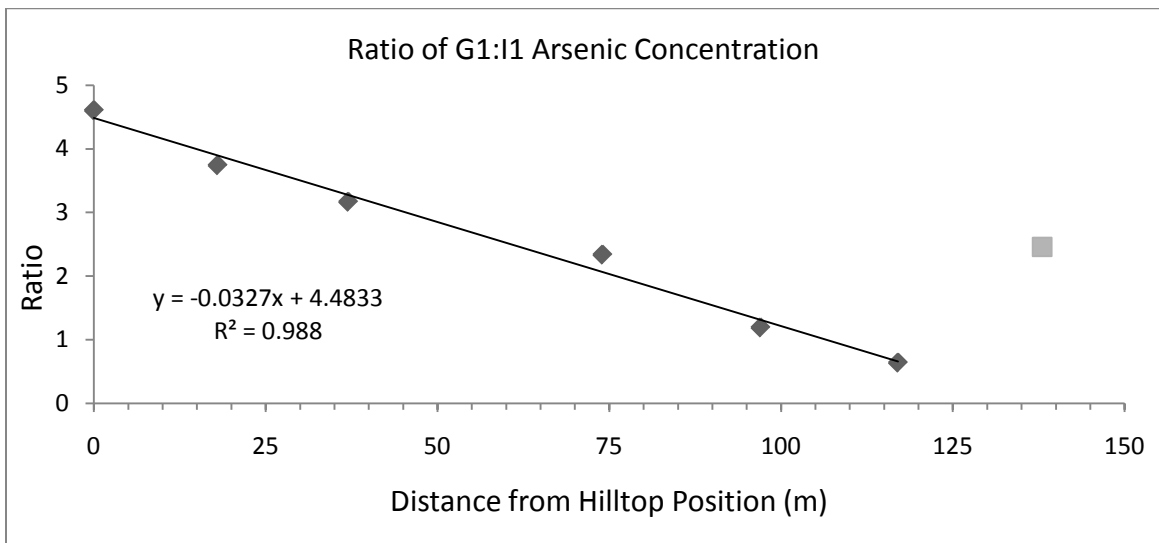

Figure A10. 6: Copper average concentration (Sample G1, G2, I1, I2) vs. post distance from hilltop sampling location. Hilltop location corresponds to 0 m, midslope position corresponds to 97 m, and toeslope position corresponds to 138 m.

Figure A10. 7: Ratio of G1:I1 Copper Concentration vs. post distance from hilltop sampling location. Hilltop location corresponds to 0 m, midslope position corresponds to 97 m, and toeslope position corresponds to 138 m.
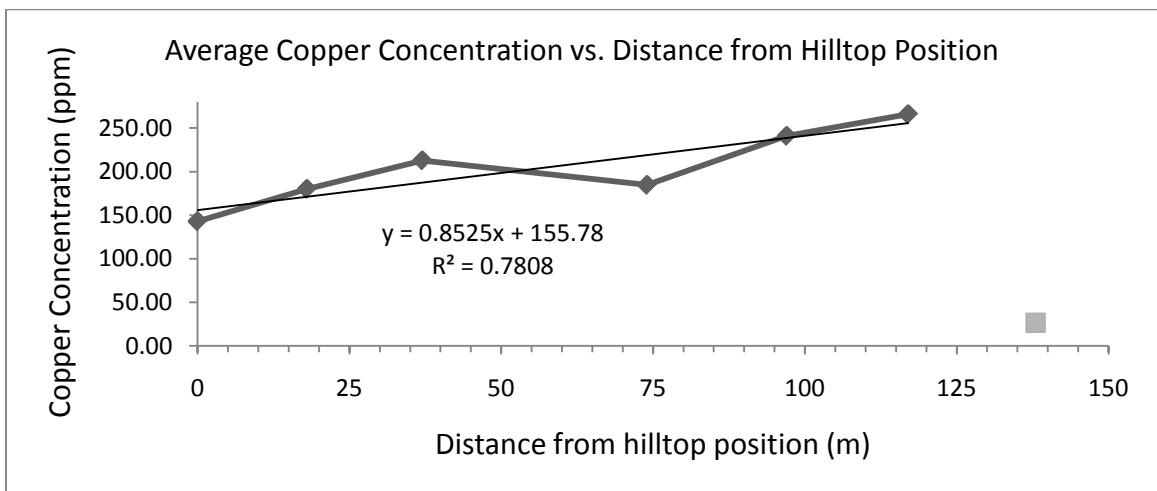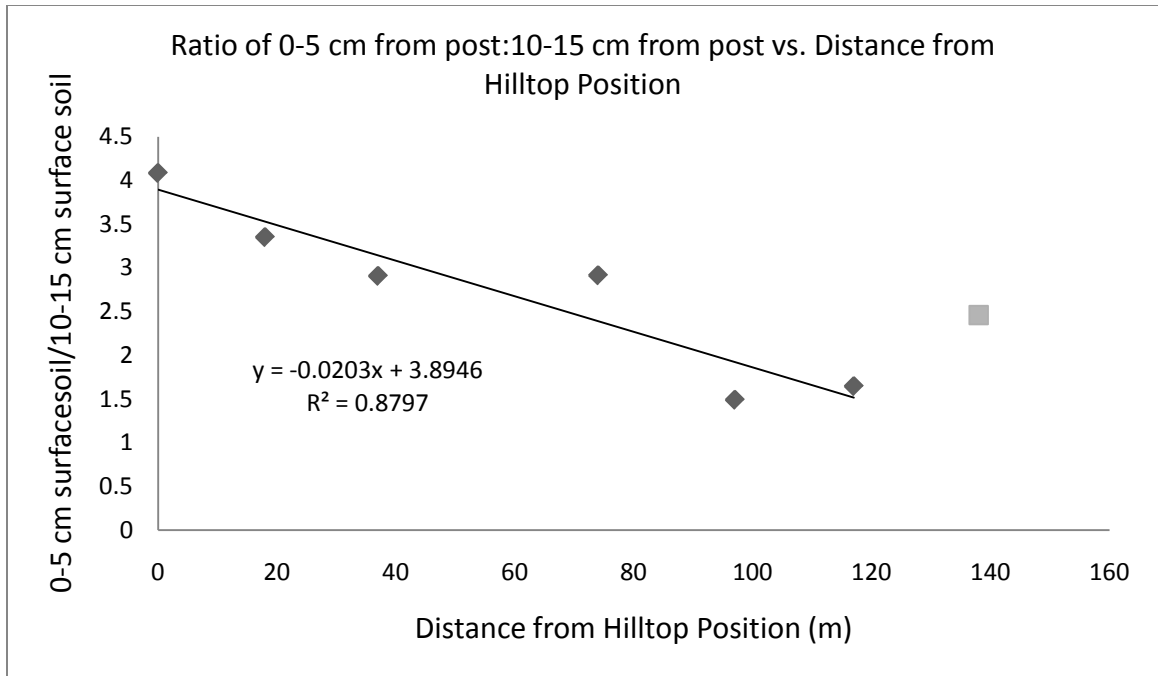
References

Natural Resources Conservation Service, United States Department of Agriculture. Official Soil Series Descriptions [Online WWW]. Available URL:"http://soils.usda.gov/technical/classification/osd/index.html". USDA-NRCS, Lincoln, NE.

Aceto M., Fedele A. (1994) RAIN WATER EFFECT ON THE RELEASE OF ARSENIC, CHROMIUM AND COPPER FROM TREATED WOOD. Fresenius Environmental Bulletin 3:389-394.

Agbenin J.O., Olojo L.A. (2004) Competitive adsorption of copper and zinc by a Bt horizon of a savanna Alfisol as affected by pH and selective removal of hydrous oxides and organic matter. Geoderma 119:85-95. DOI: 10.1016/s0016-7061(03)00242-8.

Alcacio T.E., Hesterberg D., Chou J.W., Martin J.D., Beauchemin S., Sayers D.E. (2001) Molecular scale characteristics of Cu(II) bonding in goethite-humate complexes. Geochimica et Cosmochimica Acta 65:1355-1366.

Alvarez-Puebla R.A., Valenzuela-Calahorro C., Garrido J.J. (2004a) Cu(II) retention on a humic substance. Journal of Colloid and Interface Science 270:47-55. DOI: 10.1016/j.jcis.2003.08.068.

Alvarez-Puebla R.A., Valenzuela-Calahorro C., Garrido J.J. (2004b) Retention of Co(II), Ni(II), and Cu(II) on a purified brown humic acid. Modeling and characterization of the sorption process. Langmuir 20:3657-3664. DOI: 10.1021/la0363231.

Alvarez-Puebla R.A., Valenzuela-Calahorro C., Garrido J.J. (2004c) Modeling the adsorption and precipitation processes of Cu(II) on humin. Journal of Colloid and Interface Science 277:55-61. DOI: 10.1016/j.jcis.2004.04.031.

Alvarez-Puebla R.A., dos Santos D.S., Blanco C., Echeverria J.C., Garrido J.J. (2005) Particle and surface characterization of a natural illite and study of its copper retention. Journal of Colloid and Interface Science 285:41-49. DOI: 10.1016/j.jcis.2004.11.044.

Anderson R.A. (1989) ESSENTIALITY OF CHROMIUM IN HUMANS. Science of the Total Environment 86:75-81.

Appelo C.A.J., Van der Weiden M.J.J., Tournassat C., Charlet L. (2002) Surface complexation of ferrous iron and carbonate on ferrihydrite and the mobilization of arsenic. Environmental Science & Technology 36:3096-3103. DOI: 10.1021/es010130n.

Arai Y., Elzinga E.J., Sparks D.L. (2001) X-ray absorption spectroscopic investigation of arsenite and arsenate adsorption at the aluminum oxide-water interface. Journal of Colloid and Interface Science 235:80-88. DOI: 10.1006/jcis.2000.7249.

Arai Y., Lanzirotti A., Sutton S., Davis J.A., Sparks D.L. (2003) Arsenic speciation and reactivity in poultry litter. Environmental Science & Technology 37:4083-4090.

Arias M., Perez-Novo C., Osorio F., Lopez E., Soto B. (2005) Adsorption and desorption of copper and zinc in the surface layer of acid soils. Journal of Colloid and Interface Science 288:21-29. DOI: 10.1016/j.jcis.2005.02.053.

Association A.W.P. (2005) Standards, American Wood Preservers Association, Selma, AL.

AWPA. (2005) Standards, American Wood Preservers Association, Selma, AL.

Balasoiu C.F., Zagury G.J., Deschenes L. (2001) Partitioning and speciation of chromium, copper, and arsenic in CCA-contaminated soils: influence of soil composition. Science of the Total Environment 280:239-255.

Baldwin L. (1998) Study of State Soil Arsenic Regulations, Amherst, MA.

Barcan V., Kovnatsky E. (1998) Soil surface geochemical anomaly around the copper-nickel metallurgical smelter. Water Air and Soil Pollution 103:197-218.

Bartlett R.J., Kimble J.M. (1976a) BEHAVIOR OF CHROMIUM IN SOILS .2. HEXAVALENT FORMS. Journal of Environmental Quality 5:383-386.

Bartlett R.J., Kimble J.M. (1976b) BEHAVIOR OF CHROMIUM IN SOILS .1. TRIVALENT FORMS. Journal of Environmental Quality 5:379-383.

Bauer M., Blodau C. (2006) Mobilization of arsenic by dissolved organic matter from iron oxides, soils and sediments. Science of the Total Environment 354:179-190. DOI: 10.1016/j.scitotenv.2005.01.027.

Bauer M., Blodau C. (2009) Arsenic distribution in the dissolved, colloidal and particulate size fraction of experimental solutions rich in dissolved organic matter and ferric iron. Geochimica Et Cosmochimica Acta 73:529-542.

Bisceglia K.J., Rader K.J., Carbonaro R.F., Farley K.J., Mahony J.D., Di Toro D.M. (2005) Iron(II)-catalyzed oxidation of arsenic(III) in a sediment column. Environmental Science & Technology 39:9217-9222. DOI: 10.1021/es051271/.

Bloom P.R., McBride M.B. (1979) METAL-ION BINDING AND EXCHANGE WITH HYDROGEN-IONS IN ACID-WASHED PEAT. Soil Science Society of America Journal 43:687-692.

Breslin V.T., Adler-Ivanbrook L. (1998) Release of copper, chromium and arsenic from CCA-C treated lumber in estuaries. Estuarine Coastal and Shelf Science 46:111-125.

Brubaker S.C., Jones A.J., Lewis D.T., Frank K. (1993) SOIL PROPERTIES ASSOCIATED WITH LANDSCAPE POSITION. Soil Science Society of America Journal 57:235-239.

Brun L.A., Maillet J., Hinsinger P., Pepin M. (2001) Evaluation of copper availability to plants in copper-contaminated vineyard soils. Environmental Pollution 111:293-302.

Brun L.A., Maillet J., Richarte J., Herrmann P., Remy J.C. (1998) Relationships between extractable copper, soil properties and copper uptake by wild plants in vineyard soils. Environmental Pollution 102:151-161.

Bull D.C. (2001) The chemistry of chromated copper arsenate II. Preservative-wood interactions. Wood Science and Technology 34:459-466.

Bull D.C., Harland P.W., Vallance C., Foran G.J. (2000) XAFS study of chromated copper arsenate timber preservative in wood. Journal of Wood Science 46:248-252.

Cao Y., Conklin M., Betterton E. (1995) COMPETITIVE COMPLEXATION OF TRACE-METALS WITH DISSOLVED HUMIC-ACID. Environmental Health Perspectives 103:29-32.

Cavallaro N., McBride M.B. (1980) ACTIVITIES OF CU-2+ AND CD2+ IN SOIL SOLUTIONS AS AFFECTED BY PH. Soil Science Society of America Journal 44:729-732.

Cavallaro N., McBride M.B. (1984) ZINC AND COPPER SORPTION AND FIXATION BY AN ACID SOIL CLAY - EFFECT OF SELECTIVE DISSOLUTIONS. Soil Science Society of America Journal 48:1050-1054.

Chakraborti D., Rahman M.M., Paul K., Chowdhury U.K., Sengupta M.K., Lodh D., Chanda C.R., Saha K.C., Mukherjee S.C. (2002) Arsenic calamity in the Indian subcontinent - What lessons have been learned? Talanta 58:3-22.

Chirenje T., Ma L.Q., Clark C., Reeves M. (2003) Cu, Cr and As distribution in soils adjacent to pressure-treated decks, fences and poles. Environmental Pollution 124:407-417.

Clark C.J., McBride M.B. (1984) CHEMISORPTION OF CU(II) AND CO(II) ON ALLOPHANE AND IMOGOLITE. Clays and Clay Minerals 32:300-310.

Cooper P.A. (1991) LEACHING OF CCA FROM TREATED WOOD - PH EFFECTS. Forest Products Journal 41:30-32.

Cooper P.A., ManVicar R., Ung T.Y. (1995) Relating CCA Fixation to Leaching of CCA Components from Treated Products The International Research Group of Wood Preservation IRG/WP/95-50045, Stockholm.

Dahlgren S.E. (1974) KINETICS AND MECHANISM OF FIXATION OF CU-CR-AS WOOD PRESERVATIVES .4. CONVERSION REACTIONS DURING STORAGE. Holzforschung 28:58-61.

Dahlgren S.E., Hartford W.H. (1972) KINETICS AND MECHANISM OF FIXATION OF CU-CR-AS WOOD PRESERVATIVES .1. PH BEHAVIOR AND GENERAL ASPECTS ON FIXATION. Holzforschung 26:62-&.

Dixit S., Hering J.G. (2003) Comparison of arsenic(V) and arsenic(III) sorption onto iron oxide minerals: Implications for arsenic mobility. Environmental Science & Technology 37:4182-4189. DOI: 10.1021/es030309t.

Echeverria J.C., Morera M.T., Mazkiaran C., Garrido J.J. (1998) Competitive sorption of heavy metal by soils. Isotherms and fractional factorial experiments. Environmental Pollution 101:275-284.

Elkhatib E.A., Bennett O.L., Wright R.J. (1984) ARSENITE SORPTION AND DESORPTION IN SOILS. Soil Science Society of America Journal 48:1025-1030.

Elliott H.A., Liberati M.R., Huang C.P. (1986) COMPETITIVE ADSORPTION OF HEAVY-METALS BY SOILS. Journal of Environmental Quality 15:214-219.

EPA. (2009) National Primary Drinking Water Regulations, in: E. P. A. E. 816-F-09-004 (Ed.).

Fendorf S., Eick M.J., Grossl P., Sparks D.L. (1997) Arsenate and chromate retention mechanisms on goethite .1. Surface structure. Environmental Science & Technology 31:315-320.

Flemming C.A., Trevors J.T. (1989) Copper Toxicity and Chemistry in the Environment - a Review. Water Air and Soil Pollution 44:143-158.

Frost R.R., Griffin R.A. (1977) EFFECT OF PH ON ADSORPTION OF ARSENIC AND SELENIUM FROM LANDFILL LEACHATE BY CLAY-MINERALS. Soil Science Society of America Journal 41:53-57.

Furnare L.J., Vailionis A., Strawn D.G. (2005a) Polarized XANES and EXAFS spectroscopic investigation into copper(II) complexes on vermiculite. Geochimica et Cosmochimica Acta 69:5219-5231. DOI: 10.1016/j.gca.2005.06.020.

Furnare L.J., Vailionis A., Strawn D.G. (2005b) Molecular-level investigation into copper complexes on vermiculite: Effect of reduction of structural iron on copper complexation. Journal of Colloid and Interface Science 289:1-13. DOI: 10.1016/j.jcis.2005.03.068.

Geelhoed J.S., Hiemstra T., Van Riemsdijk W.H. (1998) Competitive interaction between phosphate and citrate on goethite. Environmental Science & Technology 32:2119-2123.

Giller K.E., Witter E., McGrath S.P. (1998) Toxicity of heavy metals to microorganisms and microbial processes in agricultural soils: A review. Soil Biology & Biochemistry 30:1389-1414.

Goldberg S. (1986) CHEMICAL MODELING OF ARSENATE ADSORPTION ON ALUMINUM AND IRON-OXIDE MINERALS. Soil Science Society of America Journal 50:1154-1157.

Goldberg S. (2002) Competitive adsorption of arsenate and arsenite on oxides and clay minerals. Soil Science Society of America Journal 66:413-421.

Goldberg S., Glaubig R.A. (1988) ANION SORPTION ON A CALCAREOUS, MONTMORILLONITIC SOIL ARSENIC. Soil Science Society of America Journal 52:1297-1300.

Goldberg S., Johnston C.T. (2001) Mechanisms of arsenic adsorption on amorphous oxides evaluated using macroscopic measurements, vibrational spectroscopy, and surface complexation modeling. Journal of Colloid and Interface Science 234:204-216. DOI: 10.1006/jcis.2000.7295.

Grafe M., Eick M.J., Grossl P.R. (2001) Adsorption of arsenate (V) and arsenite (III) on goethite in the presence and absence of dissolved organic carbon. Soil Science Society of America Journal 65:1680-1687.

Grafe M., Eick M.J., Grossl P.R., Saunders A.M. (2002) Adsorption of arsenate and arsenite on ferrihydrite in the presence and absence of dissolved organic carbon. Journal of Environmental Quality 31:1115-1123.

Grafe M., Tappero R.V., Marcus M.A., Sparks D.L. (2008a) Arsenic speciation in multiple metal environments: I. Bulk-XAFS spectroscopy of model and mixed compounds. Journal of Colloid and Interface Science 320:383-399.

Grafe M., Tappero R.V., Marcus M.A., Sparks D.L. (2008b) Arsenic speciation in multiple metal environments - II. Micro-spectroscopic investigation of a CCA contaminated soil. Journal of Colloid and Interface Science 321:1-20.

Gustavsson N.B.B.D.B.S.a.R.C.S. (2001) Geochemical Landscapes of the Conterminous United States- New Map Presentations for 22 Elements, in: U. S. G. Survey (Ed.), USGS Information Services, Denver, CO.

Harter R.D. (1979) ADSORPTION OF COPPER AND LEAD BY AP AND B2 HORIZONS OF SEVERAL NORTHEASTERN UNITED-STATES SOILS. Soil Science Society of America Journal 43:679-683.

Henshaw B. (1979) FIXATION OF COPPER, CHROMIUM AND ARSENIC IN SOFTWOODS AND HARDWOODS. International Biodeterioration Bulletin 15:66-73.

Hickey M.G., Kittrick J.A. (1984) CHEMICAL PARTITIONING OF CADMIUM, COPPER, NICKEL AND ZINC IN SOILS AND SEDIMENTS CONTAINING

HIGH-LEVELS OF HEAVY-METALS. Journal of Environmental Quality 13:372-376.

Hingston J.A., Collins C.D., Murphy R.J., Lester J.N. (2001) Leaching of chromated copper arsenate wood preservatives: a review. Environmental Pollution 111:53-66.

Hopp L., Nico P.S., Marcus M.A., Peiffer S. (2008) Arsenic and chromium partitioning in a podzolic soil contaminated by chromated copper arsenate. Environmental Science & Technology 42:6481-6486.

Iglesias A., Lopez R., Fiol S., Antelo J.M., Arce F. (2003) Analysis of copper and calcium-fulvic acid complexation and competition effects. Water Research 37:3749-3755. DOI: 10.1016/s0043-1354(03)00236-7.

Kabata-Pendias A. (2001) Trace Elements in Soils and Plants. Third Edition ed. CRC Press, Boca Raton, Florida.

Kalbitz K., Solinger S., Park J.H., Michalzik B., Matzner E. (2000) Controls on the dynamics of dissolved organic matter in soils: A review. Soil Science 165:277-304.

Keon N.E., Swartz C.H., Brabander D.J., Harvey C.F., Hemond H.F. (2001) Validation of an arsenic sequential extraction method for evaluating mobility in sediments. Environmental Science & Technology 35:2778-2784. DOI: 10.1021/es001511o.

Khan B.I., Solo-Gabriele H.M., Dubey B.K., Townsend T.G., Cai Y. (2004) Arsenic speciation of solvent-extracted leachate from new and weathered CCA-treated wood. Environmental Science & Technology 38:4527-4534. DOI: 10.1021/es049598r.

Kim H., Kim D.J., Koo J.H., Park J.G., Jang Y.C. (2007) Distribution and mobility of chromium, copper, and arsenic in soils collected near CCA-treated wood structures in Korea. Science of the Total Environment 374:273-281.

Kocar B.D., Fendorf S. (2009) Thermodynamic Constraints on Reductive Reactions Influencing the Biogeochemistry of Arsenic in Soils and Sediments. Environmental Science & Technology 43:4871-4877. DOI: 10.1021/es8035384.

Kocar B.D., Herbel M.J., Tufano K.J., Fendorf S. (2006) Contrasting effects of dissimilatory iron(III) and arsenic(V) reduction on arsenic retention and transport. Environmental Science & Technology 40:6715-6721.

Korshin G.V., Frenkel A.I., Stern E.A. (1998) EXAFS study of the inner shell structure in copper(II) complexes with humic substances. Environmental Science & Technology 32:2699-2705.

Kozul C.D., Ely K.H., Enelow R.I., Hamilton J.W. (2009) Low-Dose Arsenic Compromises the Immune Response to Influenza A Infection in Vivo. Environmental Health Perspectives 117:1441-1447. DOI: 10.1289/ehp.0900911.

La Force M.J., Hansel C.M., Fendorf S. (2000) Arsenic speciation, seasonal transformations, and co-distribution with iron in a mine waste-influenced palustrine emergent wetland. Environmental Science & Technology 34:3937-3943. DOI: 10.1021/es0010150.

Lebow S. (1996) Leaching of wood preservative components and their mobility in the environment: summary of pertinent literature, in: U. F. P. Laboratory (Ed.).

Lebow S., Foster D., Lebow P. (2004a) Rate of CCA leaching from commercially treated decking. Forest Products Journal 54:81-88.

Lebow S., Foster D., Evans J. (2004b) Long-term soil accumulation of chromium, copper, and arsenic adjacent to preservative-treated wood. Bulletin of Environmental Contamination and Toxicology 72:225-232. DOI: 10.1007/s00128-003-9055-y.

Lin Z.a.R.W.P. (2000) Adsorption, desoption and oxidation of arsenic affected by clay minerals and aging process. Environmental Geology 39.

Liu E.F., Shen J., Yang L.Y., Zhang E.L., Meng X.H., Wang J.J. (2010) Assessment of heavy metal contamination in the sediments of Nansihu Lake Catchment, China. Environmental Monitoring and Assessment 161:217-227. DOI: 10.1007/s10661-008-0739-y.

Livesey N.T., Huang P.M. (1981) ADSORPTION OF ARSENATE BY SOILS AND ITS RELATION TO SELECTED CHEMICAL-PROPERTIES AND ANIONS. Soil Science 131:88-94.

Loring D.H., Rantala R.T.T. (1992) MANUAL FOR THE GEOCHEMICAL ANALYSES OF MARINE-SEDIMENTS AND SUSPENDED PARTICULATE MATTER. Earth-Science Reviews 32:235-283.

Loring J.S., Sandstrom M.H., Noren K., Persson P. (2009) Rethinking Arsenate Coordination at the Surface of Goethite. Chemistry-a European Journal 15:5063-5072. DOI: 10.1002/chem.200900284.

Malinowski E.R. (1977) DETERMINATION OF NUMBER OF FACTORS AND EXPERIMENTAL ERROR IN A DATA MATRIX. Analytical Chemistry 49:612-617.

Malinowski E.R. (1978) THEORY OF ERROR FOR TARGET FACTOR-ANALYSIS WITH APPLICATIONS TO MASS-SPECTROMETRY AND NUCLEAR MAGNETIC-RESONANCE SPECTROMETRY. Analytica Chimica Acta-Computer Techniques and Optimization 2:339-354.

Manceau A., Marcus M.A., Tamura N. (2002) Quantitative speciation of heavy metals in soils and sediments by synchrotron X-ray techniques, in: P. A. Fenter, et al. (Eds.), Applications of Synchrotron Radiation in Low-Temperature Geochemistry and Environmental Sciences, Mineralogical Soc America, Washington. pp. 341-428.

Manceau A.M., A. (2010) The nature of Cu bonding to natural organic matter. Geochimica et Cosmochimica Acta xxx:xxx.

Mandal B.K., Suzuki K.T. (2002) Arsenic round the world: a review. Talanta 58:201-235.

Manning B.A., Goldberg S. (1996) Modeling competitive adsorption of arsenate with phosphate and molybdate on oxide minerals. Soil Science Society of America Journal 60:121-131.

Manning B.A., Goldberg S. (1997a) Arsenic(III) and arsenic(V) absorption on three California soils. Soil Science 162:886-895.

Manning B.A., Goldberg S. (1997b) Adsorption and stability of arsenic(III) at the clay mineral-water interface. Environmental Science & Technology 31:2005-2011.

Marcus M.A., MacDowell A.A., Celestre R., Manceau A., Miller T., Padmore H.A., Sublett R.E. (2004) Beamline 10.3.2 at ALS: a hard X-ray microprobe for environmental and materials sciences. Journal of Synchrotron Radiation 11:239-247. DOI: 10.1107/s0909049504005837.

Martinez-Villegas N., Martinez C.E. (2008) Solid- and solution-phase organics dictate copper distribution and speciation in multicomponent systems containing ferrihydrite, organic matter, and montmorillonite. Environmental Science & Technology 42:2833-2838. DOI: 10.1021/es072012r.

Martinez C.E., McBride M.B. (1998) Solubility of Cd2+, Cu2+, Pb2+, and Zn2+ in aged coprecipitates with amorphous iron hydroxides. Environmental Science & Technology 32:743-748.

Masscheleyn P.H., Delaune R.D., Patrick W.H. (1991) Effect of Redox Potential and Ph on Arsenic Speciation and Solubility in a Contaminated Soil. Environmental Science & Technology 25:1414-1419.

McBride M.B. (1978a) COPPER(II) INTERACTIONS WITH KAOLINITE - FACTORS CONTROLLING ADSORPTION. Clays and Clay Minerals 26:101-106.

McBride M.B. (1978b) RETENTION OF CU2+, CA2+, MG2+, AND MN2+ BY AMORPHOUS ALUMINA. Soil Science Society of America Journal 42:27-31.

McBride M.B. (1982) CU-2+-ADSORPTION CHARACTERISTICS OF ALUMINUM HYDROXIDE AND OXYHYDROXIDES. Clays and Clay Minerals 30:21-28.

McBride M.B., Bouldin D.R. (1984) LONG-TERM REACTIONS OF COPPER(II) IN A CONTAMINATED CALCAREOUS SOIL. Soil Science Society of America Journal 48:56-59.

McBride M.B., Richards B.K., Steenhuis T., Russo J.J., Sauve S. (1997) Mobility and solubility of toxic metals and nutrients in soil fifteen years after sludge application. Soil Science 162:487-500.

McLaren R.G., Crawford D.V. (1973a) STUDIES ON SOIL COPPER .2. SPECIFIC ADSORPTION OF COPPER BY SOILS. Journal of Soil Science 24:443-452.

McLaren R.G., Crawford D.V. (1973b) Studies on Soil Copper .1. Fractionation of Copper in Soils. Journal of Soil Science 24:172-181.

Mehlich A. (1984) MEHLICH-3 SOIL TEST EXTRACTANT - A MODIFICATION OF MEHLICH-2 EXTRACTANT. Communications in Soil Science and Plant Analysis 15:1409-1416.

Nath B., Chakraborty S., Burnol A., Stuben D., Chatterjee D., Charlet L. (2009) Mobility of arsenic in the sub-surface environment: An integrated hydrogeochemical study and sorption model of the sandy aquifer materials. Journal of Hydrology 364:236-248.

Nickson R., McArthur J., Burgess W., Ahmed K.M., Ravenscroft P., Rahman M. (1998) Arsenic poisoning of Bangladesh groundwater. Nature 395:338-338.

Nico P.S., Ruby M.V., Lowney Y.W., Holm S.E. (2006) Chemical speciation and bioaccessibility of arsenic and chromium in chromated copper arsenate-treated wood and soils. Environmental Science & Technology 40:402-408. DOI: 10.1021/es050950q.

Nico P.S., Fendorf S.E., Lowney Y.W., Holm S.E., Ruby M.V. (2004) Chemical structure of arsenic and chromium in CCA-treated wood: Implications of environmental weathering. Environmental Science & Technology 38:5253-5260. DOI: 10.1021/es0351342.

O'Neill P. (1995) (Ed.)^(Eds.) Arsenic, Blackie, London. pp. Pages.

Oremland R.S., Stolz J.F. (2005) Arsenic, microbes and contaminated aquifers. Trends in Microbiology 13:45-49.

Oscarson D.W., Huang P.M., Defosse C., Herbillon A. (1981) OXIDATIVE POWER OF MN(IV) AND FE(III) OXIDES WITH RESPECT TO AS(III) IN TERRESTRIAL AND AQUATIC ENVIRONMENTS. Nature 291:50-51.

Paez-Espino D., Tamames J., de Lorenzo V., Canovas D. (2009) Microbial responses to environmental arsenic. Biometals 22:117-130.

Paktunc D., Foster A., Laflamme G. (2003) Speciation and characterization of arsenic in Ketza River mine tailings using x-ray absorption spectroscopy. Environmental Science & Technology 37:2067-2074. DOI: 10.1021/es026185m.

Paktunc D., Foster A., Heald S., Laflamme G. (2004) Speciation and characterization of arsenic in gold ores and cyanidation tailings using X-ray absorption spectroscopy. Geochimica et Cosmochimica Acta 68:969-983.

Pasquarello A., Petri I., Salmon P.S., Parisel O., Car R., Toth E., Powell D.H., Fischer H.E., Helm L., Merbach A.E. (2001) First solvation shell of the Cu(II) aqua ion: Evidence for fivefold coordination. Science 291:856-859.

Paulson A.J., Kester D.R. (1980) COPPER(II) ION HYDROLYSIS IN AQUEOUS-SOLUTION. Journal of Solution Chemistry 9:269-277.

Phillips E.J.P., Lovley D.R. (1987) DETERMINATION OF FE(III) AND FE(II) IN OXALATE EXTRACTS OF SEDIMENT. Soil Science Society of America Journal 51:938-941.

Pigna M., Krishnamurti G.S.R., Violante A. (2006) Kinetics of arsenate sorption-desorption from metal oxides: Effect of residence time. Soil Science Society of America Journal 70:2017-2027. DOI: 10.2136/sssaj2005.0373.

Pils J.R.V., Karathanasis A.D., Mueller T.G. (2004) Concentration and distribution of six trace metals in northern Kentucky soils. Soil & Sediment Contamination 13:37-51.

Ponizovskii A.A., Studenikina T.A., Mironenko E.V. (1999) Adsorption of Copper(II) ions by soil as influenced by organic components of soil solutions. Eurasian Soil Science 32:766-775.

Ponizovsky A.A., Allen H.E., Ackerman A.J. (2007) Copper activity in soil solutions of calcareous soils. Environmental Pollution 145:1-6. DOI: 10.1016/j.envpol.2006.04.010.

Raven K.P., Jain A., Loeppert R.H. (1998) Arsenite and arsenate adsorption on ferrihydrite: Kinetics, equilibrium, and adsorption envelopes. Environmental Science & Technology 32:344-349.

Redman A.D., Macalady D.L., Ahmann D. (2002) Natural organic matter affects arsenic speciation and sorption onto hematite. Environmental Science & Technology 36:2889-2896. DOI: 10.1021/es0112808.

Registar F. (2002) Notice of receipt of requests to cancal certain chromated copper arsenate (CCA) wood preservative products and amend to terminate certain uses of CCA products., Federal Registar. pp. 8244-8246.

Ressler T. (1997) WinXAS: A new software package not only for the analysis of energy-dispersive XAS data. Journal De Physique Iv 7:269-270.

Ressler T., Wong J., Roos J., Smith I.L. (2000) Quantitative speciation of Mn-bearing particulates emitted from autos burning (methylcyclopentadienyl)manganese tricarbonyl-added gasolines using XANES spectroscopy. Environmental Science & Technology 34:950-958.

Robinson B., Greven M., Green S., Sivakumaran S., Davidson P., Clothier B. (2006) Leaching of copper, chromium and arsenic from treated vineyard posts in Marlborough, New Zealand. Science of the Total Environment 364:113-123.

Rodriguez-Rubio P., Morillo E., Madrid L., Undabeytia T., Maqueda C. (2003) Retention of copper by a calcareous soil and its textural fractions: influence of amendment with two agroindustrial residues. European Journal of Soil Science 54:401-409.

Sadiq M. (1997) Arsenic chemistry in soils: An overview of thermodynamic predictions and field observations. Water Air and Soil Pollution 93:117-136.

Sanders J.R., Bloomfield C. (1980) THE INFLUENCE OF PH, IONIC-STRENGTH AND REACTANT CONCENTRATIONS ON COPPER COMPLEXING BY HUMIFIED ORGANIC-MATTER. Journal of Soil Science 31:53-63.

Scheinost A.C., Abend S., Pandya K.I., Sparks D.L. (2001) Kinetic controls on Cu and Pb sorption by ferrihydrite. Environmental Science & Technology 35:1090-1096.

Seibert J., Stendahl J., Sorensen R. (2007) Topographical influences on soil properties in boreal forests. Geoderma 141:139-148. DOI: 10.1016/j.geoderma.2007.05.013.

Shacklette H.T., Boerngen J.G. (1984) Element concentrations in soils and other surficial materials of the conterminous United States, in: U. S. G. Survey (Ed.).

Smedley P.L., Kinniburgh D.G. (2002) A review of the source, behaviour and distribution of arsenic in natural waters. Applied Geochemistry 17:517-568.

Smith E., Naidu R., Alston A.M. (1998) Arsenic in the soil environment: A review, Advances in Agronomy, Vol 64, Academic Press Inc, San Diego. pp. 149-195.

Smith E., Naidu R., Alston A.M. (1999) Chemistry of arsenic in soils: I. Sorption of arsenate and arsenite by four Australian soils. Journal of Environmental Quality 28:1719-1726.

Smith E., Naidu R., Alston A.M. (2002) Chemistry of inorganic arsenic in soils: II. Effect of phosphorus, sodium, and calcium on arsenic sorption. Journal of Environmental Quality 31:557-563.

Solo-Gabriele H., Townsend T. (1999) Disposal practices and management alternatives for CCA-treated wood waste. Waste Management & Research 17:378-389.

Sparks D.L. (2003) Environmental Soil Chemistry Elsevier, San Diego, Ca.

Sposito G. (2008) The Chemistry of Soils. Second Edition ed. Oxford University Press, Inc., New York.

Stilwell D., Toner M., Sawhney B. (2003) Dislodgeable copper, chromium and arsenic from CCA-treated wood surfaces. Science of the Total Environment 312:123-131.

Stilwell D.E., Gorny K.D. (1997) Contamination of soil with copper, chromium, and arsenic under decks built from pressure treated wood. Bulletin of Environmental Contamination and Toxicology 58:22-29.

Stilwell D.E., Graetz T.J. (2001) Copper, chromium, and arsenic levels in soil near highway traffic sound barriers built using CCA pressure-treated wood. Bulletin of Environmental Contamination and Toxicology 67:303-308.

Stookey L.L. (1970) FERROZINE - A NEW SPECTROPHOTOMETRIC REAGENT FOR IRON. Analytical Chemistry 42:779-&.

Strawn D.G., Baker L.L. (2008) Speciation of cu in a contaminated agricultural soil measured by XAFS, mu-XAFS, and mu-XRF. Environmental Science & Technology 42:37-42. DOI: 10.1021/es071605z.

Strawn D.G., Palmer N.E., Furnare L.J., Goodell C., Amonette J.E., Kukkadapu R.K. (2004) Copper sorption mechanisms on smectites. Clays and Clay Minerals 52:321-333. DOI: 10.1346/ccmn.2004.0520307.

Sun X.H., Doner H.E. (1996) An investigation of arsenate and arsenite bonding structures on goethite by FTIR. Soil Science 161:865-872.

Sun X.H., Doner H.E. (1998) Adsorption and oxidation of arsenite on goethite. Soil Science 163:278-287.

Sylva R.N. (1976) ENVIRONMENTAL CHEMISTRY OF COPPER(II) IN AQUATIC SYSTEMS. Water Research 10:789-792.

Sylvia D.M., J.J. Fuhrmann, P.G. Hartel, and D.A. Zuberer. (2005) Principles and applications of soil microbiology. 2 ed. Pearson, Upper Saddle River, New Jersey.

Tipping E., Griffith J.R., Hilton J. (1983) THE EFFECT OF ADSORBED HUMIC SUBSTANCES ON THE UPTAKE OF COPPER(II) BY GOETHITE. Croatica Chemica Acta 56:613-621.

Tournassat C., Charlet L., Bosbach D., Manceau A. (2002) Arsenic(III) oxidation by birnessite and precipitation of manganese(II) arsenate. Environmental Science & Technology 36:493-500. DOI: 10.1021/es0109500.

Townsend T., Solo-Gabriele H. (2001) Environmental Impacts of Treated Wood Taylor & Francis.

Tufano K.J., Fendorf S. (2008) Confounding impacts of iron reduction on arsenic retention. Environmental Science & Technology 42:4777-4783.

Uminska R. (1988) Assessment of Hazardous Levels of Trace Elements to Health in Contaminated Soils of Poland, in: I. M. Wsi (Ed.), Warszawa.

USDHHS. (2007) CERCLA Priority List of Hazardous Substances That Will Be Subject of Toxicological Profiles and Support Document, in: U. S. D. o. H. a. H. S. A. f. T. S. a. D. R. D. o. Toxicology (Ed.).

USGS. (2009) Mineral commodity summaries 2009, in: U. S. G. Survey (Ed.). pp. 195.

Valko M., Morris H., Cronin M.T.D. (2005) Metals, toxicity and oxidative stress. Current Medicinal Chemistry 12:1161-1208.

Vega F.A., Covelo E.F., Chao I., Andrade M.L. (2007) Role of different soil fractions in copper sorption by soils. Communications in Soil Science and Plant Analysis 38:2887-2905. DOI: 10.1080/00103620701663131.

Warner J.E., Solomon K.R. (1990) Acidity as a Factor in Leaching of Copper, Chromium and Arsenic from Cca-Treated Dimension Lumber. Environmental Toxicology and Chemistry 9:1331-1337.

Wauchope R.D. (1975) FIXATION OF ARSENICAL HERBICIDES, PHOSPHATE, AND ARSENATE IN ALLUVIAL SOILS. Journal of Environmental Quality 4:355-358.

Yavuz O., Altunkaynak Y., Guzel F. (2003) Removal of copper, nickel, cobalt and manganese from aqueous solution by kaolinite. Water Research 37:948-952.

Yu S., He Z.L., Huang C.Y., Chen G.C., Calvert D.V. (2004) Copper fractionation and extractability in two contaminated variable charge soils. Geoderma 123:163-175. DOI: 10.1016/j.geoderma.2004.02.003.

Zhang H., Selim H.M. (2008) Reaction and transport of arsenic in soils: Equilibrium and kinetic modeling, Advances in Agronomy, Vol 98. pp. 45-115.

Vita

Donald Roy Schwer III

Date of Birth: 01/19/1985

Place of Birth: Chicago, IL

Education:

B.S., Agricultural and Biological Engineering, University of Illinois, Dec. 2007

Employment:

Academic

Aug. 2008 – present	Graduate Research Assistant, University of Kentucky, Rhizosphere Science Laboratory
Fall 2008, Spring 2009	Teaching Assistant, University of Kentucky, PLS 366- Fundamentals of Soil Science
May 2006- August 2006	Research Assistant, United States Department of Agriculture at University of Illinois

Industry

March 2008- August 2008	Corn Breeding Intern, Monsanto at Thomasboro, IL
June 2007- August 2007	Engineer Technical Intern, Geosyntec Consultants at Chicago, IL
May 2005- August 2005	Labor/ Pre-apprentice, 3G Plumbing Inc. at Beecher, IL

Presentations:

Schwer III, D.R. April 3, 2009. Bluegrass Fences: A Biogeochemical study on the Kentucky Landscape. Plant and Soil Science Seminar. University of Kentucky. Lexington, Kentucky

Schwer III, D.R. and D.H. McNear. November 3, 2009. Concentration and Speciation of Arsenic, Chromium, and Copper in the Soil System Adjacent to Chromated Copper Arsenate Treated Lumber Fence Posts. 73rd International Annual Meeting of the Soil Science Society of America. Pittsburgh, Pennsylvania.

Society Affiliations:

Soil Science Society of America (SSSA)
Crop Science Society of America (CSA)
American Society of Agronomy (ASA)
American Society of Agricultural and Biological Engineers (ASABE)